

ANNUAL PROGRESS REPORT 1972

(NASA-CR-140708) APPLICATIONS OF THE
DIRECT PHOTON ABSORPTION TECHNIQUE FOR
MEASURING BONE MINERAL CONTENT IN VIVO.
DETERMINATION OF BODY (Wisconsin Univ.)
157 p HC \$6.25

N75-10694

CSSL 06P

G3/52

Unclas
53751

BONE MINERAL LABORATORY
UNIVERSITY OF WISCONSIN
MADISON, WISCONSIN



PROGRESS REPORT

AEC Grant No. AT-(11-1)-1422

"Determination of Body Composition In Vivo"

NASA Grant No. Y-NGR-50-002-051

"Applications of the Direct Photon Absorption
Technique for Measuring Bone Mineral
Content In Vivo"

August 1, 1972

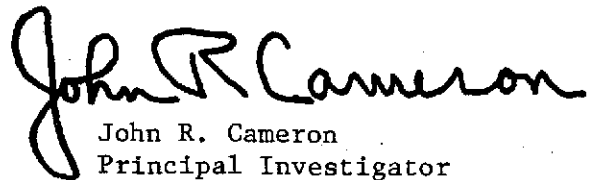
John R. Cameron, Ph.D.
Principal Investigator
Department of Radiology
University of Wisconsin Medical Center
Madison, Wisconsin 53706

FORWORD

This progress report is a summary of research on the measurement of bone mineral content and body composition, in vivo, at the University of Wisconsin from July 15, 1971 through July 15, 1972. Research support for the bone measurement laboratories comes from a variety of sources, these are: United States Atomic Energy Commission through Contract AT(11-1)-1422, the National Aeronautics and Space Administration through Grant Y-NGR-50-002-051 and the University of Wisconsin. The work represents primarily the efforts of the following: Dr. Richard B. Mazess, Dr. Philip F. Judy, Dr. Charles R. Wilson, Dr. Mark Mueller, Dr. Everett L. Smith, Dr. John M. Jurist, Robert M. Witt, John M. Sandrik, Kianpour Kianian, Warren E. Mather, Keith Jones, Clifford E. Vought, Mrs. Joyce Fischer and Mrs. Sue Kennedy. I wish to express my appreciation for their efforts.

I would like to thank Mrs. Linda Robbins, Miss Sue Bostwick and Miss Joyce Reilly for their secretarial help in preparing these reports and Miss Beth Sommers, Miss Nancy Kang, Miss Stephanie Wurdinger and Quinton Verdier for assembling these reports. I would also like to thank Orlando Canto for the illustrations.

Certain parts of this report represent work in progress which will be continued during the coming year.



John R. Cameron
Principal Investigator
August 1, 1972

August 1, 1972

ANNUAL PROGRESS REPORT ON AEC CONTRACT AT - (11 - 1) - 1422

Table of Contents

1. C00-1422-111 The Use of In Vivo Bone Mineral Determination to Predict the Strength of Bone. Abstract of Ph.D. thesis.

 . . . C. R. Wilson
2. C00-1422-112 Skeletal Growth in School Children: Maturation and Bone Mass.

 . . . R. B. Mazess and J. R. Cameron
3. C00-1422-113 Growth of Bone in School Children: Comparison of Radiographic Morphometry and Photon Absorptiometry.

 . . . R. B. Mazess and J. R. Cameron
4. C00-1422-114 Direct Readout of Bone Mineral Content Using Radionuclide Absorptiometry. Abstract.

 . . . R. B. Mazess, J. R. Cameron and H. Miller
5. C00-1422-115 Weight and Density of Sadlermiut Eskimo Long Bones. Abstract.

 . . . R. B. Mazess and R. Jones
6. C00-1422-116 Technical Information on a Rectilinear Scanner for Determination of Bone Mineral Content.

 . . . J. M. Sandrik
7. C00-1422-117 Effects of the Polyenergetic Character of the Spectrum of ^{125}I on the Measurement of Bone Mineral Content.

 . . . J. M. Sandrik and P. F. Judy
8. C00-1422-118 Improved Version of the Dual-Channel System to Measure Bone Mineral Content

 . . . R. M. Witt, C. E. Vought and R. B. Mazess

9. C00-1422-119 Comparison of Compact Scintillation Detectors for Bone Mineral Content Measurements.
 . . . R. M. Witt and R. B. Mazess
10. C00-1422-120 A Compact Scanner for Measurement of Bone Mineral.
 . . . R. B. Mazess and Y. Towliati
11. C00-1422-121 Bedrest Subject Measurements at USPHS.
 . . . P. F. Judy and J. R. Cameron
12. C00-1422-122 Prediction of Body Composition from Absorptiometric Limb Scans.
 . . . R. B. Mazess
13. C00-1422-123 Bone Mineral Content of Eskimos in Alaska and Canada: Preliminary Report.
 . . . W. Mather and R. B. Mazess
14. C00-1422-124 Progress in Clinical Use of Photon Absorptiometry.
 . . . R. B. Mazess, P. F. Judy, C. R. Wilson and J. R. Cameron
15. C00-1422-125 The Bone Mineral Content and Physical Strength of Avascularized Femoral Heads. An Experimental Study on Adult Rabbits. A Proposed Experiment.
 . . . R. M. Witt
16. C00-1422-126 Determination of Vertebral Bone Mineral Mass by Transmission Measurements.
 . . . P. F. Judy, J. R. Cameron, K. M. Jones and M. G. Ort
17. C00-1422-127 A New Material for the International Bone Mineral Standard.
 . . . A. Kabluna, R. B. Mazess and W. Mather

18. C00-1422-128 Experiences with the Use of Vibrational Techniques for the Determination of the Resonant Frequency of Bone In Vivo.
... C. R. Wilson
19. C00-1422-129 Report on the First Bone Mineral Workshop - 1971.
... R. B. Mazess
20. C00-1422-130 Interpretation of Fracture Index Charts.
... E. Smith and J. R. Cameron
21. C00-1422-131 Relationship Between Bone Mineral Contents of the Radius, Femoral Neck, Thoracic Vertebrae and Other Sites.
... C. R. Wilson and J. R. Cameron
22. C00-1422-132 Bone Mineralization and Unilateral Activity.
... R. C. Watson
23. C00-1422-133 Osteoporosis in Rheumatoid Arthritis (RA) Influence of Disease Duration, Severity, and Steroid Therapy.
... M. N. Mueller and J. M. Jurist
24. C00-1422-134 Skeletal Status in Rheumatoid Arthritis: A Preliminary Report.
... M. N. Mueller and J. M. Jurist

THE USE OF IN VIVO BONE MINERAL DETERMINATION
TO PREDICT THE STRENGTH OF BONE

Abstract of Ph.D. thesis
completed January 1972

by

Charles R. Wilson
Department of Radiology
University of Wisconsin Medical Center
Madison, Wisconsin

The importance of bone to the health of an individual is well known. However, in many instances there is a failure of the skeleton to provide adequate structural support throughout life. A progressive deterioration in skeletal integrity begins after maturity with the most serious loss of strength occurring in the femoral neck and the spine. Fractures in these areas associated with minimal trauma and often called "spontaneous" increase markedly with age. The primary factor in the increased fragility of the skeleton is the reduction in the total amount of bone present due to cortical thinning of the long bones and the increased rarefaction of the vertebrae. A determination of the amount of bone in the areas of clinical interest, i.e. the hip and spine, may provide an estimate of the strength of the bone in these areas and a measure of the risk of fracture. The bone mineral content, BMC, determined by the University of Wisconsin monoenergetic photon absorption technique, of 29 different locations on the long bones and vertebral columns of 24 skeletons were measured. Compressive tests were made on bone from these locations in which the maximum load and maximum stress were measured. Also the ultimate strain, modulus of elasticity and energy absorbed to failure were determined for compact bone from the femoral diaphysis and cancellous bone from the eighth through eleventh thoracic vertebrae. Correlations and predictive relationships between these parameters were examined to investigate the applicability of using the BMC at sites normally measured in vivo, i.e. radius and ulna in estimating the BMC and/or strength of the spine or femoral neck.

It was found that the BMC at sites on the same bone were highly correlated $r = 0.95$ or better; the BMC at sites on different bones were also highly interrelated, $r = 0.85$. The BMC at various sites on the long bones could be estimated to between 10 and 15 per cent from the BMC of sites on the radius or ulna. Also the BMC of the thoracic vertebrae could be estimated from the BMC at a site on the radius and age with a standard error of estimate of about 17 per cent. The maximum compressive stress of bone from the vertebral column was found to be closely related to the mass of bone mineral per unit volume of the vertebra. The maximum compressive stress and bone mineral per unit volume of the vertebral bone tissue declined with age at rates

of about 17 and 8 per cent per decade respectively. It was found to be possible to estimate the maximum compressive stress of bone of the vertebra qualitatively from the radial BMC, age and the dimensions of the vertebra. The radial BMC was highly related to the mineral content of the femoral neck, $r = 0.88$, and the femoral neck mineral content could be estimated with a standard error of estimate of 15 per cent. It was found that the femoral necks of all skeletons with a radial BMC of less than 0.68 gm/cm were significantly weaker than those with a radial BMC greater than this value.

The relation between the BMC and the maximum compressive load of specimens of compact bone was examined. The maximum load borne by the bone was found to be more closely related to the BMC of the specimen than to the total area. The maximum compressive stress of compact bone tissue was found to decrease about 7 per cent per decade after age 35. There was also a decline in the bone mineral per unit volume of compact bone tissue of about 3.3 per cent per decade. A model in which bone is considered a porous material was developed. The model was able to mathematically describe the age related changes in the maximum stress and the bone mineral per unit volume of compact bone.

Supported by USPHA Training Grant CA-05104

Reprinted from AMERICAN JOURNAL OF PHYSICAL ANTHROPOLOGY
Vol. 35, No. 3, November 1971 © The Wistar Institute Press 1971

Skeletal Growth in School Children: Maturation and Bone Mass

RICHARD B. MAZESS AND JOHN R. CAMERON
*Department of Radiology (Medical Physics), University of Wisconsin
Hospital, Madison, Wisconsin 53706*

ABSTRACT Skeletal growth and development was evaluated in 322 white children (age 6 to 14) using three different methods: (1) ^{125}I photon absorptiometry, (2) compact bone measures on radiographs, and (3) Greulich-Pyle skeletal age from hand-wrist radiographs. Bone mineral content, measured by photon absorptiometry, increased at an incremental rate of about 8.5% each year. Skeletal age was a poor predictor of skeletal status, i.e., bone mineral content (14% error), and did not decrease the predictive error substantially more than did chronological age. Gross morphology (height and weight) was in fact a better predictor of bone mineral content than were skeletal age, chronological age, and radiographic morphometry. Skeletal age deviations were correlated with deviations in body size. A bone mineral index was devised which was independent of body size and this index was also independent of skeletal age. Skeletal age is imprecise (3 to 6 months error) and the range of variation in normal children (13 months) overlaps the maturational delay of the malnourished and diseased. The difficulties in using skeletal maturation are discussed and it is suggested that particular maturational indices be used which better indicate skeletal growth than does a composite skeletal age.

Traditionally osseous growth and development has been assessed using the linear dimensions of anthropometry, but these measures have been supplemented, and even supplanted, by indicators of skeletal maturation and determinations of skeletal status (i.e., the amount and the distribution of bone, strength, modulus of elasticity, and skeletal dynamics). The ossification patterns used for assessment of skeletal maturation have been shown to have some relationship to linear growth of bones, and in fact can be used to predict stature increments and adult stature. However, stature, and even bone lengths, are only moderately associated with skeletal status, and skeletal maturation therefore might be expected to demonstrate an even lower degree of association. If the latter hypothesis is in fact demonstrable then skeletal maturation would be of little utility as an indicator of skeletal status in either abnormal or normal children, nor would it be of primary use in assessing the influences of environmental variables such as disease, nutrition, activity levels, and stress on skeletal status.

The chief difficulty in testing the above hypothesis is the difficulty in finding acceptable criteria of skeletal status. The amount of bone itself is unacceptable since individuals will vary widely in size depending on their genetic background. This difficulty can be overcome in part by referencing the amount of bone to either the size of the skeleton or to overall body size. The amount of bone can be measured by several non-destructive methods. We have used the measurement of compact bone on radiographs and scanning with radioisotope photon absorptiometry since these are the most commonly used and practical methods.

METHODS

Measurements were made on 322 white school age children (age 6 to 14 years) in Middleton, Wisconsin. The age and sex distribution is given in table 1. The direct photon absorption method (Cameron and Sorenson, '63; Cameron, Mazess, and Sorenson, '68; Cameron, '70; Sorenson and Cameron, '67) was used to measure bone mineral content. The monoenergetic

photon source was ^{125}I (27.4 keV). Linear scans were made across the distal third of the radius and across the mid-humerus on all subjects, and across the distal third of the ulna on 128 subjects. In addition to mineral content, the bone width was determined from the width of the absorptiometric scan and the mineral-width ratio was calculated as an indicator of the mineral content per unit bone width. The precision and accuracy of this method have been demonstrated to be very high (less than 2% error), and the absorptiometric scan is related not only to local mineral content but to the weight of individual long bones and to total skeletal weight (Mazess, '71).

Measurements of the bone image on a radiograph (Meema, '63; Virtama and Helela, '69) have been widely used in clinical settings and in surveys of skeletal growth and development. The thickness of the total bone and of the medullary canal were measured by two observers with Helios calipers on a standard radiograph (36-inch FFD); the site measured was the same as for the absorptiometric scan on the distal radius. Compact bone thickness was derived. In addition, the total cross-sectional area and the area of the compact bone were calculated assuming a circular model (Frisancho, Garn and Ascoli, '70). The ratio of compact to total bone thickness and area were also calculated as these ratios are commonly used indices of skeletal status.

Skeletal age determinations were done from hand-wrist radiographs using the atlas of Greulich and Pyle ('59). A variety of weighting formulae and other schemes have been advocated by various investigators, and, in using the Greulich-Pyle method we have simply selected a common method, the success and failure of which is probably fairly representative of analogous techniques. Two observers were trained to do skeletal age assessments. The error (RMS) in repeat measurements ($n = 141$) by the same observer was 5.23 months (4.64%). For the 316 films on which determinations were possible the between observer error (RMS) was 5.17 months (4.41%). Both observers systematically scored skeletal ages about 3.7 months below chronological ages (girls -2.1 months and boys -5.3 months).

RESULTS

A. Age changes in morphology and the skeleton. Skeletal age in each age group of girls closely approximated the chronological age, but in boys the skeletal age was markedly below chronological age during the early school years, and also to some extent during adolescence (table 1). Skeletal and chronological ages were nevertheless highly correlated ($r = 0.92$ in girls and 0.88 in boys) but the error in predicting skeletal age from chronological age was rather large (11.1 months in girls and 14.7 months in boys). Apparently a deviation of ± 1 year in skeletal age may

TABLE 1
Means and coefficients of variation for age and skeletal age in school children

Age	Boys					Girls				
	CA ¹			SA ²		CA			SA	
	N	Mean	C/V ³	Mean	C/V	N	Mean	C/V	Mean	C/V
<i>years</i>										
6	16	79	4	67	28	11	80	3	79	12
7	26	90	4	80	18	19	91	3	93	13
8	25	101	4	98	18	15	103	3	103	13
9	25	113	3	110	16	22	115	3	111	9
10	28	126	3	124	12	29	125	3	120	9
11	23	137	2	133	9	20	137	2	135	8
12	19	148	2	142	8	13	153	2	152	9
13	11	161	2	154	9	15	161	2	158	9
14	5	170	1	163	8	4	172	2	170	5

¹ CA, chronological age.

² SA, skeletal age.

³ C/V, coefficient of variation.

be observed in supposedly normal children. Height and weight values were similar to those usually seen in well-nourished American white children, and the arm circumferences and skinfolds were not unusual (McCammon, '70).

Bone mineral content was moderately correlated with age ($r = 0.74$ to 0.80), and the increase was fairly linear, amounting to an average of about 10.5% year or an incremental rate of about 8.5% each year. The bone width and mineral-width ratio increased at an average annual rate of 4.5% or an incremental rate of 4% each year. Radiographic morphometry showed a somewhat similar pattern to bone mineral age changes. Total and compact bone thickness increased on the average about 3.8% annually while medullary canal diameter increased only 2.6%. The calculated total and compact bone cross-sectional areas increased to a far greater extent (on the average 8% annually) than did the thicknesses. In contrast, there was virtually

no change (0.5% annually) in the ratio of compact to total bone thickness or area.

B. Associations of chronological and skeletal age. The correlations of skeletal and chronological age with morphology, bone mineral and radiographic morphometry are given in table 2. There was a fairly high association of age with gross morphology, a moderate association with arm circumference, and no association with fatfold thickness. A moderate age association was evident for the bone mineral content of the three bones studied ($r = 0.74$) and there was a somewhat lower degree of association with both bone width ($r = 0.59$) and mineral-width ratio ($r = 0.65$). The correlations of age with radiographic morphometry were somewhat lower than those with absorptiometry, reflecting the greater errors of the former method. These correlations showed skeletal age to be somewhat more highly associated with morphology and skeletal measurements than was chronological age. However, use of skeletal age

TABLE 2

Correlation coefficients between chronological and skeletal ages and morphology, bone mineral measurements, and radiographic morphometry

	Chronological age	Skeletal age
Morphology		
Height	0.88	0.91
Weight	0.77	0.82
Arm circumference	0.56	0.64
Fatfold	0.04	0.14
Bone mineral		
Radius		
Mineral	0.75	0.78
Width	0.59	0.63
Mineral/width	0.71	0.73
Humerus		
Mineral	0.75	0.77
Width	0.64	0.66
Mineral/width	0.65	0.66
Ulna		
Mineral	0.68	0.72
Width	0.49	0.53
Mineral/width	0.57	0.60
Radiographic morphometry		
Thickness		
Total	0.52	0.57
Medullary	0.23	0.24
Compact	0.54	0.61
Area		
Total	0.53	0.58
Compact	0.58	0.64
Ratios		
Thickness (compact bone/total)	0.11	0.14
Area (compact bone/total)	0.10	0.13

increased the correlation coefficient only slightly (0.03) and increased predictive accuracy by only a few per cent.

C. Morphology and bone mineral measurements. Increases of body size (height, weight) are associated ($r = 0.81$) with increases of bone mineral content, and to a somewhat lesser extent ($r = 0.65$ to 0.70) with increases in bone width and in the mineral-width ratio (table 3). Height was not more closely associated with bone measurements than weight, but both height and weight were more highly associated than was arm circumference. Fatfold thickness was very poorly associated with the bone variables. Standardized regression coefficients and partial correlation coefficients were obtained from multiple regression analysis; these indicated that height and weight were equally important in explaining the variance of the bone measurements.

The correlations of morphological features with radiographic morphometry were substantially lower than those with absorptiometry, apparently reflecting the larger errors of the former measurements.

D. Deviant growth and development. A closer examination of the associations among skeletal age, morphology, and bone mineral was made by studying the deviation of observed from predicted values (using sex-specific regressions derived from this same sample). Height, weight, and bone mineral content (radius and humerus) were predicted for chronological age. A bone mineral index was devised using an average for the radius and humerus of the results from six regres-

sions with the following independent variables:

1. chronological age	$r = 0.75$
2. height	$r = 0.83$
3. weight	$r = 0.82$
4. bone width	$r = 0.86$
5. bone width, and age	$r = 0.91$
6. age, height, and weight	$r = 0.85$

The difference between predicted and observed values were expressed relative to the observed values to get per cent deviations. The associations among these deviations are shown in table 4. Height and weight deviations were moderately associated reflecting the concomitant growth in both parameters. Skeletal age deviations were associated with height and weight ($r = 0.4$ to 0.6), and also to some extent with bone mineral content ($r = 0.38$). There was only a very low degree of association, however, between bone mineral index and height, weight, or skeletal age deviations. It therefore appeared that deviations of skeletal age were associated to some extent with body size, and that the association with bone mineral content was secondary to this morphological relationship. The lack of association between bone mineral index and either skeletal age or morphological deviations indicated the dominant influence of body size and skeletal size on bone mineral content; when these factors were taken into account the associations with morphology and skeletal age deviations dropped appreciably.

The relative deviations in children with delayed (more than -10%), normal ($\pm 9\%$), and advanced (more than

TABLE 3

Correlation coefficients between morphological features and absorptiometric measurements

	Height	Weight	Arm circumference	Fatfold
Radius				
Mineral content	0.84	0.83	0.69	0.17
Width	0.72	0.73	0.62	0.15
Mineral content/width	0.72	0.68	0.57	0.15
Humerus				
Mineral content	0.82	0.82	0.65	0.12
Width	0.71	0.73	0.59	0.20
Mineral content/width	0.69	0.65	0.52	0.00
Ulna				
Mineral content	0.78	0.78	0.74	0.29
Width	0.61	0.61	0.56	0.16
Mineral content/width	0.61	0.59	0.57	0.27

TABLE 4

Associations among relative deviations (%) of observed from predicted values in school children

Variable 1	Variable 2	Correlations	
		Boys (n = 144)	Girls (n = 178)
Height for chron. age	Weight for chron. age	0.68	0.66
Skeletal — chron. age	Height for chron. age	0.62	0.52
Skeletal — chron. age	Weight for chron. age	0.43	0.51
Skeletal — chron. age	Bone mineral for chron. age	0.39	0.37
Skeletal — chron. age	Bone mineral index	0.22	0.16
Height for chron. age	Bone mineral index	0.26	0.09
Weight for chron. age	Bone mineral index	0.24	0.23

TABLE 5

Relative deviations (%) of observed from predicted values in children with delayed (more than -10%), normal ($\pm 9\%$), and advanced (more than 10%) skeletal ages

		Boys			Girls		
		Delayed	Normal	Advanced	Delayed	Normal	Advanced
Number		58	106	14	19	111	14
Skeletal — chron. age	\bar{X}	-20.5	0.3	20.9	-14.0	-1.6	17.5
	SD	9.7	4.8	10.7	4.2	5.0	8.7
Height for chron. age	\bar{X}	-2.9	0.8	5.5	-4.1	0.2	4.1
	SD	3.8	3.1	4.0	3.9	3.5	3.2
Weight for chron. age	\bar{X}	-11.5	-1.2	19.8	-20.1	-1.9	11.4
	SD	14.8	16.0	16.3	18.1	16.6	10.6
Bone mineral for chron. age	\bar{X}	-8.0	-0.3	11.8	-7.9	-1.8	7.2
	SD	12.6	13.0	9.1	12.2	13.7	10.1
Bone mineral index	\bar{X}	-3.2	-0.3	1.7	-0.6	-1.6	1.9
	SD	7.2	7.9	5.1	5.8	8.5	6.2

+10%) skeletal ages are given in table 5. As is often the case more males than females were delayed. Height, weight, and bone mineral predicted for age tended to be distributed with skeletal age; delayed children, both male and female, had smaller body size and less than usual bone mineral while the reverse was the case for children with advanced skeletal age. This tendency was not evident at all in the bone mineral content predicted for body size or for skeletal size, and this was evidenced clearly by the distribution of the bone mineral index in the normal and deviant groups.

DISCUSSION

A. *Skeletal maturation.* There is no need to concern ourselves here with the various investigations of the optimal techniques for assessing maturation, weighting of different bone centers, selection of optimal bones or groups of bones, or com-

parisons among overall methods. Whatever the procedures used there seems to be substantial errors of about equal magnitude for both intra- and inter-observer reliability (for example: Acheson et al., '63; House, '50; Johnston and Jahina, '65; Mainland, '53, '54; Roche et al., '70). Errors as low as one month and as high as 12 months have been reported; the most typical value is about five months, or about the same as noted in the present study, though some claim routine errors to decline to three months with experience. The fairly large magnitude of these errors has suggested to several workers that a series of repeat determinations should be made by each of several observers so that the error associated with each assessment is minimized. One result of the high imprecision may be a diminution of the apparent degree of communality among bones of an area or among different areas, and an obfuscation of the

associations between maturation and growth indicators. It is important to examine the degree to which poor communality of skeletal maturation, and poor association of maturation with growth indicators, contribute to the prevailing vague notions (Falkner, '58) of the functional import of skeletal maturation.

There is only a moderate degree of communality in ossification timing ($r = 0.3$ to 0.5) and rate of maturation ($r = 0.7$ to 0.8) in bones of a limited area, and an even lower communality ($r = 0.3$) among bones of different body areas (Garn and Rohmann, '59; Garn et al., '64; Roche, '70; Roche and French, '70). Several workers have suggested the obvious possibility of selecting bones with a high degree of communality as a more practical and representative skeletal reference than such commonly used composites as hand-wrist skeletal age. It is doubtful that poor precision is responsible for the low communality although it may contribute to it; more probably the variation reflects wide differences among bones in susceptibility to environmental influences in the expression of genetic influences (Garn et al., '63), and in environment-gene interactions (Garn and Rohmann, '66). Given variation of this nature, maturation indices derived by averaging could not reflect clear environmental or genetic influences; a composite skeletal age in no way clarifies this complex interaction of forces.

There have been some indications that populations subject to nutritional deprivation, environmental stress, or diseases have a maturational delay compared to more advantaged groups, but the magnitude of the delay is variable and there is not a close association between the degree of biological stress and maturation. For example, in frank nutritional failure there is some increase in epiphyseal "anomalies" but skeletal age is delayed by only about 13 months compared to controls (Snodgrass, et al., '55; Dreizen, et al., '58). In these same studies many normal children were delayed and had anomalies, while some of the undernourished children showed no maturational delay or anomalies. Cahn and Roche ('61) found no correlation between maturation and

either calcium intake or disease history in normal Australian children. Sontag and Lipford ('43) actually found a higher incidence of disease among fast-growing children, and showed that illness did not cause delay of centers or alterations of sequence. Garn, et al. ('66) showed that Central American children with protein-calories malnutrition were no more retarded in ossification than healthy village controls though both the affected and control groups fell below U.S. White standards. The affected children had significantly less compact bone than the controls. During up to a year or more of recovery, the increment in ossification of hospitalized children was no greater than expected. The effects of illness or undernutrition or maturation therefore appear quite variable though in all cases the effects on growth are quite marked.

The poor association of growth indicators and skeletal maturation is even more evident in normal children than in those subject to stress. Various investigators have found low or non-existent associations between skeletal maturation and growth variables (Garn, et al., '61; Johnston, '64; Moss and Noback, '58; Noback, et al., '60; Olura, '56). Even the associations between maturation and growth of the same bones is rather low (Roche and Davila, '70). Moreover, the overall pattern of discordance may vary with age. For example, Frischano et al. ('70) have shown that delays in skeletal maturity in several populations are much less marked in adolescence than childhood although the greatest retardation of growth in these populations occurred in adolescence. The present study indicated that skeletal maturation was only a slightly better indicator of skeletal status than was chronological age, and in fact was, like radiographic morphometry, a poorer indicator than either bone or body size.

Now, just as there is a "rational" approach to selection of bones on the basis of communality (Garn et al., '64) so can bones be selected on the basis of their association with growth variables. Johnston ('64) pointed out that maturation is not a unitary process reflecting a single underlying physiological mechanism, and suggested that the utility of a scale of

skeletal maturation would be dependent on the ability to select the appropriate maturation indicator for the growth variable being studied. Our data suggest that a composite skeletal age was not an appropriate scale for bone mineral growth in normal children; this might be remedied by selecting a set of interrelated bones which is also highly associated with bone mineralization. It seems, however, that the purpose of a maturation index is not in this diagnostic domain. Instead we suggest that certain bones be selected for their value in predicting the future growth ("growth potential") of a particular parameter, such as bone mineral, under various defined conditions. For example, one may select a set of bones which best predicts the potential for bone mineral growth during recovery from protein-calorie malnutrition, and these bones could quite conceivably differ from those which best predict the potential elongation of a bone during either normal growth or growth during chronic caloric shortage.

There seems little value in use of even exact observations of skeletal maturation as an indicator of status since: (a) ossification timing, duration, rate and sequence are quite variable, (b) there is a low degree of communality in maturation, (c) maturation at different areas is variably affected by different environmental influences, (d) there is a complex gene-environment interaction in expression of maturation, and (e) maturation is neither highly nor uniformly associated with growth indicators. On the other hand the ability of skeletal maturation in selected areas to serve as an index of growth potential of specific parameters under specific conditions remains to be investigated.

B. Skeletal status. Skeletal maturation is associated with large uncertainties in measurement and interpretation, and there is in fact only modest conceptual or practical basis in using this as an adjunct to, or even worse as a substitute for, an indicator of growth status. The measurement of bone mineral content by photon absorptiometry is one of several convenient alternatives which provide a more direct and error-free assessment of skeletal growth than the above methods.

Most investigators (Cameron, '70) reference the bone mineral content to the bone width in order to eliminate the effects of skeletal size. In the present work we took the additional step of referencing mineral content to age, height and weight in order to provide indices independent of body size. This was necessary as bone mineral content was highly correlated with both bone width ($r = 0.85$), and height and weight ($r = 0.83$). The partial correlations of both age and skeletal age with bone mineral content dropped from $r = 0.75$ to less than $r = 0.10$ when body size was held constant. Use of skeletal size and body size references has aided in more specific evaluation of children with bone disorders (unpublished observations), and will aid in differentiating such children from those with uniform retardation of body and skeletal size.

The analysis of deviations from predicted values (section D) demonstrated that the bone mineral content, referenced to body size and skeletal size, was in fact independent of not only body size but of skeletal age. This may merely reflect the sporadic occurrence of aberrant mineralization patterns in this normal population. However, about 5% of the children had a bone mineral index two standard deviations or more (mean of 20%, or about 2.5 standard deviations) below normal; even in these children skeletal age averaged only 6% (7 months) below chronological age, and there was no association between degree of demineralization and maturational delay. These findings suggest that skeletal age relates primarily to body size and not to skeletal status. If this is the case one may ask, as did Falkner ('58), if maturation and body size are associated, and if maturation does not provide information on skeletal growth independent of body size, then why measure maturation? The answer depends on the supposed ability of skeletal maturation to predict the subsequent course of growth and development. As yet, however, the ability of skeletal maturation to provide enhanced prediction of bone mineralization and skeletal growth under specific environmental influences has not been demonstrated, and consequently the ability of maturational measures to materially enhance either individual or popu-

lational comparisons of growth status remains in doubt.

ACKNOWLEDGMENTS

Supported by AEC grant AT-(11-1)-1422 and NASA grant Y-NGR-50-002-051. During part of this time RBM was supported through an NIH postdoctoral fellowship. The staff and students of St. Bernard's School aided our studies. Substantial help was given by Mrs. J. R. Cameron, Bob Witt, Joyce Fischer, Sue Kennedy, Ellie Sosne, Barbara Binns, Bob Jones, Monica Jaehning and the staff of the Cosmic Medicine Laboratory.

LITERATURE CITED

- Acheson, R. M., G. Fowler, E. I. Fry, M. Janes, P. Urbano and J. J. Van der Werf Ten Bosch 1963 Studies in the reliability of assessing skeletal maturity from x-rays. I. Greulich-Pyle Atlas, *Hum. Biol.*, 35: 317-349.
- Cahn, A., and A. F. Roche 1961 The influence of illness and calcium intake on the rate of skeletal maturation in children. *Brit. J. Nutr.*, 14: 411-417.
- Cameron, J. R., ed 1970 Proceedings of Bone Measurement Conference. U. S. Atomic Energy Commission Conf-700515; U. S. Dept. of Commerce, Springfield, Va.
- Cameron, J. R., and J. Sorenson 1963 Measurement of bone mineral *in vivo*: an improved method. *Science*, 142: 230-232.
- Cameron, J. R., R. B. Mazess and J. A. Sorenson 1968 Precision and accuracy of bone mineral determination by direct photon absorptiometry. *Invest. Radiol.*, 3: 141-150.
- Dreizen, S., R. M. Snodgrass, H. Webb-Peploe and T. D. Spies 1958 The retarding effect of protracted undernutrition on the appearance of the postnatal ossification centers in the hand and wrist. *Hum. Biol.*, 30: 253-264.
- Falkner, F. 1958 Skeletal maturation: an appraisal of concept and method. *Am. J. Phys. Anthropol.*, 16: 381-396.
- Frisancho, A. R., S. M. Garn and W. Ascoli 1970 Childhood retardation resulting in reduction of adult body size due to lesser adolescent skeletal delay. *Am. J. Phys. Anthropol.*, 33: 325-336.
- Garn, S. M., and C. G. Rohmann 1959 Communalities of the ossification centers of the hand and wrist. *Am. J. Phys. Anthropol.*, 17: 319-323.
- 1966 Interaction of nutrition and genetics in the timing of growth and development. *Pediatric Clinics of N. A.*, 13: 353-379.
- Garn, S. M., C. G. Rohmann and A. A. Davis 1963 Genetics of hand-wrist ossification. *Am. J. Phys. Anthropol.*, 21: 33-40.
- Garn, S. M., C. G. Rohmann and M. A. Guzman 1966 Malnutrition and skeletal development in the pre-school child. In: *Pre-School Child Malnutrition*. Nat'l. Acad. Sci. — Nat'l. Research Council, Washington, D. C.
- Garn, S. M., C. G. Rohmann and M. Robinow 1961 Increments in hand-wrist ossification. *Am. J. Phys. Anthropol.*, 19: 45-53.
- Garn, S. M., F. N. Silverman and C. G. Rohmann 1964 A rational approach to the assessment of skeletal maturation. *Ann. Radiol.*, 7: 297-307.
- Greulich, W. W., and S. I. Pyle 1959 *Radiographic Atlas of Skeletal Development of Hand and Wrist*. 2nd ed. Stanford Univ. Press, Stanford, Calif.
- House, R. W. 1950 A summary of forty-nine radiologists' opinions of the skeletal age limits of apparently normal six-year old children. *Am. J. Roentgen.*, 64: 442-445.
- Johnston, F. E. 1964 The relationship of certain growth variables to chronological and skeletal age. *Hum. Biol.*, 36: 16-27.
- Johnston, F. E., and S. B. Jahina 1965 The contribution of the carpal bone to the assessment of skeletal age. *Am. J. Phys. Anthropol.*, 23: 349-354.
- Mainland, D. 1953 Evaluation of the skeletal age method of estimating children's development. I. Systematic errors in the assessment of roentgenograms. *Pediatrics*, 12: 114-129.
- 1954 Evaluation of the skeletal age method of estimating children's development. II. Variable errors in the assessment of roentgenograms. *Pediatrics*, 13: 165-173.
- Mazess, R. B. 1971 Estimation of bone and skeletal weight by direct photon absorptiometry. *Invest. Radiol.*, 6: 52-60.
- McCammon, R. W. 1970 *Human Growth and Development*. Charles C Thomas, Springfield.
- Meema, H. E. 1963 Cortical bone atrophy and osteoporosis as a manifestation of aging. *Am. J. Roentgen.*, 89: 1287-1295.
- Moss, M. L., and C. R. Noback 1958 A longitudinal study of digital epiphyseal fusion in adolescence. *Anat. Rec.*, 131: 19-32.
- Noback, C. R., M. L. Moss and E. Leszczynska 1960 Digital epiphyseal fusion of the hand in adolescence — a longitudinal study. *Am. J. Phys. Anthropol.*, 18: 13-18.
- Olura, K. 1956 A study on the standard of evaluating physical maturation degree through measurement of carpal bones radiograph and the validity of this standard. *Jap. J. Educ. Psychol.*, 4: 1-12.
- Roche, A. F. 1970 Associations between the rates of maturation of the bones of the hand-wrist. *Am. J. Phys. Anthropol.*, 33: 341-348.
- Roche, A. F., and G. H. Davila 1970 Associations between the rates of maturation and growth in the short bones of the hand. *Am. J. Phys. Anthropol.*, 33: 349-356.
- Roche, A. F., C. G. Rohmann, N. Y. French and G. H. Davila 1970 Effect of training on replicability of assessments of skeletal maturity (Greulich-Pyle). *Am. J. Roentgen.*, 108: 511-515.
- Snodgrass, R. M., S. Dreizen, C. Currie, G. S. Parker and T. D. Spies 1955 The association between anomalous ossification centers in the hand skeleton, nutritional status, and the rate of skeletal maturation in children five to four-

- teen years of age. Am. J. Roentgen., 74: 1037-1048.
- Sontag, L. W., and J. Lipford 1943 The effect of illness and other factors on the appearance pattern of skeletal epiphyses. J. Pediatrics, 23: 391-409.
- Sorenson, J. A., and J. R. Cameron 1967 A reliable *in vivo* measurement of bone mineral content. J. Bone Jt. Surg., 49A: 481-497.
- Virtama, P., and T. Helela 1969 Radiographic Measurements of Cortical Bone. Acta Orthop. Scand. Suppl., 293.

GROWTH OF BONE IN SCHOOL CHILDREN: COMPARISON OF RADIOGRAPHIC MORPHOMETRY AND PHOTON ABSORPTIOMETRY

RICHARD B. MAZESS AND JOHN R. CAMERON

*Department of Radiology (Medical Physics)
University of Wisconsin Hospital
Madison, Wisconsin 53706*

(Received 20 December 1971)

Skeletal growth was measured in 322 white children (age 6 to 14 years) using ^{125}I photon absorptiometry and compact bone measures on radiographs. Bone mineral content, measured by photon absorptiometry, increased on the average 10.5% per year or at an incremental rate of about 8.5% each year. Radiographic measures of compact bone were imprecise, and did not accurately reflect bone mineral content. The error in predicting mineral content from compact bone area was about 12%, or 50% larger than the annual increment of bone. The large imprecision (5 to 10%) and inaccuracy of radiographic morphometry limit its use in assessing skeletal status, especially in growing children.

INTRODUCTION

Several methods are available for examining skeletal growth and development (Garn and Rohmann, 1966) but objective evaluations and intercomparisons of these methods have been limited. For example, skeletal age is widely used but is conceptually vague and may be of little pragmatic value in both diagnosis and prognosis (Falkner, 1958; Johnston, 1964; Mazess and Cameron, 1971) since the relationship of ossification to growth is quite labile. Measurements of bone length are fairly reliable and easy to perform, but provide only a unidimensional description of growth which may be quite unrelated to skeletal robusticity. Two methods, radiographic morphometry and photon absorptiometry, which appear to afford more sensitive indications of skeletal status, are compared in this report.

Radiographic morphometry consists of the measurement of the dimensions of the bone image on a conventional radiograph (Barnett and Nordin, 1969; Meema, 1963; Virtama and Helela, 1969). Compact bone thickness, or a calculated area, and various ratios have been derived. Such measurements are widely used in surveys of skeletal status, rather than clinical situations, in particular to compare groups

of adults and to gauge the extent of bone loss with aging (Garn, Rohmann and Wagner, 1967; Meema and Meema, 1969; Meema, Bunker and Meema, 1965; Smith and Walker, 1964). Morphometry also has been used to evaluate growth in children (Garn, Rohmann and Nolan, 1964; Smithgall, Johnston, Malina and Galbraith, 1966; Garn and Wagner, 1969) and has been shown to be a more sensitive indicator of nutritional status in protein-calorie malnutrition than was ossification status (Garn, Rohmann and Guzman, 1966).

The photon absorptiometric method of measuring bone mineral content has been developed over the past decade (Cameron and Sorenson, 1963; Sorenson and Cameron, 1967; Cameron, 1970). A low energy (20 to 100 keV) radionuclide source is passed at uniform speed across a bone and the transmitted radiation is measured with a scintillation detector-single channel analyzer system. The mineral mass of a section of bone at the scan site is measured with an error of only 1 to 3% (Cameron, Mazess, and Sorenson, 1968; Mazess, Cameron and Sorenson, 1970). Absorptiometric scans on humans are related not only to the mineral content at the scan site but to the weight of the long bone on which the scan is made and to the total skeletal weight (Mazess, 1971; Horsman, Bulusu, Bentley and Nordin, 1970). The precision of this method on standards or with careful repositioning on humans is about 1%; the precision is about 2 to 3% in routine clinical operation and 5% in field surveys. Absorptiometry has now had widespread application in clinical observations, normative surveys and nutritional evaluations of adults and has been used as well for diagnosis, and evaluating treatment, in childhood diseases (Schuster, Reiss and Kramer, 1970).

METHODS

The direct photon absorption method was used to measure the bone mineral content of 322 white school age (6 to 14 years) children from Middleton, Wisconsin. Linear scans were made with a ^{125}I source at the distal third of the radius and across the mid-humerus on all children, and at the distal third of the ulna on 128 subjects. Bone width and the mineral-width ratio were also derived from the absorptiometric scans.

Radiographic morphometry was done with Helios calipers on standard radiographs (36 inch FFD). The thickness of the total bone and

the medullary canal diameter were measured at the absorption scan site on the radius thereby permitting direct comparisons of the two methods. Compact bone thickness was derived, and total cross-section area and the area of the compact bone were calculated assuming a circular model (Garn and Wagner, 1969). The commonly used ratios of compact to total bone thickness and area were also calculated.

Skeletal age (Greulich and Pyle, 1959) determinations were done by two observers from hand-wrist radiographs. There was a 5 month error both for repeat measurements by the same observers and for inter-observer differences. The errors of skeletal maturation measurement and its relation to bone growth were discussed in a previous paper (Mazess and Cameron, 1971).

RESULTS

Precision of Radiographic Morphometry

The remeasurement error ($n = 113$ cases) for both total and medullary thickness was about 0.12 mm; similar values were noted in a series of radiographs on adults (Mazess, Cameron, and Sorenson, 1970). This measurement error amounted to about 1% of the total width and 2 to 3% of the medullary canal width; this resulted in about a 4% error in compact bone thickness and area. In adults when repeat measurements were done on repeat films rather than the same film the magnitude of the errors increased two- or three-fold. The inter-observer errors are given in Table 1. The magnitude of the absolute errors was about the same in children as had been observed in adults (about 0.3 mm in compact bone thickness and 4mm in compact bone area); the adults, due to their larger bones, showed a slightly smaller relative error for some variables. Still there was about a 5% error for both compact bone thickness and area in both children and adults. This analysis indicated that the relatively high precision of caliper measurement was deceptive since there were substantial difficulties both by the same observer and by different observers in locating the margins of the medullary canal. This lead to subsequent errors in derivative measurements such as compact bone thickness and area; these errors might be even greater with refilming. Even though the overall error of individual radiographic measurements may be high, the precision in the present series was lowered by using the average of values from two observers.

TABLE 1
BETWEEN OBSERVER ERRORS OF RADIOGRAPHIC MORPHOMETRY ON THE
RADIUS SHAFT IN SCHOOL CHILDREN ($N = 308$) AND IN
ADULTS ($N = 240$; MAZESS ET AL., 1970.)

	Errors		Percent Errors	
	Children	Adults	Children	Adults
<i>Thickness (MM)</i>				
Total	0.19	0.11	1.80	0.83
Medullary	0.27	0.25	5.58	2.93
Compact	0.32	0.26	5.44	5.03
<i>Area (MM²)</i>				
Total	3.25	2.60	3.52	1.65
Compact	3.72	4.45	5.16	4.82
<i>Compact/Total (%)</i>				
Thickness	2.59	1.72	4.72	4.57
Area	2.32	2.24	2.93	3.74

Relationship of Radiographic Morphometry and Bone Mineral

Measurements on the radiograph were made at the same spot where photon absorptiometric scans were done, thereby enabling direct evaluation of radiographic morphometry. The radiographic width of the bone was associated with the scan width ($r = 0.88$) but it systematically overestimated the actual width by about 2% in both males and females. The mean width from the radiograph was 10.74 mm while that from the scan was 10.51 mm. The difference of 0.2 mm probably represents the magnification due to parallex.

Compact bone thickness was not highly correlated with bone mineral content ($r = 0.73$; SEE = 94 mg or 16%). Total bone cross-sectional area was more highly correlated ($r = 0.78$) but the error was still too high for useful prediction (SEE = 85 mg or 14%). The best predictor of mineral content was calculated area of the compact bone; the correlation was 0.84 but the predictive error was still fairly large (SEE = 75 mg or 12%).

The regressions of thickness and of area on bone mineral content are shown in Figure 1. There was only a small sex difference over the age range of school children so that a single regression could be used without introducing substantial errors. Such a validation appears necessary wherever radiographic morphometry is used, but this would still limit the validity to grouped data rather than individual cases.

Morphological features, such as height and weight, appeared in fact to be better predictors of bone mineral content than was radiographic

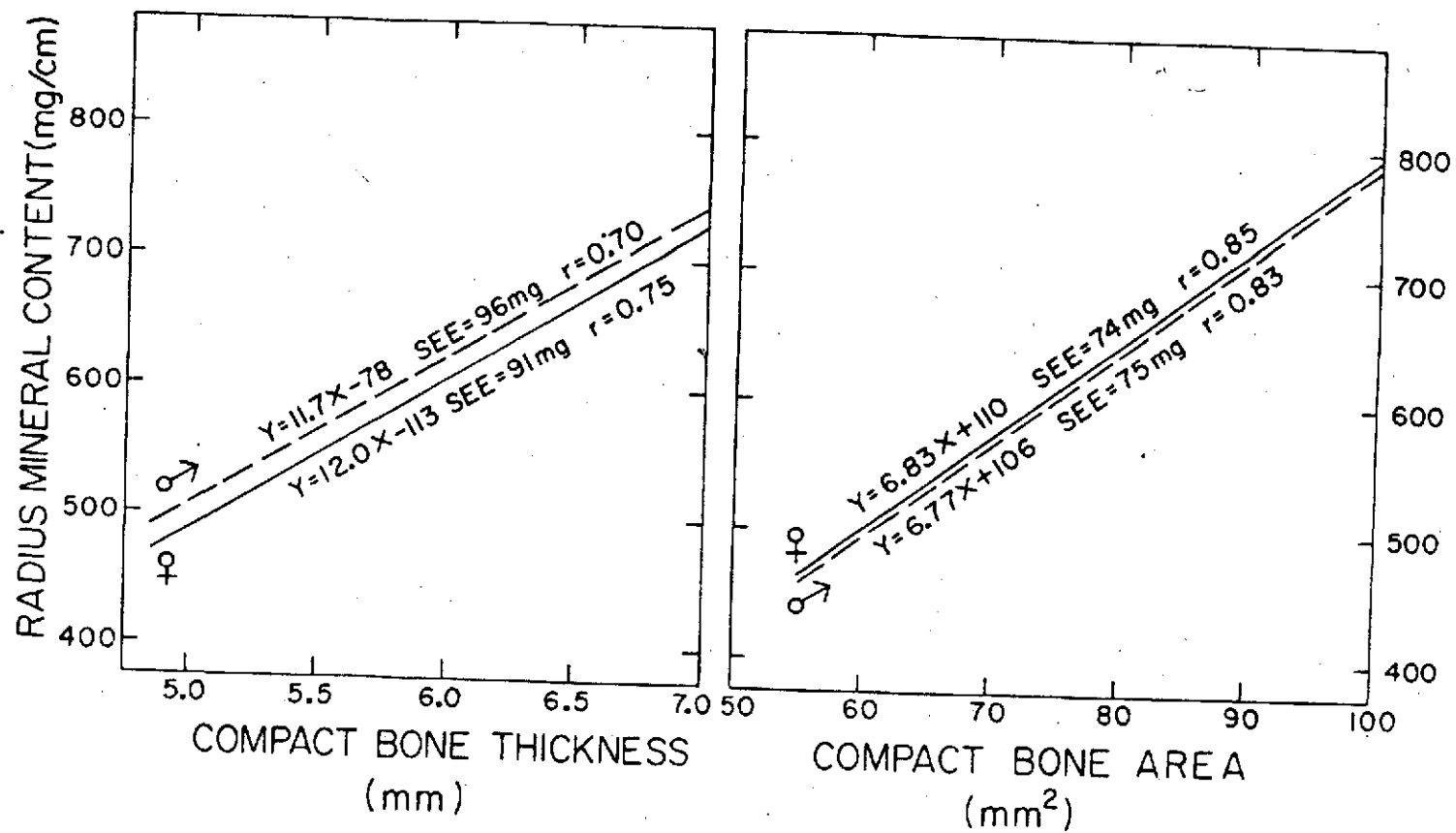


FIGURE 1
Compact bone thickness and area versus bone mineral content of the radius in school children.

morphometry; the predictive errors of the latter variables were only about 12 to 13%, or about the same as the predictive error of compact bone area.

Age Change in Morphology and the Skeleton

Age and sex specific values for the morphological variables are given in Table 2; corresponding values for bone mineral measurements and for radiographic morphometry are given in Tables 3 and 4. The children in the present study were morphologically similar to other American white children (McCammon, 1970) and the skeletal ages were generally within the normal range of variation (± 1 year) at a given chronological age. Bone mineral content of the radius, humerus, and ulna showed a fairly linear increase with age (Table 3 and Figure 2). The average yearly change was about 10.5% or an annual incremental change of 8.5%. There was an average annual increase of 4.5%, or an annual incremental rate of 4%, in both bone width and mineral-width ratio. The rate of increase in bone mineral content and the mineral-width ratio was slightly greater in females than in males, apparently reflecting the earlier adolescent growth spurt of the females. Radiographic morphometry (Table 4) exhibited a somewhat similar pattern of increase. The average annual increase in total and compact bone thickness was 3.8% while the increase in medullary canal diameter was 2.6%. There was some suggestion that the medullary canal did not increase in size during early adolescence, and in fact may decrease. However, the effect seemed less marked on the radius than the large endosteal deposition reported for the metacarpal (Johnston and Smithgall-Watts, 1969). The increases in total and compact bone cross-sectional area were larger (averaging 8% annually) than the increases of thickness, and were more nearly comparable to the bone mineral increases. The ratios of compact to total bone thickness or area showed little age change.

The age-sex specific coefficients of variation averaged 13.8% for bone mineral content, 10.2% for bone width, and 9.5% for the mineral-width ratio. For total and compact bone thicknesses the variation was about 11%, while for medullary canal thickness and total and compact bone area it was almost 20%. The ratio of compact to total bone thickness showed a variation of about 11.8% while the area ratio was much less variable—7.3%.

DISCUSSION

Radiographic morphometry has been widely used in assessing skeletal status but the present data suggest that its utility in measurement of children is even less than demonstrated in adults (Mazess et al, 1970). The errors for repeat measurement of a fixed diameter are rather small, but definition of the medullary canal width is extremely difficult. This leads to large (4 to 6%) errors for both intra- and inter-observer comparisons. The errors would be even larger with refilming and repositioning. Errors of 5 to 10% have been reported by various workers (Adams, Davies and Sweetnam, 1969; Anderson, Shimmins and Smith, 1966; Garn, Feutz, Colbert and Wagner, 1966; Morgan, Spiers, Pulvertaft, and Fourman, 1967; Mazess, Cameron, and Sorenson, 1970; Saville, 1967).

Such errors of precision in fact limit the accuracy of determinations, but even with repeat measurements by two observers the accuracy (15% error) in predicting mineral content is not high (Mazess et al, 1970). Such large errors virtually preclude use of radiographic morphometry for individual assessment and in particular for assessment of increments where the error may be several times the magnitude of the actual increment. In school age children with an annual increment of only 8 to 10% in bone mineral these errors are substantial and would effectively prohibit evaluation of changes occurring over periods less than two or three years in duration.

There has been little direct validation of radiographic morphometry, and the existent studies suggest that the method is not an accurate indicator of physical bone parameters. The original studies of Virtama and Mahonen (1960) for example show a correlation of only 0.71 between compact bone thickness and mineral content of finger bones. Virtama and Talkka (1962) predicted the density of the humerus and femur from a compact bone ratio, but though the relationship was significant the predictive errors appeared large. Kivilaakso and Palolampi (1965) also showed relatively large errors in predicting density of ulnae. The results of Garn et al (1966) showed a correlation of only 0.6 between morphometry and the mineral mass obtained by radiographic photodensitometry, but the large errors of the latter method may have contributed to the low correlation. Van Gerven, Armalagos and Bartley (1969) demonstrated that radiographic mea-

TABLE 2
MEANS AND COEFFICIENTS OF VARIATION FOR AGE AND MORPHOLOGY IN SCHOOL CHILDREN

Age	Number		Age (months)		Skeletal Age (months)		Height (cm)		Weight (kg)		Arm Circum. (cm)		Skinfold Triceps (mm)	
	F	M	F	M	F	M	F	M	F	M	F	M	F	M
Means														
6	11	16	80	79	79	67	122.8	120.8	22.1	22.2	172	170	11.1	9.2
7	19	26	91	90	93	80	128.4	127.3	24.3	25.0	178	181	10.1	10.0
8	15	25	103	101	103	98	132.3	134.7	26.6	27.6	193	190	11.1	8.3
9	22	25	115	113	111	110	137.6	139.8	30.2	32.0	193	195	12.4	9.4
10	29	28	125	126	120	124	141.8	144.6	33.2	35.3	200	204	12.7	9.8
11	20	23	137	137	135	133	149.5	148.6	40.5	37.6	216	214	13.8	11.0
12	13	19	153	148	152	142	156.8	153.9	42.9	45.7	210	228	11.8	12.6
13	15	11	161	161	158	154	158.9	157.6	45.4	49.7	216	235	7.3	8.6
14	4	5	172	170	170	163	164.9	163.1	59.7	54.2	249	237	9.7	7.0
Coefficients of Variation														
6			3	4	12	28	5	4	19	12	8	8	24	33
7			3	4	13	18	5	4	16	15	8	10	29	45
8			3	4	13	18	4	6	14	24	9	13	29	38
9			3	3	9	16	6	4	21	22	11	12	37	32
10			3	3	9	12	5	4	19	23	12	13	35	42
11			2	2	8	9	4	3	23	14	17	21	36	48
12			2	2	9	8	5	6	17	22	8	13	32	52
13			2	2	9	9	4	6	17	27	10	16	31	61
14			2	1	5	8	4	4	24	20	16	10	85	23

GROWTH OF BONE IN SCHOOL CHILDREN

TABLE 3
MEANS AND COEFFICIENTS OF VARIATION FOR BONE MINERAL MEASUREMENTS OF SCHOOL CHILDREN, MINERAL (MG), WIDTH (MM) AND MINERAL-WIDTH RATIO (MG/MM)

Age	Radius						Humerus						Ulna					
	Mineral		Width		M/W		Mineral		Width		M/W		Mineral		Width		M/W	
	F	M	F	M	F	M	F	M	F	M	F	M	F	M	F	M	F	M
Means																		
6	436	466	9.1	9.5	47.5	48.6	943	1018	13.7	14.4	69.2	70.9	354	343	7.6	8.1	46.6	42.1
7	457	510	9.1	10.0	49.9	50.9	1001	1109	14.3	14.7	69.8	75.7	374	411	8.2	8.6	45.9	48.2
8	490	557	9.4	10.2	52.2	54.3	1106	1249	14.9	15.6	74.2	80.2	413	480	8.8	9.1	47.2	52.7
9	542	584	9.7	10.5	55.6	55.4	1216	1276	15.7	15.9	77.3	79.9	481	475	8.4	8.2	52.5	51.8
10	565	633	9.9	11.1	56.6	57.3	1226	1442	15.8	16.8	77.4	85.7	473	554	8.6	9.5	53.6	58.6
11	645	691	10.8	11.3	59.6	61.0	1354	1478	16.5	17.2	81.7	85.9	540	567	9.6	9.8	55.0	58.0
12	716	763	11.3	12.0	63.1	62.9	1533	1662	17.3	19.0	88.1	87.1	595	595	10.4	10.4	57.0	57.0
13	742	781	11.5	12.6	64.0	61.6	1627	1624	18.2	18.0	89.4	90.6
14	878	792	12.1	11.9	71.9	66.0	1875	1855	19.1	19.8	98.1	93.2
Coefficients of Variation																		
6	18	11	12	9	10	8	11	12	13	12	10	8	16	10	7	7	15	8
7	12	14	10	8	8	8	11	15	8	14	7	7	14	12	9	13	12	9
8	12	15	9	10	9	9	14	12	9	11	8	7	17	12	9	11	17	11
9	13	12	10	10	6	7	11	13	9	8	7	9	9	15	13	10	9	12
10	17	13	11	10	9	13	12	14	9	10	8	9	16	14	12	7	9	13
11	18	16	11	12	12	8	18	10	11	8	12	8	26	10	12	11	16	9
12	12	16	10	11	8	9	16	13	12	9	9	8	...	10	7	8
13	13	17	10	12	8	8	12	14	9	11	9	13
14	14	18	14	12	2	10	6	19	6	12	5	12

TABLE 4
MEANS AND COEFFICIENTS OF VARIATION FOR RADIOGRAPHIC MORPHOMETRY OF THE RADIUS SHAFT IN SCHOOL CHILDREN

Age	Thickness (mm)						Area (mm ²)				Compact/Total (%)			
	Total		Medullary		Compact		Total		Compact		Thickness		Area	
	F	M	F	M	F	M	F	M	F	M	F	M	F	M
Means														
6	9.4	10.0	4.4	4.6	5.0	5.4	70	79	54	62	54	54	78	79
7	9.7	10.3	4.4	4.8	5.2	5.5	75	84	58	65	54	54	79	78
8	9.6	10.6	4.2	4.9	5.4	5.7	73	89	59	69	56	54	81	78
9	9.9	10.8	4.4	5.2	5.5	5.6	78	93	62	71	56	52	80	77
10	10.3	11.2	4.6	5.0	5.7	6.2	84	101	67	80	56	55	80	80
11	11.2	11.4	4.8	5.2	6.3	6.2	99	103	80	81	56	55	81	79
12	11.5	12.0	5.2	5.7	6.3	6.3	105	113	82	87	55	53	79	77
13	11.6	12.2	4.9	5.5	6.7	6.6	107	117	87	92	58	55	82	79
14	11.7	12.3	4.8	5.5	7.0	6.8	109	120	91	95	60	56	84	80
Coefficients of Variation														
6	12	10	24	20	15	13	25	20	23	20	15	12	10	7
7	12	8	20	17	10	10	23	15	20	14	9	10	6	7
8	8	10	18	20	12	13	16	20	16	19	11	12	7	8
9	12	9	28	16	9	11	23	18	17	17	14	10	9	6
10	12	11	21	20	12	13	24	22	22	21	11	11	7	7
11	10	9	19	21	15	10	20	19	22	16	12	12	7	7
12	9	9	28	16	11	11	18	17	11	17	17	10	11	6
13	10	9	22	21	12	14	19	18	18	18	12	14	7	9
14	11	13	18	23	7	14	22	26	19	25	6	13	3	8

GROWTH OF BONE IN SCHOOL CHILDREN

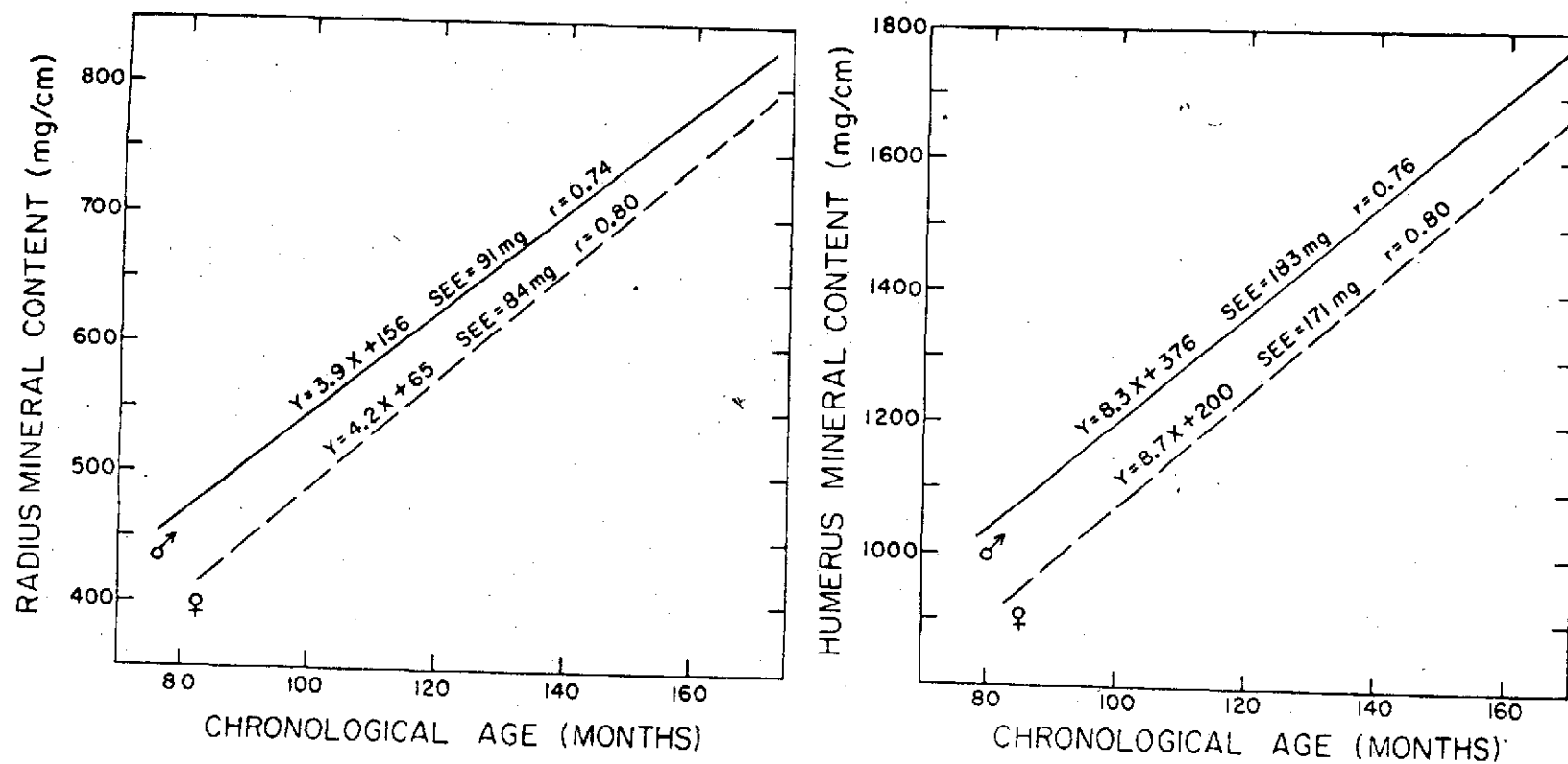


FIGURE 2
Age changes in the bone mineral content of the radius and the humerus in school children.

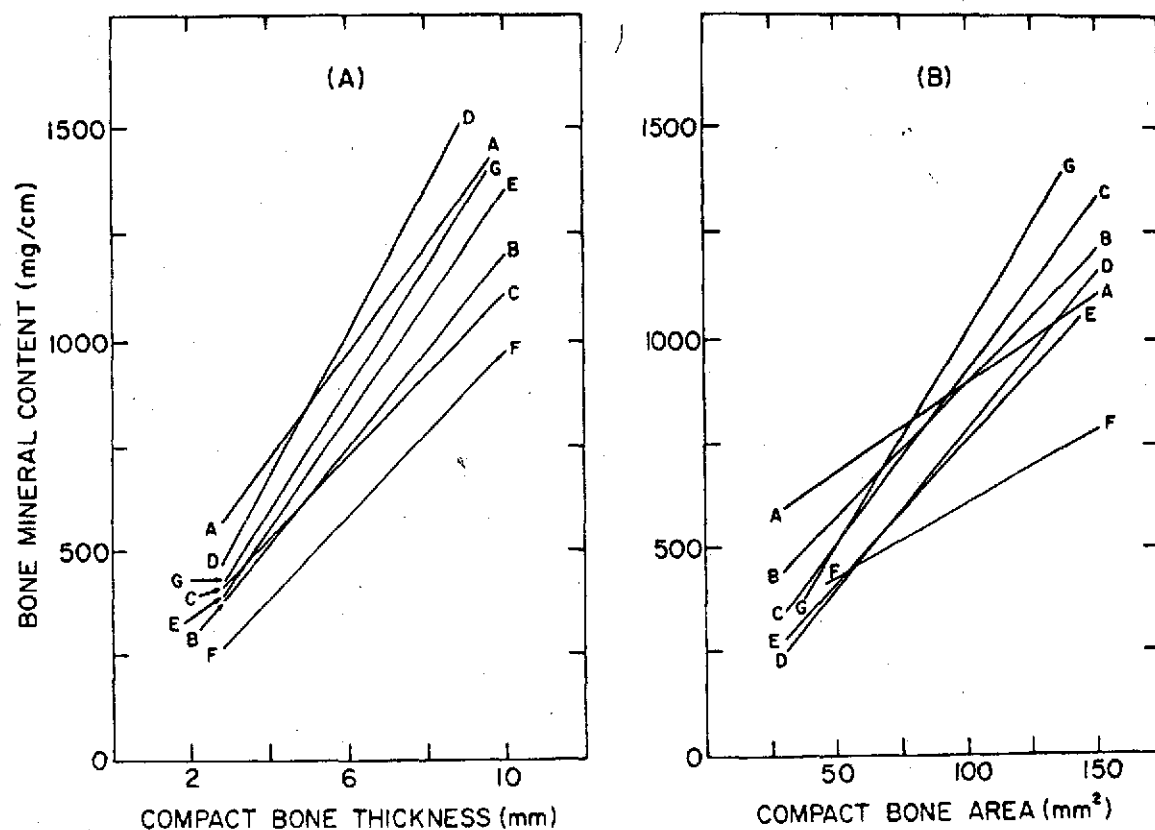


FIGURE 3

Compact bone thickness and area versus bone mineral content on the radius and ulna in adults (data from Mazess et al 1970). Regressions at the different sites differ leading to systematic errors when using radiographic morphometry.

surements of compact bone were poorly correlated with actual caliper measurements of the excised bones, and that large errors resulted from the fact that the compact bone thickness in a given plane was not representative of the thicknesses at other locations. The cross-sectional shape of the bone varies with age and sex prohibiting any facile generalizations about a "tubular" bone model.

Such variations in anatomical shape may be responsible for the relatively poor precision and accuracy of morphometry, and make it mandatory to have regression adjustment of morphometric results to render intelligible interpretations in terms of actual skeletal changes. For example, between the ages of 85 and 165 months males and females increased mineral content by 64% and 80% respectively; compact bone thickness increased by only 22% and 33%, while compact bone area increased by only 46% and 64%. Direct use of compact bone measurements underestimated the magnitude of the age changes, and also exaggerated the extent of male-female differences during this period. A further complication arises since in adults one finds differences between bones, and even among locations on the same bone, with regard to the magnitude of the errors (Mazess et al, 1970), and to regression relationship with mineral content (see Figure 3); in growing children these factors could lead to even greater variability and uncertainties. Consequently, radiographic morphometry can be used only when steps are taken to minimize errors of precision and when validation of the measurement in terms of mineral content has been accomplished. The resultant measurements would be of use in population studies though not for individual assessments, except where the magnitude of individual differences are very large (for example, protein-calorie malnutrition or several years of growth). The mere measurement of a large number of subjects does not insure the validity of results. For example Garn and Wagner (1969) have estimated total skeletal mass, and dietary mineral requirements, based on radiographic morphometry of the second metacarpal in thousands of subjects. The representativeness of this site and this bone, the accuracy of the local measurement, and the validity of the extrapolation to the total skeleton have not been demonstrated. Such majestic speculation, though perhaps correct, must be viewed with candor: like the fabled emperor more substantial clothing, in the form of validation, is required prior to public acceptance.

It appears that radiographic morphometry has a large imprecision and substantial inaccuracy which limit its use in assessment of skeletal status. Certainly in the normal children of this study it would be preferable to use height or weight as a predictor of mineral content, since in fact these morphological variables were more highly correlated than were radiographic measurements. The validity and usefulness of radiographic morphometry seems questionable, and utilization of such a technique without further scientific justification may merely add unwarranted radiation to growing children.

ACKNOWLEDGMENTS

Supported by AEC grant AT-(11-1)-1422 and NASA grant Y-NGR-50-002-051. During part of this time RBM was supported through an NIH postdoctoral fellowship. The staff and students of St. Bernards school aided our studies. Substantial help was given by Mrs. J. R. Cameron, Bob Witt, Joyce Fischer, Sue Kennedy, Mrs. F. Lantz, Ellie Sosne, Barbara Binns, Bob Jones, Monica Jaehnig and the staff of the Cosmic Medicine Laboratory.

REFERENCES

- ADAMS, P., DAVIES, G. T., & SWEETNAM, P. M. 1969. Observer error and of the metacarpal. *Brit. J. Radiol.* 42, 192-197.
- ANDERSON, J. B., SHIMMINS, J., & SMITH, D. A. 1966. A new technique for measurement of metacarpal density. *Brit. J. Radiol.* 39, 443-450.
- BARNETT, E., & NORDIN, B. E. C. 1960. The radiological diagnosis of osteoporosis: a new approach. *Clin. Radiol.* 11, 166-174.
- CAMERON, J. R. (ed). 1970. *Proceedings of Bone Measurement Conference*. U.S. Atomic Energy Commission Conf-700515; U.S. Dept. of Commerce, Springfield, Va.
- CAMERON, J. R., & SORENSON, J. 1963. Measurement of bone mineral *in vivo*: an improved method. *Science* 142, 230-232.
- CAMERON, J. R., MAZESS, R. B., & SORENSON, J. A. 1968. Precision and accuracy of bone mineral determination by direct photon absorptiometry. *Invest. Radiol.* 3, 141-150.
- FALKNER, F., 1958. Skeletal maturation: an appraisal of concept and method. *Am. J. Phys. Anthropol.* 16, 381-396.
- GARN, S., & ROHMANN, C. G. 1966. Interaction of nutrition and genetics in the timing of growth and development. *Pediatric Clinics of N. A.* 13, 355-379.
- GARN, S. M., & WAGNER, B. 1969. The adolescent growth of the skeletal mass and its implications to mineral requirements. In: F. Heald (ed)—*Adolescent Nutrition and Growth*. Appleton-Century-Crofts, N.Y. pp. 139-161.
- GARN, S. M., FEUTZ, E., COLBERT, C., & WAGNER, B. 1966. Comparison of cortical thickness and radiographic microdensitometry in the measurement of bone loss. In: G. D. Whedon, W. F. Neumann, and D. W. Jenkins (eds)—*Progress in Development of Methods in Bone Densitometry*, NASA-SP-64. Washington, D.C. (pp. 65-77).

- GARN, S. M., ROHMANN, C. G., & GAUZMAN, M. A. 1966. Malnutrition and skeletal development in the pre-school child. In: *Pre-School Child Malnutrition*. Nat'l Acad. Sci.—Nat'l Research Council, Washington, D.C.
- GARN, S. M., ROHMANN, C. G., & NOLAN, P. JR. 1964. The developmental nature of bone changes during aging. In: *Relations of Development and Aging*. J. E. Birren (ed). C. C. Thomas, Springfield.
- GARN, S. M., ROHMANN, C. G., & WAGNER, B. 1967. Bone loss as a general phenomenon in man. *Fed. Proc.* **26**, 1729-1736.
- GREULICH, W. W., & PYLE, S. I. 1959. *Radiographic Atlas of Skeletal Development of Hand and Wrist*. (2nd ed) Stanford Univ. Press, Stanford, California.
- HORSMAN, A., BULUSU, L., BENTLEY, H. B., & NORDIN, B. E. C. 1970. Internal relationships between skeletal parameters in twenty-three male skeletons. In: J. R. Cameron (ed) *Proceedings of the Bone Measurement Conference*. U.S. Atomic Energy Commission Conference—700515; U.S. Dept. of Commerce, Springfield, Va. pp. 365-382.
- JOHNSTON, F. E. 1964. The relationship of certain growth variables to chronological and skeletal age. *Human Biol.* **36**, 16-27.
- JOHNSTON, F. E., & SMITHGALL-WATTS, E. 1969. Endosteal desposition of bone at the midshaft of the second metacarpals of adolescent females. *Anatom. Rec.* **163**, 67-70.
- KIVILAASKO, F., & POLAMPI, E. 1965. On the density of the ulna and on the relationship between density and cortical thickness. *Acta Anat.* **60**, 325-329.
- MAZESS, R. B. 1971. Estimation of bone and skeletal weight by direct photon absorptiometry. *Invest. Radiol.* **6**, 52-60.
- MAZESS, R. B., & CAMERON, J. R. 1971. Skeletal growth in school children: maturation and bone mass. *Am. J. Phys. Anthropol.* **35**, 399-407.
- MAZESS, R. B., CAMERON, J. R., & SORENSON, J. A. 1970. A comparison of radiological methods for determining bone mineral content. In: G. D. Whedon and J. R. Cameron (eds)—*Progress in Methods of Bone Mineral Measurement* (pp. 455-479), U.S. Dept. Health, Educ., and Welfare, Supt. of Documents, Washington, D.C.
- MCCAMMON, R. W. 1970. *Human Growth and Development*. C. C. Thomas, Springfield.
- MEEMA, H. E. 1963. Cortical bone atrophy and osteoporosis as a manifestation of aging. *Am. J. Roentgen.* **89**, 1287-1295.
- MEEMA, H. E., & MEEMA, S. 1969. Cortical bone mineral density versus cortical thickness in the diagnosis of osteoporosis: a roentgenologic-densitometric study. *J. Am. Ger. Soc.* **17**, 120-141.
- MEEMA, H. E., BUNKER, M. L., & MEEMA, S. 1965. Loss of compact bone due to menopause. *Obstet. Gynecol.* **26**, 333-343.
- MORGAN, D. B., SPIERS, F. W., PULVERTAFT, C. N., & FOURMAN, P. 1967. The amount of bone in the metacarpal and the phalanx according to age and sex. *Clin. Radiol.* **18**, 101-108.
- SAVILLE, P. D. 1967. A quantitative approach to simple radiographic diagnosis of osteoporosis; its application to the osteoporosis of rheumatoid arthritis. *Arthr. Rheumat.* **10**, 416-422.
- SCHUSTER, W., REISS, H., & KRAMER, K. 1970. The objective assessment of disorders of bone mineralization in congenital and acquired skeletal diseases in childhood. *Ann. Radiol.* **8**, 255-265.
- SMITH, R. W. JR., & WALKER, R. R. 1964. Femoral expansion in aging women: implications for osteoporosis and fractures. *Science* **145**, 156-157.
- SMITHGALL, E. B., JOHNSTON, F. E., MALINA, R. M., & GALBRAITH, M. A. 1966. Developmental changes in compact bone relationships in the second metacarpal. *Human Biology* **38**, 141-151.

- SOERENSON, J. A., & CAMERON, J. R. 1967. A reliable *in vivo* measurement of bone mineral content. *J. Bone Jt. Surg.* **49A**, 481-497.
- VAN GERVEN, D. P., ARMELAGOS, G. J., & BARTLEY, M. H. 1969. Roentgenographic and direct measurement of femoral cortical involution in a prehistoric Mississippian population. *Am. J. Phys. Anthropol.* **31**, 23-38.
- VIRTAMA, P., & HELELA, T. 1969. *Radiographic Measurements of Cortical Bone*. *Acta Orthop. Scand. Suppl.* 293.
- VIRTAMA, P., & MAHONEN, H. 1960. Thickness of the cortical layer as an estimate of the mineral content of finger bones. *Brit. J. Radiol.* **33**, 60-62.
- VIRTAMA, P., & TELKKA, A. 1962. Cortical thickness as an estimate of mineral content of human humerus and femur. *Brit. J. Radiol.* **35**, 632-633.

DIRECT READOUT OF BONE MINERAL CONTENT USING
RADIONUCLIDE ABSORPTIOMETRY *

Richard B. Mazess, John R. Cameron and Harry Miller
Intern. J. Applied Radiation & Isotopes (in press)

ABSTRACT

A device has been constructed and tested which provides immediate readout of bone mineral content and bone width from absorptiometric scans with low-energy radionuclides (such as ^{125}I). The basis of this analog system is a logarithmic converter-integrator coupled with a precision linear ratemeter. The system provided accurate and reliable results on standards and ashed bone sections. The standard deviation for measurements on standards over a year was about 1%; the standard deviation for the residuals about the regression line predicting the ash weight of bone sections was about 1.5%, but part of this appeared due to variability in the bone sections rather than due to limitations of the instrumentation. Clinical measurements were made on about 100 patients with the direct readout system, and these were highly correlated with the results from digital scan data on the same patients. The direct readout system has been used successfully in field studies and surveys as well as for clinical observations. Such an analog system has several advantages over previously-used digital handling of scan data, including lower operational and equipment costs, greater mobility, and immediate availability of results.

* Reprint of the article available upon request

WEIGHT AND DENSITY OF SADLERMIUT ESKIMO LONG BONES

Richard B. Mazess and Robert Jones
Human Biology (in press) *

The weights of six long bones and the densities (water displacement) of three of these were measured in the Sadlermiut Eskimo skeletal series (67 adults). Weights and densities of these appendicular bones were intercorrelated. Older adults of both sexes had about 10% to 15% lower bone weights and densities than younger adults. As in previous work on bone sections, the Sadlermiut had bone densities comparable to those of elderly Negroes and higher than those of elderly Whites, but if correction is made for age and for methodological differences the Sadlermiut were more nearly comparable to Whites and lower in density than Negroes. Sex differences in Sadlermiut bone weights and densities were smaller than in Whites or Negroes.

Supported through NASA-Y-NGR-50-002-051 and AEC-(11-1)-1422. The Sadlermiut skeletons were collected by W.S. Laughlin, C.F. Merbs and R. Chown on grants from NIH and the Rockefeller Foundation in 1959, and W. Taylor, Canadian National Museum, kindly provided the bones for analysis. Age and sex determinations were done by W.S. Laughlin, R. Meier, C.F. Merbs and W. Wilson; Jeanne Mazess and Sari Prowler kindly helped measure the bones.

* Reprints of this article available upon request

TECHNICAL INFORMATION ON A RECTILINEAR SCANNER
FOR DETERMINATION OF BONE MINERAL CONTENT

by

John M. Sandrik
Department of Radiology
University of Wisconsin Medical Center
Madison, Wisconsin

In a previous report (1) the operation of a recently constructed rectilinear scanner for use in the photon absorptiometric determination of bone mineral content was discussed. With this scanner an area of 15 cm x 15 cm can be scanned in a raster pattern with a scanning speed of 2 mm/sec in the "y-direction". Stepping increments in the "x-direction" can be 0.71, 1.38, 2.71, 5.38 or 10.73 mm in length at a speed of 0.62 mm/sec. The stepping motor can also be operated continuously at either 0.62 or 1.25 mm/sec for bringing the scanner to the desired scanning site. A photo of the completed scanner is shown in Figure 1.

This report includes the mechanical drawings and electronic schematics which were used to construct the scanner and the electronic control system. A set of these drawings has also been sent to the Division of Technical Information of the U.S. Atomic Energy Commission. Also included in this report are some technical notes describing those drawings and explaining the details of construction and some suggestions for improvement of the original system.

Construction Drawings

Figures 2 and 3 are isometric projections of completed sections of the scanner. The support roller for the scanning assembly referred to in Figure 3 was added to counteract the torque loading of the ball-bushings due to the detector assembly. This torque produced an unsteady scanning motion, which was markedly improved by the addition of the support roller. In what follows that part of the scanner shown in Figure 3 will be termed the linear scanning system (LSS).

The scanner base plate is shown in Figure 4. The dowel pins referred to were found to be unnecessary and were not used. Also shown in Figure 4 is the lead screw for moving the LSS during the stepping operation. The ends of the screw on each side of the threaded section were machined to mate with the ball-bearings used to support the screw in the scanner end plates.

The LSS is supported by the lead screw and the guide rod, which are fastened to the scanner end plates (Figure 5). Similarly the source and detector system moves along guide rods supported by the scanning platform end plates (Figure 6). Since this pair of guide rods must be parallel as well as the lead screw and guide rod supporting the LSS, both pairs of end plates must be machined as a set. The dowel pins referred to in these drawings were also found to be unnecessary.

The carriers to which the LSS are attached are shown in Figures 7 and 8. The carrier in Figure 7 has been designed to house a 1/2-inch I.D. ball-bushing, while that in Figure 8 houses the lead nuts (also shown in Figure 8), which are threaded onto the lead screw and pressed into the carrier. A similar set of carriers for the source and detector system are drawn in Figure 9. These house 3/8-inch I.D. ball-bushings.

The platform which attaches the LSS to the stepping mechanism is shown in Figure 10. The scan motor, drive belt pulleys, and idler are also mounted on this plate.

Electrical Schematics

Figure 11 is the schematic of the power supply for the scanner. Since this is a hybrid control system consisting of relays, discrete electronics, and integrated circuits, many voltage levels were required.

Automatic control of the scanning and stepping operations during a measurement is achieved with the electronics diagrammed in Figures 12, 13, 14 and 15. The circled numbers, e.g. (5) refer to the pin number on the plug which connects the control system to the scanner. Relays GR1 and GR2 are DPDT general relays with 5000 ohm coil resistance and 2.8 mADC activating current. Relays LR1, LR2, LR3 and LR4 are 6PDT latch relays with latch coil resistance of 200 ohms and reset coil resistance of 275 ohms. The operating voltage of these relays is 26.5 VDC.

The truth table for the J-K flip-flops (Figure 12) is as follows (2):

t_n		t_{n+1}	
S	C	Q	\bar{Q}
1	1	Q_n	\bar{Q}_n
1	0	1	0
0	1	0	1
0	0	\bar{Q}_n	Q_n

where t_n is the time period prior to the negative transition of the clock pulse at T (terminal 2) and Q_n is the state of the Q output (terminal 10) in the period t_n . In this application the flip-flops are operated with the S and C inputs grounded such that the Q output alternates between 1 and 0 after each negative transition of the clock pulse.

The following is the sequence of operations that occurs assuming that the scanner is just completing a scan in the forward direction.

1. The scanner activates the Front Scan Limit Switches (FSLS) #1 and #2 (Figure 13).
 - a. FSLS #1 energizes the latch coil of LR1 reversing the direction of the scan motor (Figure 14).
 - b. FSLS #2 energizes GR1 which then energizes the latch coil of LR2.

2. Contacts on LR2

- a. Remove the 110 VAC from the scanning motor and apply DC for dynamic braking (Figure 14).
 - b. Remove the DC braking from the stepping motor and apply 110 VAC (Figure 15).
 - c. Remove the 3 VDC from the C_D input of the flip-flops enabling them to begin timing, clocked by the Schmitt Trigger connected to the T input of the first flip-flop (Figure 12).
3. When the Q output of the flip-flop selected by the "Step-Length" switch changes from the 0 to the 1 state, GR2 is energized (Figure 12).
4. GR2 energizes the reset coil of LR2, thus reversing all of the conditions established in step 2, resetting the Q outputs of the flip-flops to the 0 state, and beginning the next linear scan in the reverse direction.

When the scanner contacts the Rear Scan Limit Switches all of the above operations are the same except that stated in 1a. In this case it is the reset coil of LR1 which is activated.

Suggested Improvements

In the process of making this system operable it has become apparent that the major improvement which could be made in the existing control system is the replacement of the relays with solid state switching devices. The transients produced in the coils and contacts of the relays interfered with the I.C. timing circuit. Reliable operation has been obtained by connecting capacitors across most of these coils and contacts to quiet their operation. In the course of evolution of this control system GR1 and GR2 have become "vestigial organs" in that they merely activate other relays. These can (and will) be eliminated, improving the noise problem somewhat.

The versatility of the entire system could be significantly enhanced by replacing the hysteresis synchronous motors used for both scanning and stepping with step motors. These motors, with their control systems, would increase the flexibility of the system by allowing a greater range of scanning speeds and stepping increments.

REFERENCES

1. Sandrik, J.M., Mazess, R.B., Vought, C.E. and Cameron, J.R.; Rectilinear Scanner for Determination of Bone Mineral Content, U.S. Atomic Energy Commission Report COO-1422-96 (June, 1971).
2. Motorola Semiconductors Products, Inc.; The Integrated Circuit Data Book (August, 1968).

ACKNOWLEDGEMENTS

I wish to thank Orlando Canto who prepared the mechanical drawings and electrical schematics.

This work is supported in part by the U.S. Atomic Energy Commission through contract AT-(11-1)-1422.

REPRODUCIBILITY OF THE
ORIGINAL PAGE IS POOR

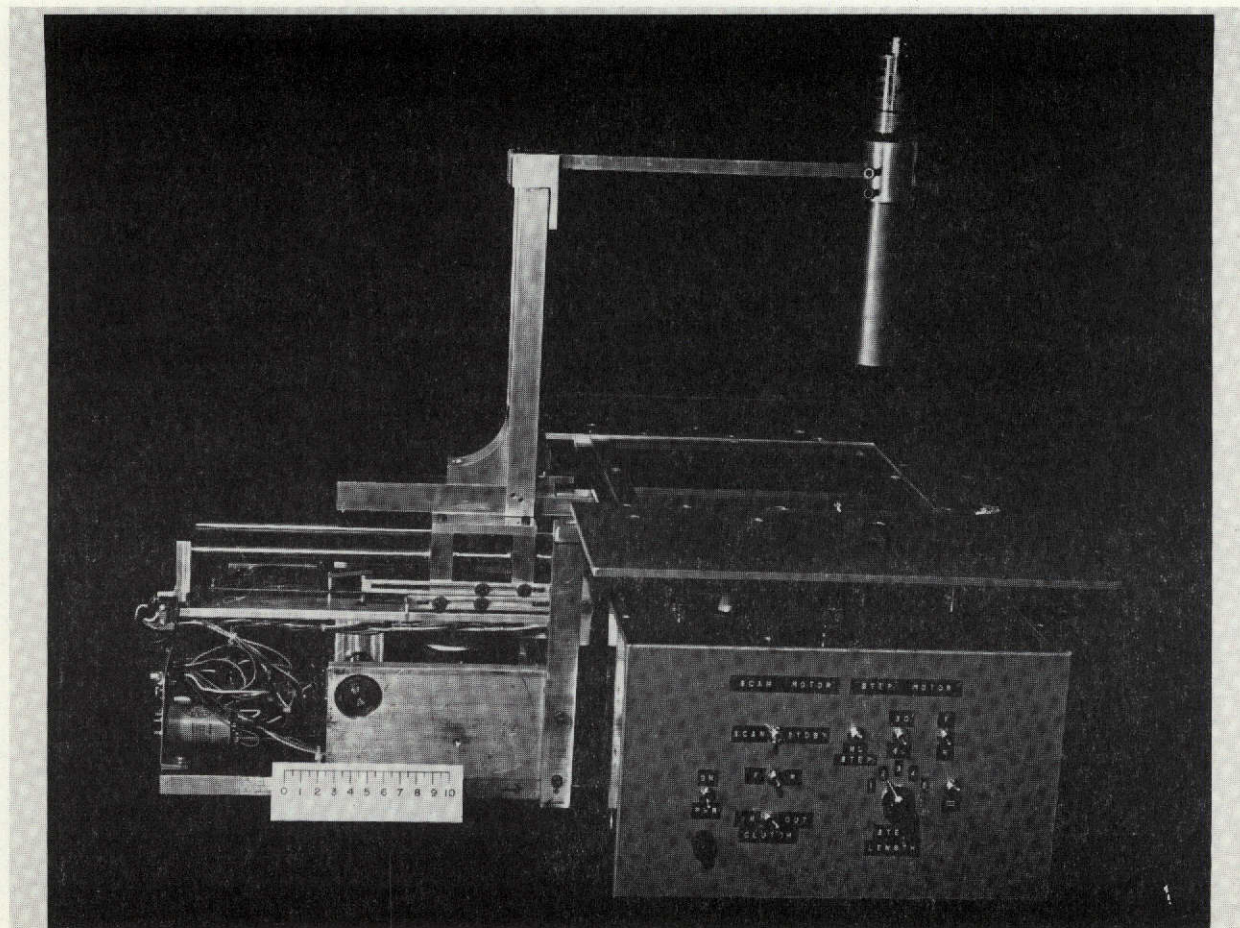


Fig. 1. Photograph of the assembled rectilinear scanner with its control panel. The range of the scanner is 15 cm square. It has a scanning speed of 2 mm/sec and five step lengths, which are selected from the control panel. Scale is in cm.

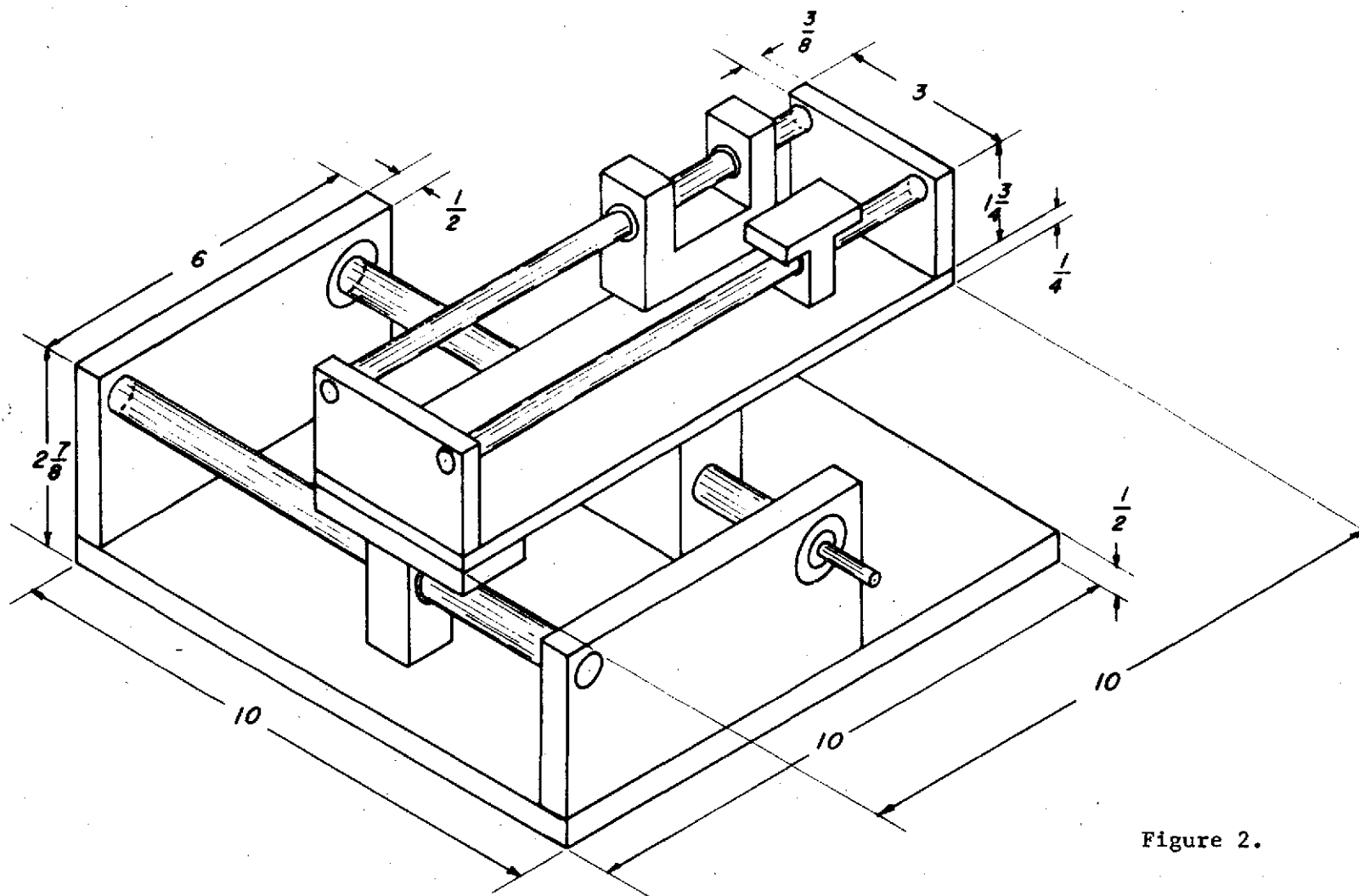


Figure 2.

X-Y SCANNER

PLATES MADE OF ALUMINUM. GUIDE RODS
60 C ROCKWELL STAINLESS STEEL. LEAD
SCREW 14MM X $1\frac{1}{4}$ MM PITCH STAINLESS STEEL
ALL DIMENSIONS IN INCHES. SCALE $\frac{1}{2}'' = 1''$

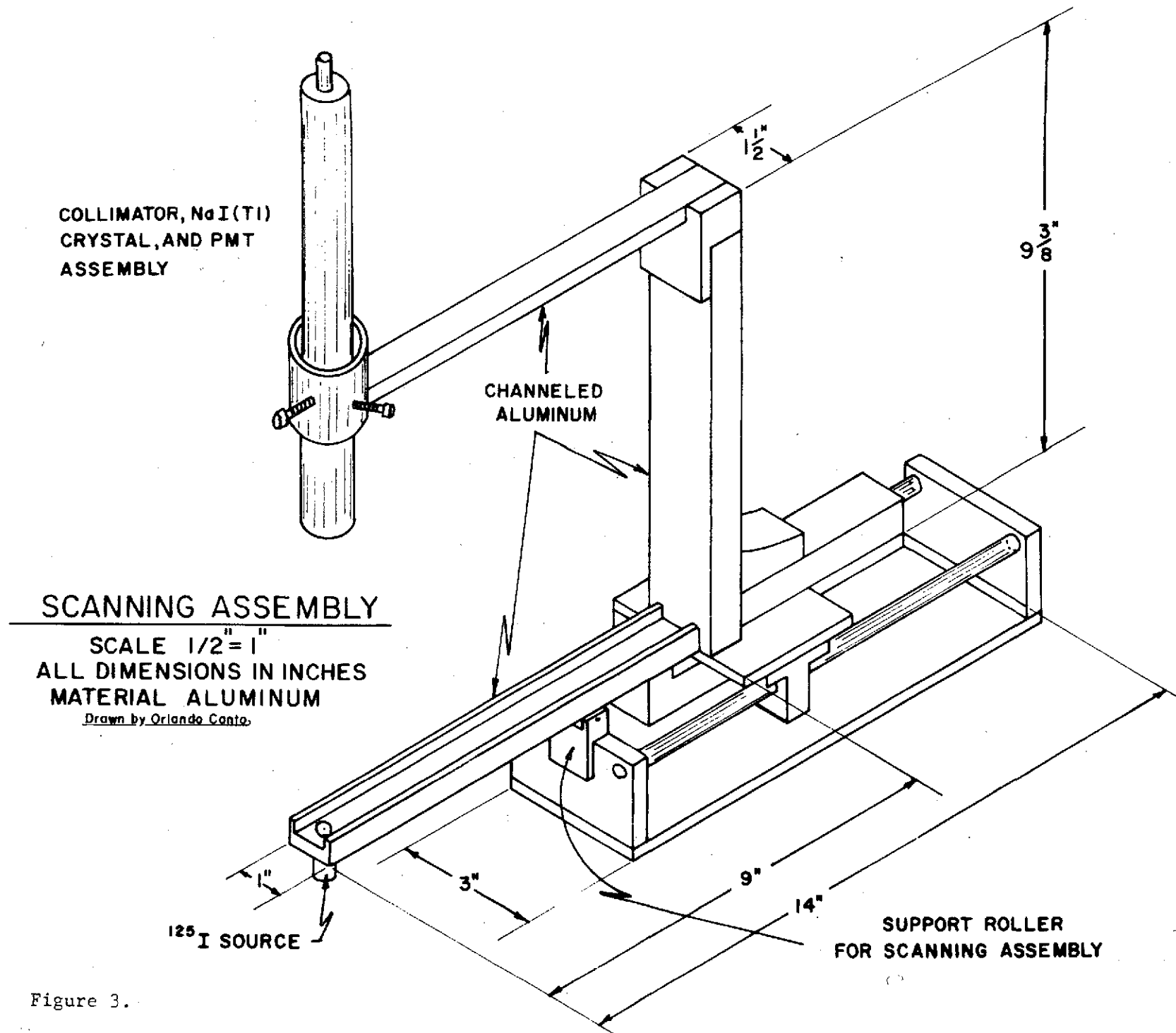
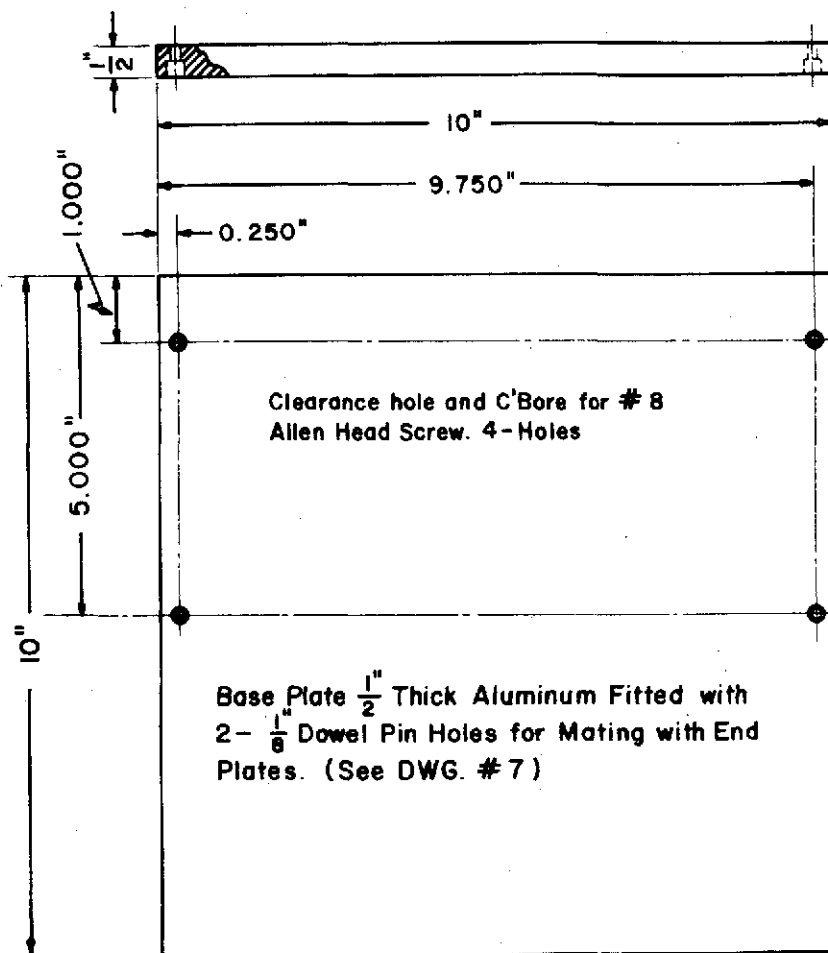


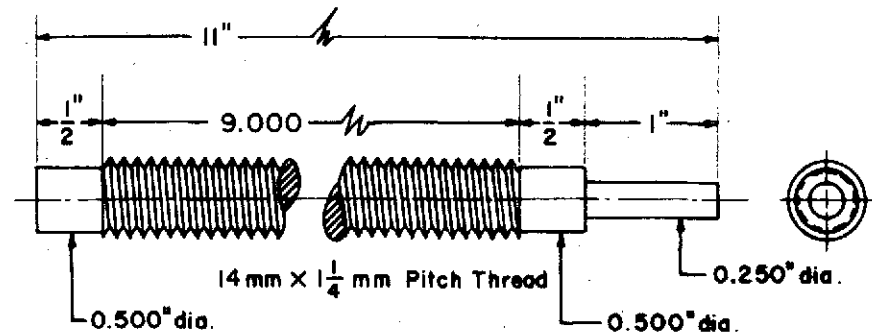
Figure 3.



Scale $\frac{1}{2}'' = 1''$

ALL DIMENSIONS IN INCHES

"SCANNER BASE PLATE"



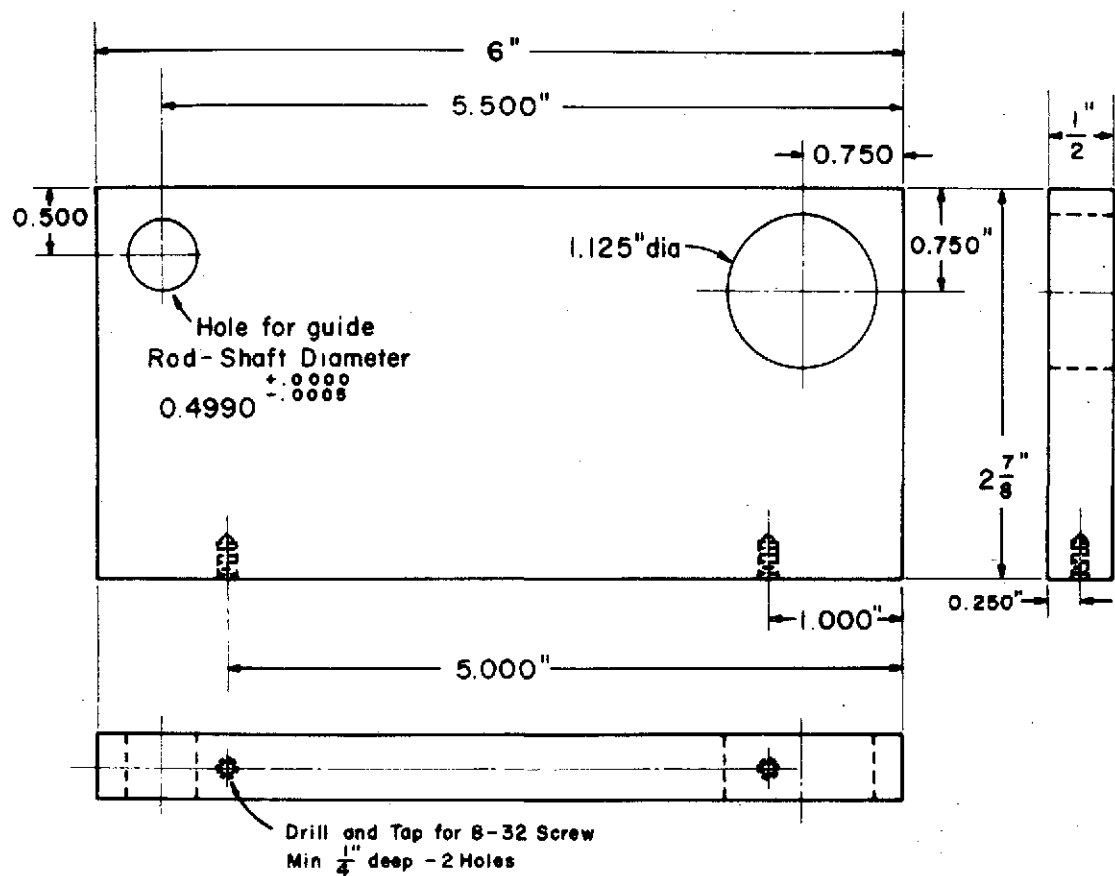
LEAD SCREW

Material Stainless Steel

Scale 1" = 1"

Figure 4.

SCANNER END PLATES - TWO REQUIRED: MACHINE AS A SET



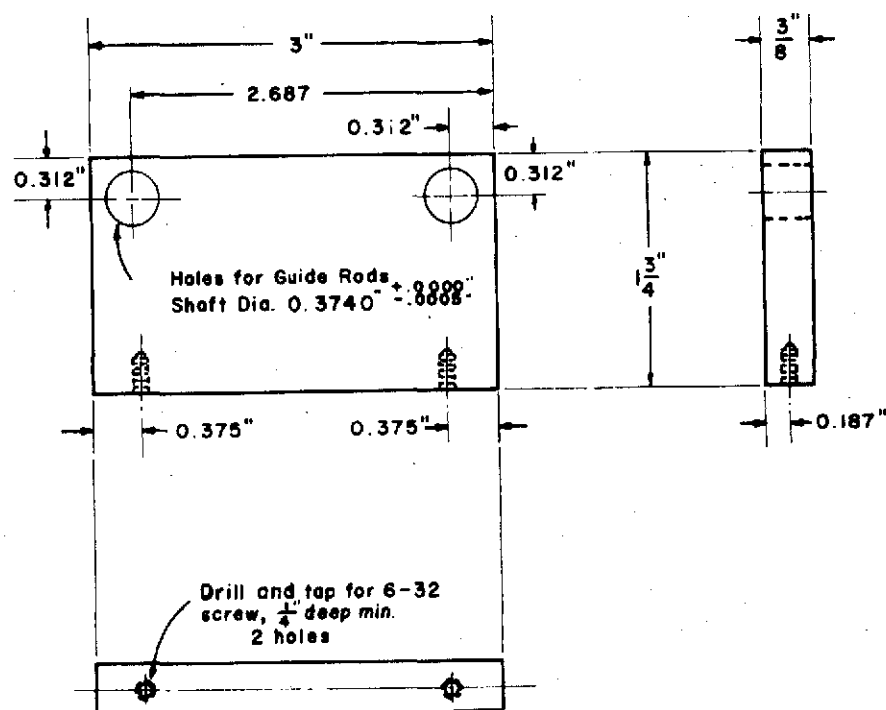
TWO PLATES TO BE MADE AS A SET.
EACH PLATE IS TO BE FITTED WITH
2 $\frac{1}{8}$ " DOWEL PINS FOR ASSEMBLY WITH
BASE PLATE. (DWG. #12)

END PLATES TO BE MADE OF ALUMINUM.
BEARINGS and GUIDE ROD FIXED AT ENDS
WITH SET SCREWS.

ALL DIMENSIONS IN INCHES
SCALE 1"=1"

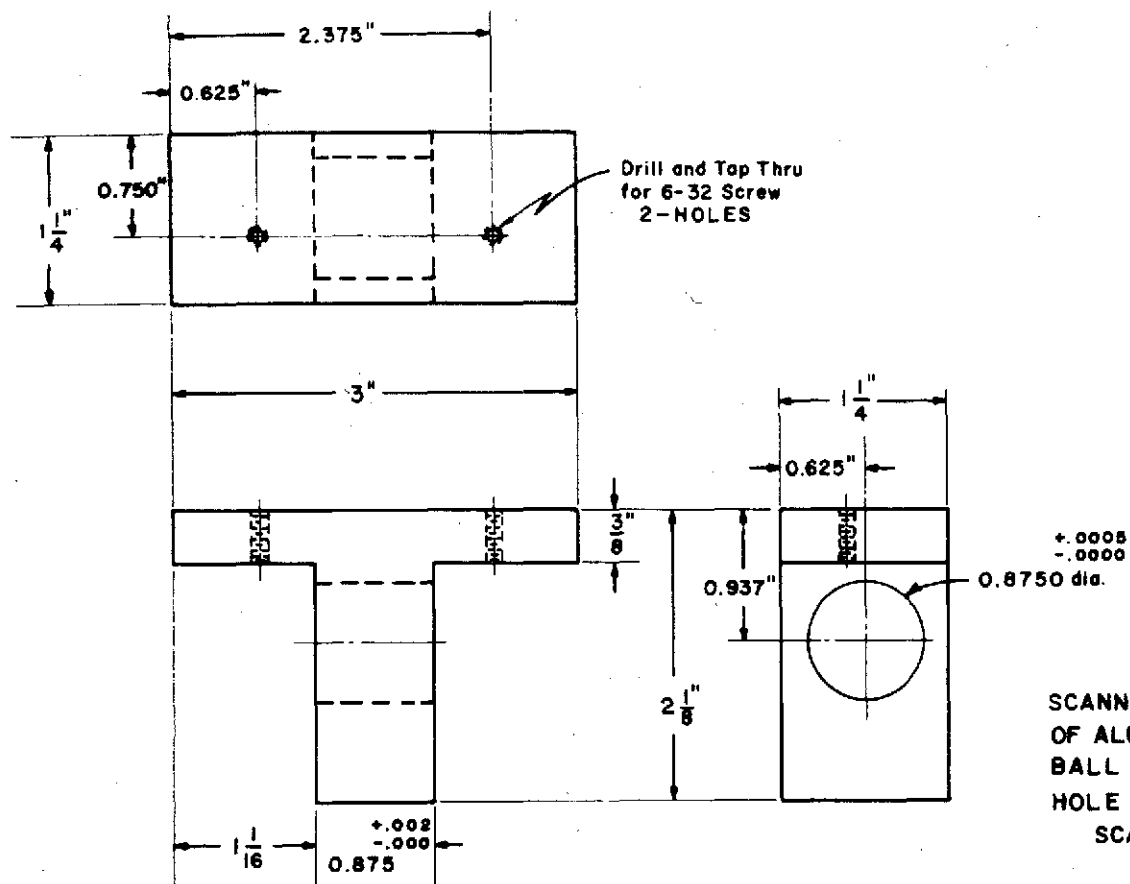
Figure 5.

SCANNING PLATFORM END PLATES, 2 REQUIRED
MACHINE AS A SET



END PLATES TO BE MADE OF ALUMINUM
EACH END PLATE IS TO BE FITTED WITH
2- $\frac{1}{8}$ " DOWEL PINS FOR ASSEMBLY TO
SCANNER PLATFORM. (DWG # 11)
GUIDE RODS FIXED TO END PLATES BY
SET SCREWS.
ALL DIMENSIONS IN INCHES.
SCALE 1" = 1"

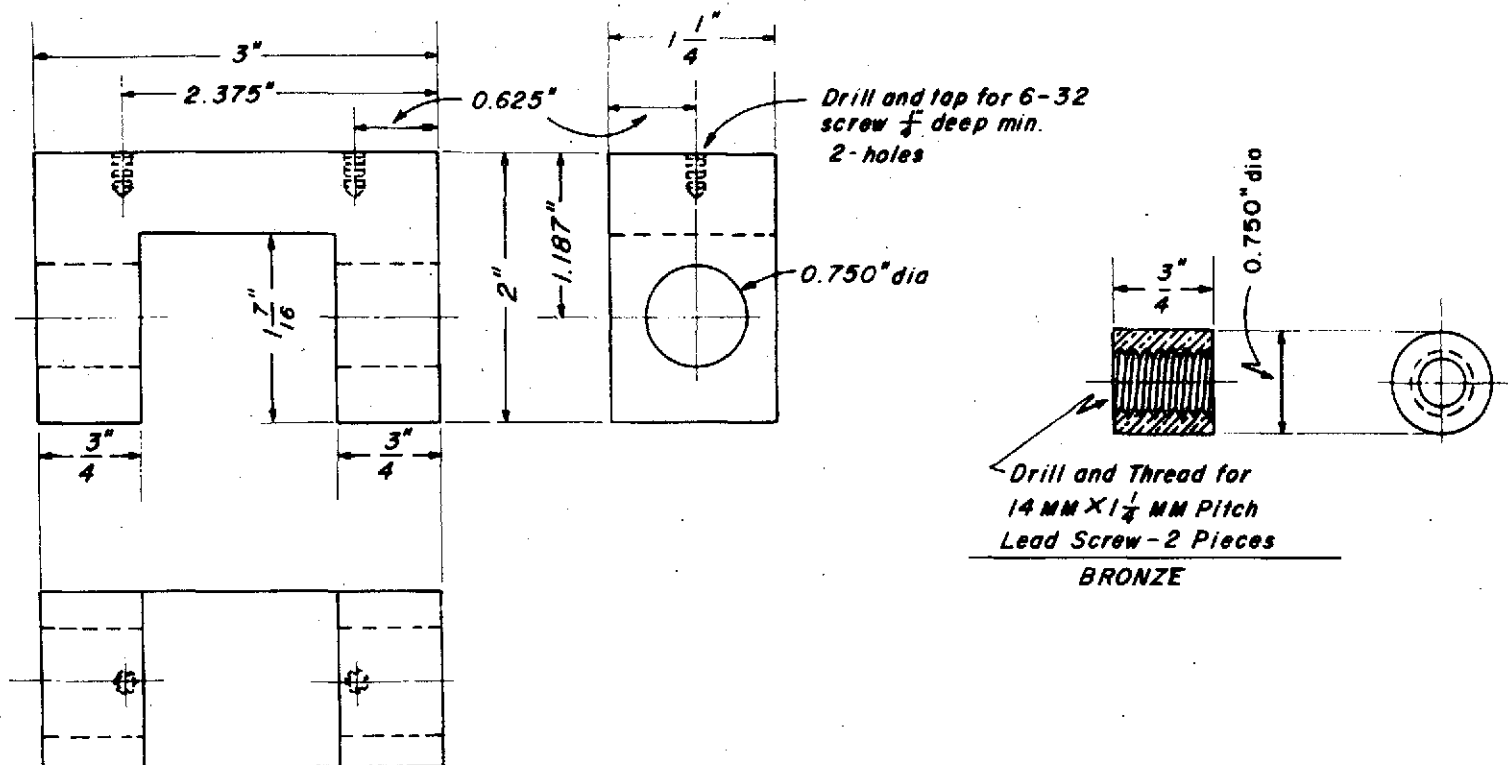
Figure 6.



SCANNER PLATFORM CARRIER TO BE MADE
OF ALUMINUM.
BALL BUSHING TO BE INSERTED INTO $\frac{7}{8}$ "
HOLE and FIXED WITH C-CLIPS.
SCALE 1"=1" All dimensions in inches

SCANNER PLATFORM CARRIER

Figure 7.

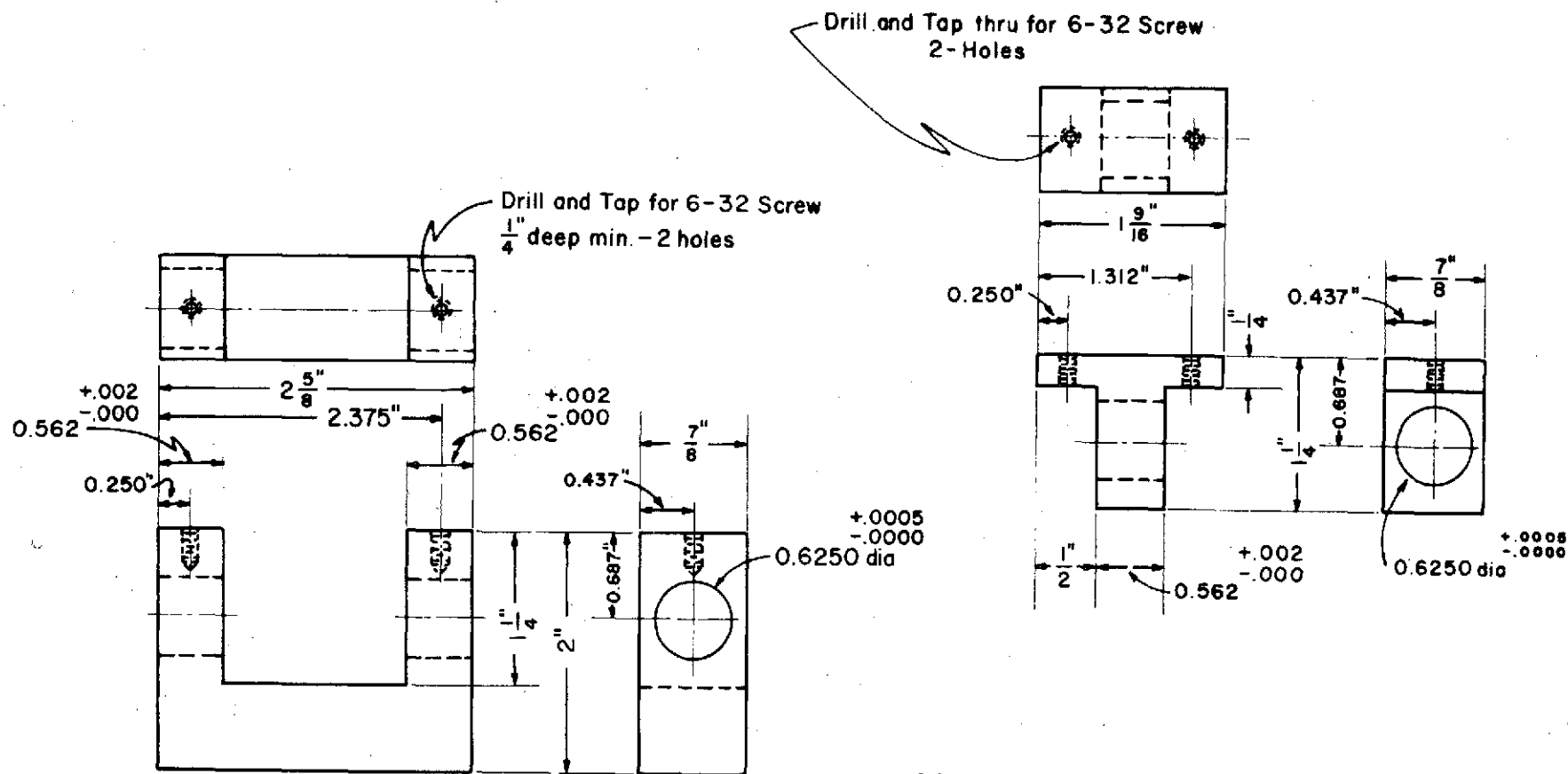


SCANNER PLATFORM MADE OF ALUMINUM
TWO NUTS MADE OF BRONZE. NUTS PRESS
FITTED INTO CARRIER WITH NUTS THREADED
ON LEAD SCREW.

SCANNER PLATFORM CARRIER and LEAD NUTS

SCALE 1" = 1", ALL DIMENSIONS IN INCHES
EXCEPT AS NOTED

Figure 8.



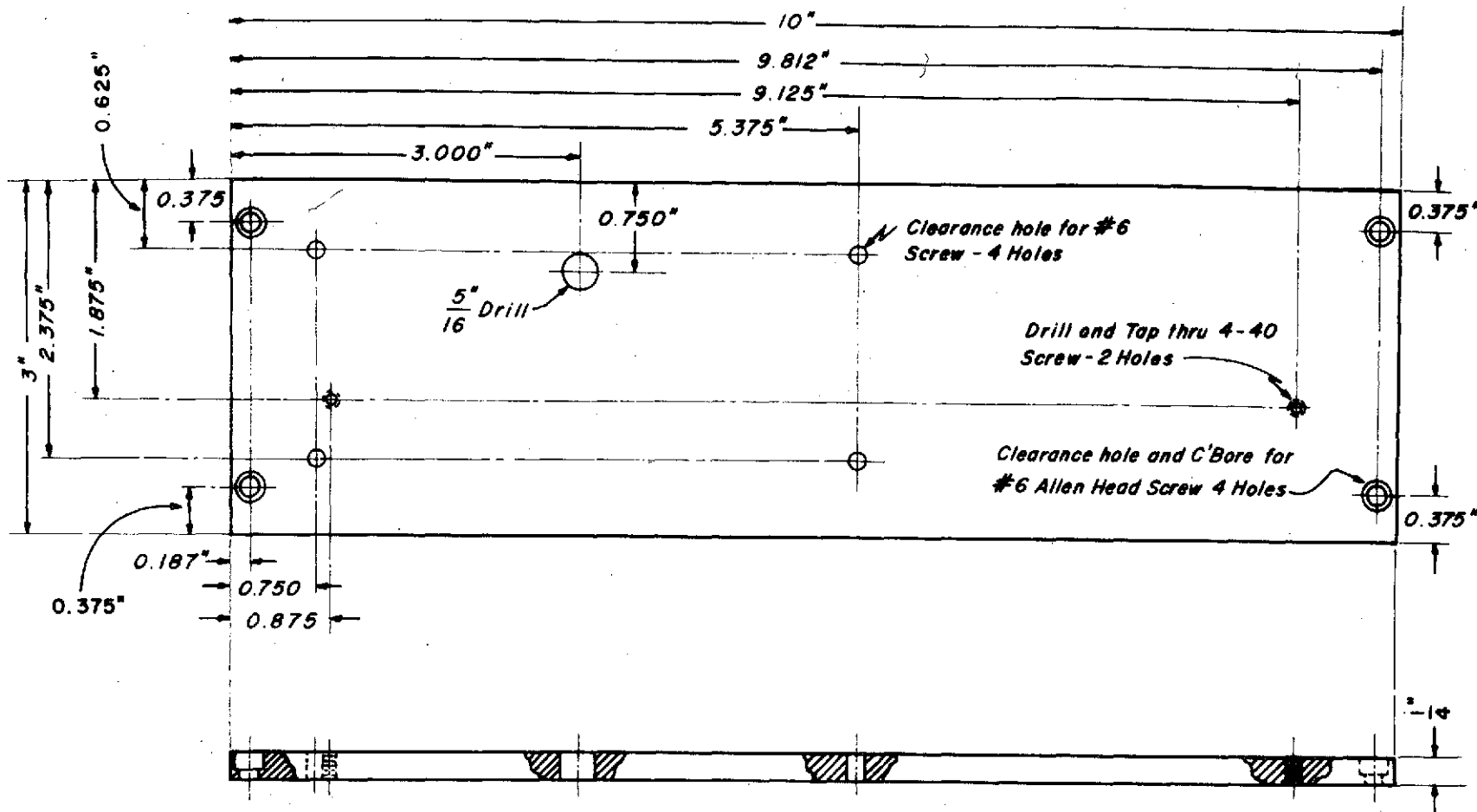
SCANNER TABLE CARRIERS

CARRIERS - 1 OF EACH TYPE TO BE MADE OF ALUMINUM. BALL BUSHINGS INSERTED INTO $\frac{5}{8}"$ HOLE and FIXED WITH C-CLIPS

SCALE 1" = 1"

ALL DIMENSIONS IN INCHES

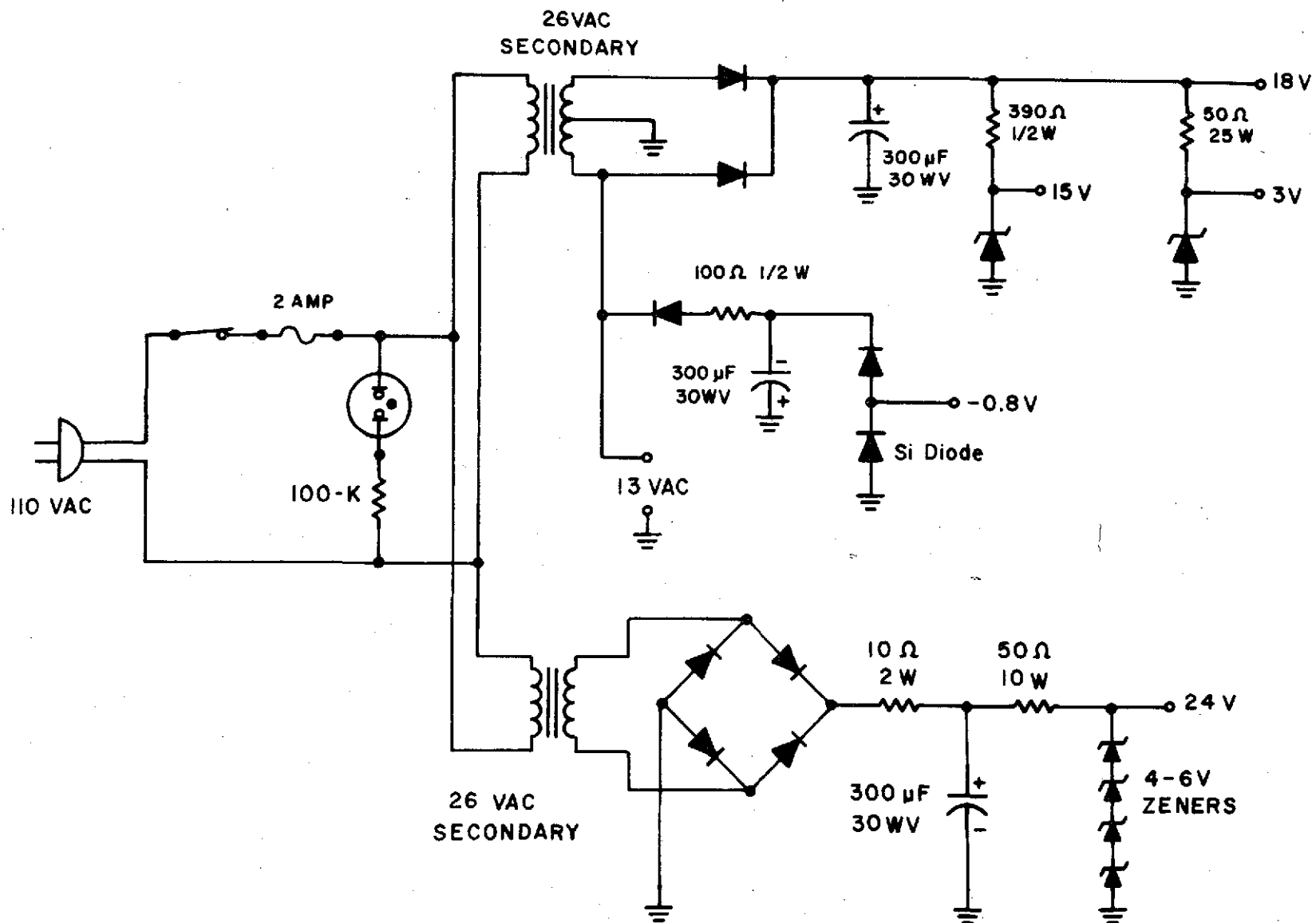
Figure 9.



SCANNER PLATFORM

PLATFORM TO BE MADE FROM $\frac{1}{4}$ " ALUMINUM PLATE
 2- $\frac{1}{8}$ " DOWEL PIN HOLES ARE TO BE DRILLED FOR
 MATING PLATFORM WITH END PLATES (See Dwg. #6)
 ALL DIMENSIONS IN INCHES
 SCALE 1" = 1"

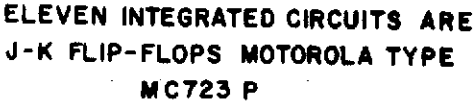
Figure 10.



POWER SUPPLY

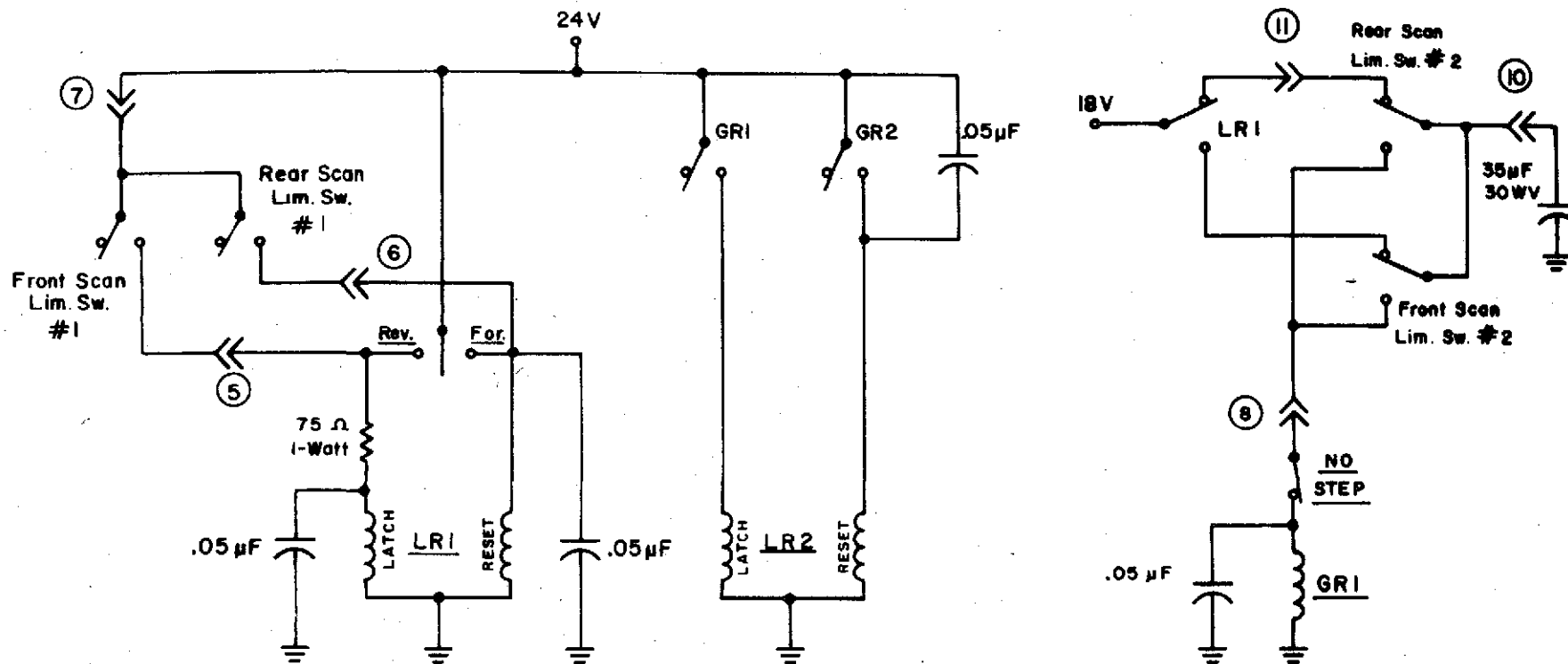
DRAWN BY ORLANDO

Figure 11.



DRAWN BY ORLANDO

Figure 12.



RELAY CONTACTS SHOWN IN POSITIONS OCCUPIED
DURING FORWARD MOTION OF SCANNER. LATCHING
RELAYS ARE IN "RESET" CONDITION.

RELAY SYSTEM

DRAWN BY ORLANDO

Figure 13.

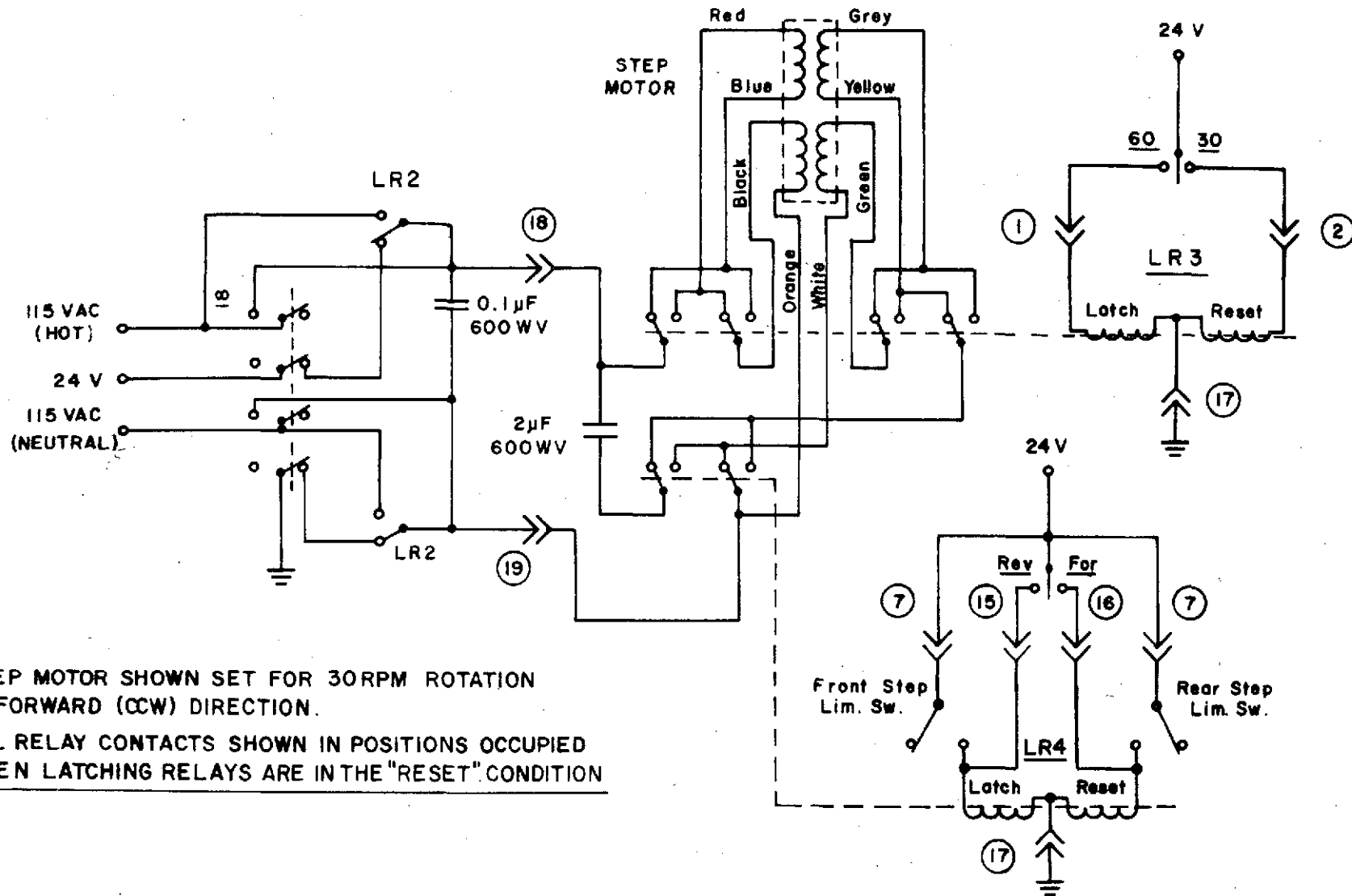


Figure 15.

STEP MOTOR CONTROL

Drawn by Orlando Canto

Effects of the Polyenergetic Character of the Spectrum of ^{125}I
on the Measurement of Bone Mineral Content

by

John M. Sandrik and Philip F. Judy
Department of Radiology
University of Wisconsin Medical Center
Madison, Wisconsin

Abstract

The spectrum of the radionuclide ^{125}I , which is extensively used for measurements of bone mineral content (BMC), consists of five photon energies ranging from 27.2 to 35.4 keV. The effect on the measurement of BMC due to the preferential attenuation of the low energy components of this spectrum in bone mineral (hydroxyapatite) and soft tissue has been investigated. A theoretical examination of this effect was made by calculating the exponential attenuation of each component of the spectrum individually and then summing the attenuation factors weighted by the fractional contribution to the spectrum of each component. The results of similar calculations for aluminum in water were found to be in good agreement with measurements indicating the validity of the above method for predicting hardening effects. The measurements and calculations were also performed with different thicknesses of tin filtration in the beam. Values of BMC determined by the above method and by a linear estimator were found to agree to $\pm 1\%$ over the range 0.6 to 1.5 g/cm² of hydroxyapatite. Variations in soft-tissue cover changed the value of BMC by 0.5% to 1.0% per cm of unit density material. The largest effect was due to variations of tin filtration which can change the value of BMC by 0.12% to 0.16% per μm of tin. These calculations indicate that the variation between tin filters used in measurements of BMC should be limited to $\pm 2.5 \mu\text{m}$.

As a polyenergetic beam of radiation passes through matter the low energy components of the beam are usually more strongly attenuated than the high energy components. This effect is termed "hardening" since the increasing proportion of the high energy components results in more penetrating or "harder" radiation. The spectrum of ^{125}I , the radionuclide most extensively used for photon absorptiometric measurements of bone mineral content (BMC), consists of five photon energies ranging from 27.2 to 35.4 keV. The effect of hardening on BMC measurements is such that the measured bone mass does not increase linearly with the mass of the bone. That is, values of BMC measured for bones of large mass are less than the values which would be obtained by linear extrapolation from measurements of bones of smaller mass. Such an extrapolation is only valid if the photon source is monoenergetic and consequently exhibits exponential attenuation in matter.

Although the spectrum of ^{125}I can be made more nearly monoenergetic by filtration with tin, which has a K-absorption edge at 29.2 keV, variation of the thickness of tin filtration among sources can also change the measured BMC.¹¹ Both the effect of variation of tin filtration and the effect of hardening of the ^{125}I spectrum will be discussed in this paper.

In developing the theory of the improved method of bone mineral measurement by the photon absorptiometric method, Cameron and Sorenson² assumed that the photon source is essentially monoenergetic; that is, the attenuation of its radiation is exponential. In a later article Sorenson and Cameron¹⁰ reported that an ^{125}I source filtered with 0.1 mm of tin did show exponential absorption over three decades of attenuation. However, in the same paper there was also a discussion of the observation of a slight non-linearity in the plot of the mineral content measured by the photon absorption method as a function of the mass of the measured bone section after ashing. This non-linearity was attributed partly to the finite cross-section of the photon beam. The same type of non-linearity which these investigators observed is produced by hardening of the ^{125}I spectrum as the beam passes through the measured bone and adjacent soft tissue.

Theoretical Estimate of the Hardening Effect

The attenuation of a discrete spectrum of radiation can be generally described by the equation

$$I = I_0 \sum_{i=1}^n f_i \exp \left\{ - \sum_{k=1}^m \mu_{k,i} \rho_k t_k \right\}$$

where I = the intensity of the radiation after attenuation

I_0 = the unattenuated intensity of the radiation

n = the number of components in the radiation spectrum

f_i = the fraction of photons in the beam having the energy of the i^{th} spectral component

m = the number of absorbers in the beam

$\mu_{k,i}$ = the mass attenuation coefficient of the k^{th} absorber at the energy of the i^{th} spectral component

ρ_k = the density of the k^{th} absorber

t_k = the thickness of the k^{th} absorber.

In making a determination of the BMC two measurements are required: the count rate I_0^* through a thickness t_{ST} of soft tissue only and the count rate I through the thickness t_{BM} of bone mineral plus the thickness $(t_{\text{ST}} - t_{\text{BM}})$ of soft tissue. The total thickness of soft tissue plus mineral is assumed to be constant for all points of measurement. With this assumption and the further assumption that the photon source is monoenergetic the quantity $\ln(I_0^*/I)$ can be shown to be linearly related to the mass of bone mineral in the path of the photon beam. However, considering the ^{125}I spectrum to consist of five discrete components, and defining the mass per unit area, M ,

of a substance as the product of its density, ρ , and its thickness, t , leads to a relation for $\ln(I_o^*/I)$ as a function M_{BM} and M_{ST} obtained from the previous equation, which is

$$\ln(I_o^*/I) = \ln \left\{ \frac{\sum_{i=1}^5 f_i \exp \{ -\mu_{ST,i} M_{ST} \}}{\sum_{i=1}^5 f_i \exp \{ -\mu_{ST,i} M_{ST} + [(\rho_{ST}/\rho_{BM})\mu_{ST,i} - \mu_{BM,i}] M_{BM} \}} \right\} \quad (1)$$

where the subscripts ST and BM refer to soft tissue and bone mineral, respectively.

The effects of photon energy shifts due to inelastic scattering have been excluded in this derivation since the geometry of our apparatus permits detection of photons singly scattered through a maximum angle of 12° . Compton scattering of a 30 keV photon through this angle would yield a scattered photon decreased in energy by about 40 eV from the incident photon energy. Such an energy shift would be unresolvable in a NaI(Tl) detector.

Experimental Estimate of the Hardening Effect

To demonstrate the validity of Equation 1 for predicting the effect of hardening due to the mineral component of the system on the measured value of $\ln(I_o^*/I)$, measurements were made on an aluminum step-wedge. The wedge had eight steps ranging in thickness from 0.164 cm to 1.593 cm; it was made from 2024 aluminum alloy, which has a density of 2.77 g/cm³.¹ The wedge was immersed in 4 cm of water; however, the effective water depth was 4.75 cm including the lucite water container and support platform. The effect of hardening due to soft tissue surrounding the absorber was determined by measuring $\ln(I_o^*/I)$ for a 0.5 cm thick section of bovine bone covered with various thicknesses of lucite.

The third effect which was examined was the variation of $\ln(I_o^*/I)$ with the thickness of tin filtration in the ¹²⁵I beam. Measurements were made with 0, 1, 2, and 3 filters in the beam with each filter being 25 μ m thick, having been cut from a commercially prepared sheet of tin foil with a thickness of 0.001 ± 0.0005 inches. In all of the above experiments point measurements were made to avoid the effect of the finite cross-section of the beam, an effect peculiar to scanning measurements.

The measurements were made with a NaI(Tl) crystal detector, a photomultiplier tube, and a Baird-Atomic Model 530 Spectrometer. In order to observe the entire photopeak, the lower level of the pulse height analyzer was set at 7 keV and the window was set at 38 keV. These settings bracket the photopeak, permitting the detection of the five components of the spectrum while minimizing the contributions of equipment noise and background to the signal.

Results

As can be seen in Figures 1 and 2, Equation 1 is a valid model for predicting the hardening effects due to both bone mineral and soft tissue.

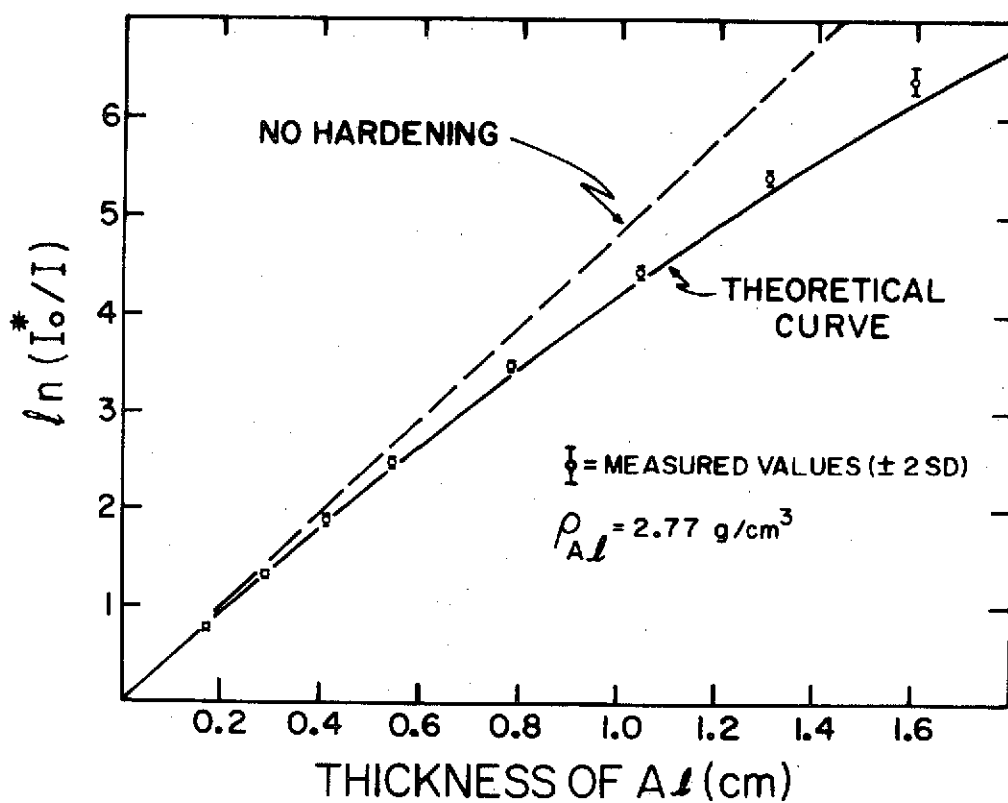


Figure 1. The effect on the measurement of bone mineral content of hardening of the ^{125}I spectrum in mineral. For these measurements the mineral was simulated by aluminum. The $\ln(I_0^*/I)$ is a measure of bone mineral content.

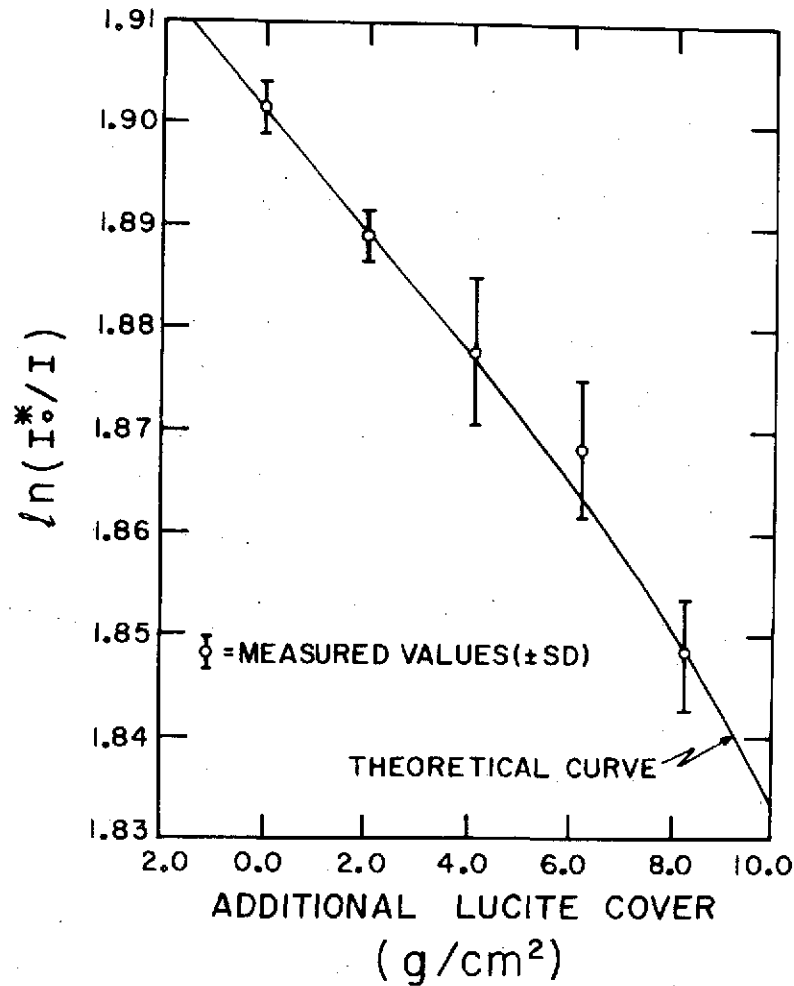


Figure 2. The effect on the measurement of bone mineral content of hardening of the ^{125}I spectrum in soft tissue. Soft tissue variations were simulated by varying the amount of lucite over a section of bovine bone. If there were no hardening effect, the curve would be horizontal.

Figure 1, a plot of $\ln(I_0^*/I)$ as a function of thickness of aluminum, illustrates the effect of increasing the mass of the absorber on the value of $\ln(I_0^*/I)$. The theoretical curve indicates values calculated using Equation 1 and the points are measured values using an unfiltered ^{125}I source; the error bars indicate ± 2 S.D. The effect on $\ln(I_0^*/I)$ of increasing the soft-tissue cover is shown in Figure 2, a plot of $\ln(I_0^*/I)$ as a function of the thickness of lucite covering the section of bovine bone. The points are the measured values (\pm S.D.), and the curve indicates values calculated according to Equation 1.

The mass attenuation coefficients used in these calculations were obtained from interpolations of published values.⁵ Tabulations of the fractional composition of the ^{125}I spectrum have also been published.³ The values used for the calculations are shown in Table I.

The attenuation coefficients of the aluminum and the water for the K_α radiation of the ^{125}I spectrum were independently determined by the Ross balanced filters technique.^{6,8,9} This method involves measuring the transmitted intensity of the beam filtered alternately by a copper and a tin filter. The thicknesses of the two filters are chosen so that the attenuation of each filter is the same for the $K_{\beta 1}$, $K_{\beta 2}$, and γ photons in the ^{125}I beam. The difference of the transmitted intensities for the two filtrations is due to the K_α radiation alone. A plot of this difference as a function of the thickness of the absorber in the beam yielded K_α attenuation coefficients of $2.047 \pm .014$ (SD) cm^2/g for the aluminum and $0.4245 \pm .0003$ (SD) cm^2/g for the water. These mass attenuation coefficients are in good agreement with the theoretical values.

Effect of Hardening on Point Measurements

To give some approximation of the magnitude of the effect on point measurements of BMC due to hardening of the ^{125}I spectrum in both bone mineral and soft tissue, a comparison was made of the values of $\ln(I_0^*/I)$ as a function of the bone mineral mass, M_{BM} (g/cm^2), computed by Equation 1 and by a linear estimator. The linear estimator was a best-fit linear regression of a set of data calculated by Equation 1 over the range of M_{BM} from $0.45 \text{ g}/\text{cm}^2$ to $1.5 \text{ g}/\text{cm}^2$. Assuming that the total tissue thickness, which is also t_{ST} , is 7 cm and the tin filtration is $51 \mu\text{m}$, a thickness commonly used in BMC measurements, the resulting regression is:

$$\langle \ln I_0^*/I \rangle = 2.103 \times M_{\text{BM}} (\text{g}/\text{cm}^2) + 0.102 \quad (2)$$

with a standard error of estimate of 0.017. The usual practice is to derive a linear equation to obtain M_{BM} as a function of $\ln(I_0^*/I)$. Equation 2 represents the inverse of such a relation, which could be obtained if actual measurements were made of bones over a broad range of mass values with the total of the tissue plus bone thickness held constant by the addition of suitable quantities of bolus material.

Since Equation 2 has no explicit dependence on the value of t_{ST} , it will be insensitive to changes of the amount of soft-tissue cover. However, the values of $\ln(I_0^*/I)$ decrease as t_{ST} increases as is evident

TABLE I

Values used in theoretical calculations of hardening of ^{125}I spectrum

Component and Energy (keV)	Fraction of Spectrum	Mass attenuation coefficients, (cm^2/g)			
		Aluminum	Hydroxyapatite	Water	Tin
$\text{K}_{\alpha 1}$ (27.5)	.517	2.0290	2.6311	.4182	8.9739
$\text{K}_{\alpha 2}$ (27.2)	.264	2.0851	2.7061	.4259	9.2181
$\text{K}_{\beta 1}$ (31.0)	.140	1.4673	1.8821	.3430	38.4212
$\text{K}_{\beta 2}$ (31.7)	.031	1.3866	1.7744	.3344	36.0697
γ (35.4)	.049	1.0511	1.3294	.2948	26.4779

from Figure 2. Hence the ratio $\langle \ln(I^*/I) \rangle / \ln(I_o^*/I)$ increases with t_{ST} . This effect is shown in Figure 3, in which this ratio is plotted as a function of M_{BM} (g/cm² of hydroxyapatite) for several values of t_{ST} . For a particular value of M_{BM} the ratio increases by 0.5% to 1% per cm of soft-tissue cover. This corresponds to a decrease of $\ln(I_o^*/I)$ of essentially the same magnitude due to hardening in the soft tissue.

Also apparent from Figure 3 is the hardening effect due to the hydroxyapatite (HA). For $M_{BM} \geq 1.2$ g/cm², and for the range of t_{ST} from 3 cm to 9 cm, the ratio $\langle \ln(I_o^*/I) \rangle / \ln(I_o^*/I)$ increases at the rate of 3.3% to 5.5% per g/cm² of HA. In particular for the case $t_{ST} = 7$ cm, the calibration condition, the curve rises by 5% per g/cm² of HA. In the range of M_{BM} from 0.6 g/cm² to 1.5 g/cm² of HA, the ratio is constant to within $\pm 1\%$ for all values of t_{ST} . In the region $M_{BM} \lesssim 0.6$ g/cm² the ratio increases rapidly since $\langle \ln(I_o^*/I) \rangle$ approaches a finite value while $\ln(I_o^*/I)$ approaches zero as M_{BM} approaches zero.

Effect of Hardening on a Scan Measurement

The above comparison of a linear estimator of $\ln(I_o^*/I)$ and Equation 1 can be extended to yield the magnitude of the error due to hardening effects to be expected in a scan measurement. In this case values of $\ln(I_o^*/I)$ and $\langle \ln(I_o^*/I) \rangle$ were calculated at 1 mm intervals across a hypothetical upper arm to obtain values of $\sum \ln(I_o^*/I)$ and $\sum \langle \ln(I_o^*/I) \rangle$ for a cylindrical humerus. Measurements of 17 excised humeri indicated that an average outer diameter is 1.8 cm and an average inner diameter is 0.9 cm in the midshaft region. Calculations were made assuming values of $t_{ST} = 7$ cm and $t_{ST} = 8$ cm. With the assumption that cortical bone is composed of 1/3 HA and 2/3 soft tissue, by volume, values of M_{BM} were determined which ranged from 0.82 g/cm² at 1 mm from the geometrical edge of the bone, to 1.5 g/cm² at 5 mm from the center of the bone. Using Equation 2 to obtain a value of $\sum \langle \ln(I_o^*/I) \rangle$ and Equation 1 to obtain a value of $\sum \ln(I_o^*/I)$ resulted in the ratio $\sum \langle \ln(I_o^*/I) \rangle / \sum \ln(I_o^*/I) = 1.001$ for $t_{ST} = 7$ cm, the calibration condition; for $t_{ST} = 8$ cm, the ratio was 1.012. This example indicates that errors due to hardening can be minimized by calibrating the system for the same range of bone mass values over which later measurements are to be made. Also, since variation in total tissue thickness can introduce an error as large as 1% per cm deviation from the calibration tissue thickness, measurements should be made with this thickness standardized in order to maximize the precision and accuracy of the measurement.

Effects of Tin Filtration on the BMC Measurement

The calculations of the previous section were performed under the assumption that there were 51 μ m of tin filtration in the beam: a filtration in common use for BMC measurements. Tin is the element of choice because it has a K-absorption edge at 29.2 keV. Hence tin filtering makes the ¹²⁵I beam more nearly monoenergetic by selective attenuation of the $K_{\beta 1}$ (31.0 keV), the $K_{\beta 2}$ (31.7 keV), and the γ (35.0 keV) radiation. However, variations of the thickness of tin filtration in the beam can lead to considerable errors in the BMC measurements. Computations using Equation 1 indicate that the magnitude of $\ln(I^*/I)$ increases with increasing tin filtration at the rate of 0.12% to 0.16% per μ m of tin over the range of

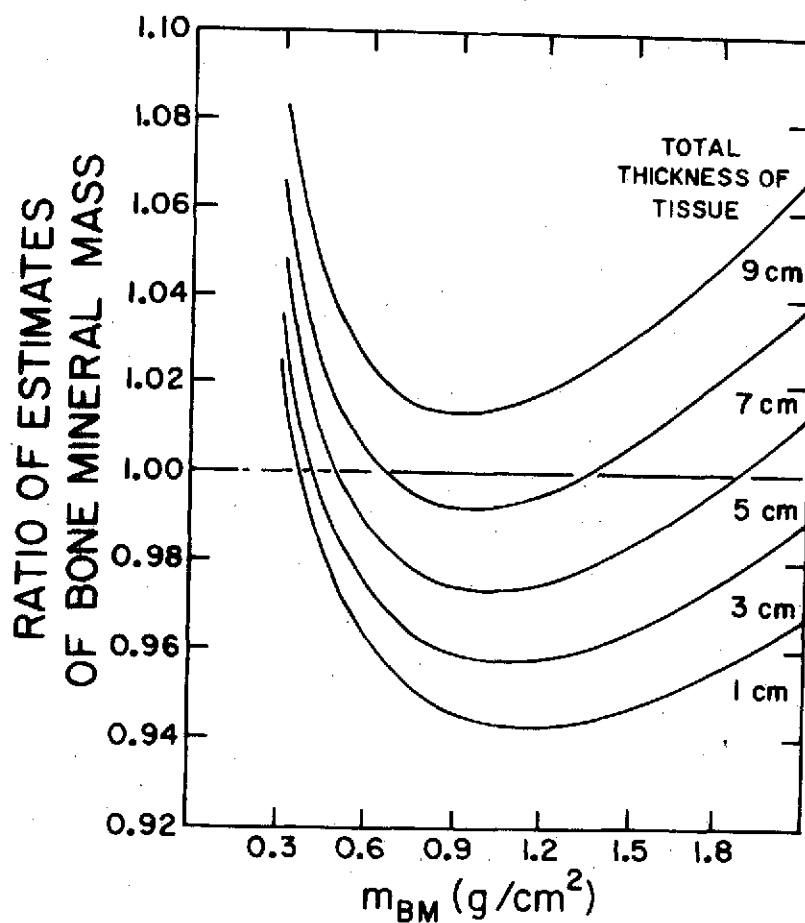


Figure 3. Comparison of a particular linear estimator of bone mineral content and Equation 1 (see text). Values on the ordinate are ratios of $\langle \ln(I^*/I) \rangle / \ln(I^*/I)$ where the numerator has been calculated by the linear estimator and the denominator by Equation 1. Abscissa values represent thicknesses of hydroxyapatite.

zero to $76 \mu\text{m}$ of tin filtration and with absorber thicknesses of 0.3 to 2.1 g/cm^2 of HA. Measurements on the aluminum step-wedge over the same range of tin filtration and a similar range of absorber thickness showed an increase in $\ln(I^*/I)$ of 0.12% to 0.20% per μm of tin. This effect is displayed in Figure 4, which contains plots of the ratio of $\ln(I^*/I)$ calculated with tin filtration to the same quantity calculated without filtration as a function of the thickness of tin filtration and for several thicknesses of HA. Specifically, these measurements imply that in order to hold the variation of measured BMC due to variation of tin filtration to $\sim 1\%$ the thickness of filters used with different sources should be controlled to $\pm 2.5 \mu\text{m}$.

One method of maintaining constant filter thickness is to use the same filter on each ^{125}I source used for BMC measurements. Since such a filter would be subject to considerable handling, it should be protected, possibly by laminating it between thin sheets of lucite. Uniformity of thickness among several filters could be achieved by making transmission measurements of the filters and selecting those for which the transmitted count rates are within the required limits.

The problems of tin filter variations can be eliminated entirely by not using any filter. Although this tactic will lead to a less mono-energetic beam, the hardening effects can be minimized by calibrating the system over a wide range of BMC values. For example, a linear regression, similar to that described previously, was determined for values of $\ln(I^*/I)$ as a function of M_{BM} , but in this case no tin filtration was assumed. Computation of $\sum \langle \ln(I^*/I) \rangle$ for the hypothetical upper arm scan produced the ratios $\sum \langle \ln(I^*/I) \rangle / \sum \ln(I^*/I) = 0.997$ with 7 cm tissue thickness, the calibration thickness assumed, and 1.010 with 8 cm tissue thickness assumed.

Eliminating the filter will also provide a considerable increase of the photon fluence. For example, our use of $60 \mu\text{m}$ of tin filtration reduces the photon fluence by $\sim 50\%$. Removing the tin filter (and also broadening the spectrum accepted by the pulse height analyzer) will permit longer use of present sources or the purchase of lower activity, less expensive sources for future use.

Conclusion

Apparently hardening effects are sufficiently small that a linear relation between BMC and $\ln(I^*/I)$ can predict the BMC to within $\pm 1\%$. However, in order to maintain this accuracy the measuring apparatus must be calibrated over the same range of BMC values that will be encountered in practice. Significant errors in accuracy, $\sim 5\%$ per g/cm^2 of HA, can be introduced into measurements of BMC outside the range of calibration. Although the errors due to variations in soft-tissue cover are small, $\lesssim 1\%$ per cm of unit density material, some control of total tissue thickness should be instituted in order to increase the precision of the measurement. Finally, errors in accuracy and precision can be minimized by control of the amount of tin filtration used in the beam. These errors can be removed by elimination of the tin filter or at least minimized by quality control of the thickness of the filters used on the ^{125}I sources.

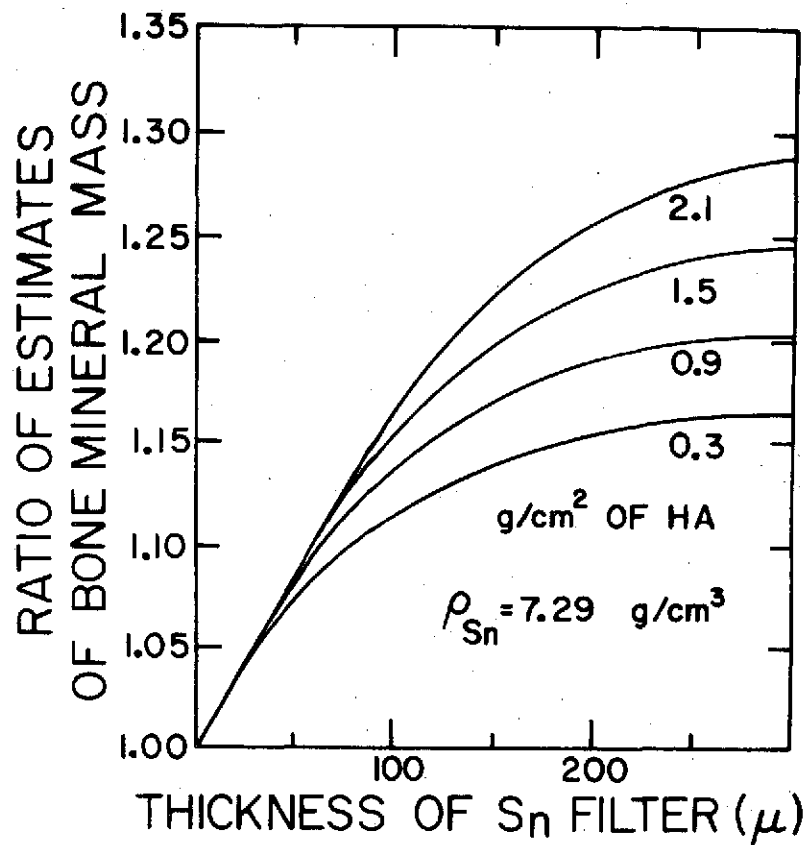


Figure 4. The effect of variation of tin filtration on measurement of bone mineral content. Values on the ordinate are ratios of $\ln(I_0^*/I)$ calculated with tin filtration to the same quantity calculated without tin filtration.

References

1. Aluminum Company of America; Alcoa Aluminum Handbook, Pittsburgh, Pennsylvania, 1962.
2. Cameron, J.R. and Sorenson, J.A.; "Measurement of Bone Mineral In Vivo: An Improved Method", Science 142: 230-232, 1963.
3. Ertl, H.H., Feinendeger, L.E. and Heiniger, H.J.; "Iodine-125, a Tracer in Cell Biology: Physical Properties and Biological Aspects", Phys. Med. and Biol. 15: 447-456, 1970.
4. Evans, R.P.; "X-ray and γ -ray Interactions", in Radiation Dosimetry, Vol. I, F.H. Attix and W.C. Roesch (eds.), Academic Press, New York 1968.
5. Hubbell, J.H.; Photon Cross-Sections, Attenuation Coefficients, and Energy Absorption Coefficients from 10 keV to 100 GeV, NSRDS-NBS 29, National Bureau of Standards, Washington, D.C., 1969.
6. Kirkpatrick, P.; "On the Theory and Use of Ross Filters", Review of Scientific Instruments 10: 186, 1939.
7. McMaster, W.H., Kerr Del Grande, N., Mallett, J.H. and Hubbell, J.H.; Compilations of X-ray Cross Sections, UCRL-50174, Lawrence Radiation Laboratory, Livermore, California, 1969.
8. Ross, P.A.; "Polarization of X-rays", Physical Review 28: 425, 1926 (Abstract).
9. Ross, P.A.; "A New Method of Spectroscopy for Faint X-radiations", J. of Optical Soc. of America and Review of Scientific Instruments 16: 433, 1928.
10. Sorenson, J.A. and Cameron, J.R.; "A Reliable In Vivo Measurement of Bone Mineral Content", J. of Bone and Joint Surgery 49-A, No. 3: 481-497, 1967.
11. Witt, R.M., Mazess, R.B. and Cameron, J.R.; Spectral Difference in Commercial ^{125}I Photon Sources, USAEC Report COO-1422-99, June 1971.

Acknowledgements

I wish to thank Orlando Canto who prepared the figures for this paper.

Computer services at the Madison Academic Computing Center were made available through a grant from the Graduate School Research Committee of the University of Wisconsin.

Partial support was also provided by funds from the Biomedical Sciences Support Committee and by NASA Grant No. Y-NGR-50-002-051.

IMPROVED VERSION OF THE DUAL-CHANNEL SYSTEM
TO MEASURE BONE MINERAL CONTENT

By

R. M. Witt, C. E. Vought and R. B. Mazess
Department of Radiology
University of Wisconsin Medical Center
Madison, Wisconsin

Certain modifications and improvements have been made on the breadboard two-channel system described in last year's report (1). The charge amplifier has been redesigned and various other changes have been made to decrease the deadtime of the complete system. The entire breadboard has been made compatible with existing equipment. A 60-Hz timer was constructed with a preset count mode so that the system could function as nuclear pulse counting device in our laboratory. The dual-channel system is now composed of the following components: an amplifier; two single-channel analyzers; two five-decade scalars; two six-decade data buffers; two address control boards; two five-decade visual numeric displays; a one decade preset 60-Hz timer; and associated control switches, potentiometers, and connectors.

Charge Amplifier

A new charge amplifier which is composed of discrete components was constructed with an FET input to handle the capacitive load of the detector cable. The output pulse has a 200 nsec risetime and a 20 μ sec decay time constant.

Pulse Shaping Network

The input circuit to the pulse shaping stage was changed to provide a "zero" to cancel the 20 μ sec "pole" response of the charge loop. The capacitor coupling the pulse shaping stage and the linear amplifier stage was decreased providing a second differentiation of the CR-RC shaped pulse. The second differentiation creates a bipolar pulse and eliminates the baseline shift which occurred at high count rates ($>10^4$). The bipolar pulse has a total length of 6 μ s and a crossover point at about 1.5 μ s.

Single Channel Analyzer-Comparator Logic Dead Time

The comparator logic sequence remains the same, but the time constants of the monostable vibrators in the comparator logic circuit have been decreased to more rapidly process the shorter amplifier pulse. The new processing time of the system is 3.8 μ s. The measured processing time of the entire detector-to-analyzer system is 5 μ s. The comparator logic circuit is a paralyzable type so that the dead time can be corrected with an analytic function at excessive count rates. With a processing time of 5 μ s the system can count at 10 kHz with 5% count loss.

Scaler Displays

Two five-decade numeric digital displays which are TTL logic compatible were added to the scaler outputs. These displays consist of a decoder/driver IC and a 4 x 7 dot array of light emitting diodes (LED) (Hewlett-Packard Series 5082-7300).

Compatibility of Scaler Control and Buffered Output

Our present digital acquisition system is composed entirely of commercial components all built to nuclear instrument module, NIM, standards (2). The data collection and output components consist of a digital magnetic tape interface (NE-25)*, and two addressable, buffered scalars (NS-30A)*. Both the data buffers and the addressing controls are contained on separate printed circuits, P.C., boards. To make the scaler control logic and the scaler outputs compatible with the existing data acquisition system two address control boards and two buffer boards were purchased and connected to the two scalars of the dual-channel system.

Data Buffer Boards

The data buffer boards are compatible with the TTL logic of 7400 series scalars used in the dual-channel system and contain 24 bits of storage which is enough for six decades of BCD data.

Address Control Board

The address control board contains an address coder programmable from 0 to 99, the run flip-flop (Q and \bar{Q}) to start and stop the scalars, and various control gates to operate the data buffers and reset the scalars. The control signals (START, STOP, and RESET) to operate the address control can be generated either locally by push buttons on the dual-channel system or by remotely by the interface device. To control all the scalars simultaneously an ADDRESS OVERRIDE, AO, signal must also be generated and sent to each address control board.

Magnetic Tape Interface Device

The magnetic tape interface device provides the necessary control signals to the address control boards to simultaneously control all scalars, and the necessary control circuitry to write the contents of the scaler buffers serially onto digital magnetic tape. The interface only writes data from components which respond to the proper addressing codes.

Both the address control board and the interface require a PRESET STOP signal which indicates the termination of a fixed time interval or the accumulation of a fixed number of counts. Upon receiving a PRESET STOP signal, the address control board stops the scalars and allows their contents to transfer to the data buffers and the interface device records all scaler buffers which respond to the addressing commands.

* Harshaw Chemical Company, Inc.

Timer

A 60-Hz timer was designed and built to provide an elapsed time counter and a PRESET STOP signal for the Address Control board and interface. Two versions of the timer were designed, Figures 4a and 4b. For the version used in the dual-channel system the timer flip-flop is controlled by the Address Control board run flip-flop and the PRESET STOP signal is sent out via the local control signal output connector. In the second version the timer flip-flop is directly controlled by push buttons and the PRESET STOP signal is directly returned to the flip-flop to automatically clear all dividers and counters at the end of each time period.

For both versions the time base is supplied by a regenerative switch which converts the 60-Hz power-line sine waveform directly into a fast fall-time clock pulse followed by a $\div 6$ counter to give a time base of 100 millisecond pulses. The 10 pps signal is then divided by 10 and 100. The Timer Mode Switch can select which divider output pulse is sent to the decade counter. Thus the time base can be scaled by 1, 10 or 100.

The counter is a one decade BCD counter whose output is compared with the output of a one decade BCD thumbwheel switch. When the counter is the same as the thumbwheel switch setting, a PRESET STOP signal is sent out. When the timer is controlled by the Address Control board, it has the feature that it can be stopped and put into "Hold" and then restarted without affecting the elapsed time.

All dividers and counters are set to zero by the RESET signal from the timer flip-flop. However, since the start signal is not synchronized with the 60-Hz time base, each Start-Stop cycle has an error of one clock cycle or 16 millisecond with the 60-Hz timer.

Packaging of the Breadboard

Since the dual-channel system has been designed to be compatible with other devices which are built to Nuclear Instrument Module (NIM) standards, the breadboard unit was also mounted in a standard NIM module. All components composing the improved dual-channel system fit into a standard three-width NIM module, Figures 1, 2. All important controls and connectors, and scaler displays are located on the front panel, Figure 3. The dimensions of the unit are 102.9 mm wide x 207.7 mm high, and 248.8 mm deep. The complete unit weighs 2.27 kg.

Control Configurations

The dual-channel system has been designed to provide flexible control and all connectors are compatible with our existing NIM digital acquisition system. The unit has three front panel push buttons: Start, Stop, and Reset. Each push button provides a +5 volt pulse along with a +5 volt ADDRESS OVERRIDE signal. These local control

signals along with the PRESET STOP signal from the internal timer are available at an output connector on the rear of the module. Another rear connector serves as an input for these same control signals. A third 50-pin connector provides parallel connections between the different NIM modules for the data, address and control signals. Depending on the interconnections, the unit can be controlled locally or remotely.

Local Control

If a cable is connected between the local control signal output and input connectors, the dual-channel system can be controlled by its front panel push buttons and its internal 60-Hz preset timer. If the unit is connected to a compatible scaler via the 50-pin connectors, it can provide parallel control of these devices with the front panel push buttons and the internal timer.

Remote Control Mode

If the dual-channel system is connected to a compatible interface device via the 50-pin connector, the unit can be remotely controlled by the interface in both its automatic and manual modes. When controlled by the interface, the contents of the buffered scalers can be written onto digital magnetic tape. In the above configuration the push buttons on the dual-channel system and the interface are connected in parallel. To avoid erroneous control signals all operations should be initiated by the interface controls. If a compatible remote timer with a preset stop signal is connected to the dual-channel system via the local signal input connector, the system can be controlled by the interface, but with the external timer providing the timer base to the scalers.

Conclusion

In addition to serving as a prototype for the inflight electronics package for bone mineral determinations, the dual-channel system in its present configuration can be used with our present digital acquisition system. The dual-channel system is suitable for both the single photon and the two photon techniques of determining bone mineral content, BMC (3,4). Since the unit is more compact than our present system, it would be more suitable as a portable field unit for making preflight, postflight, and other ground base measurements of BMC where a digital system is required.

References

1. Sitzman, J.C., Vought, C.E. and Mazess, R.B., Preliminary Report on a Dual Photon Bone Mineral Measuring Instrument, USAEC Report C00-1422-98 (1971).
2. Judy, P.F., Ort, M.G., Kianian, K. and Mazess, R.B., Developments in the Dichromatic Attenuation Technique for the Determination of Bone Mineral Content In Vivo, USAEC Report C00-1422-97 (1971).
3. Judy, P.F. and Cameron, J.R., A Dichromatic Method for the Measurement of Bone Mineral Content, USAEC Report C00-1422-60 (1969).
4. Cameron, J.R. and Sorenson, J.A., Measurement of Bone Mineral In Vivo; An Improved Method, Science 142: 230-232 (1963).

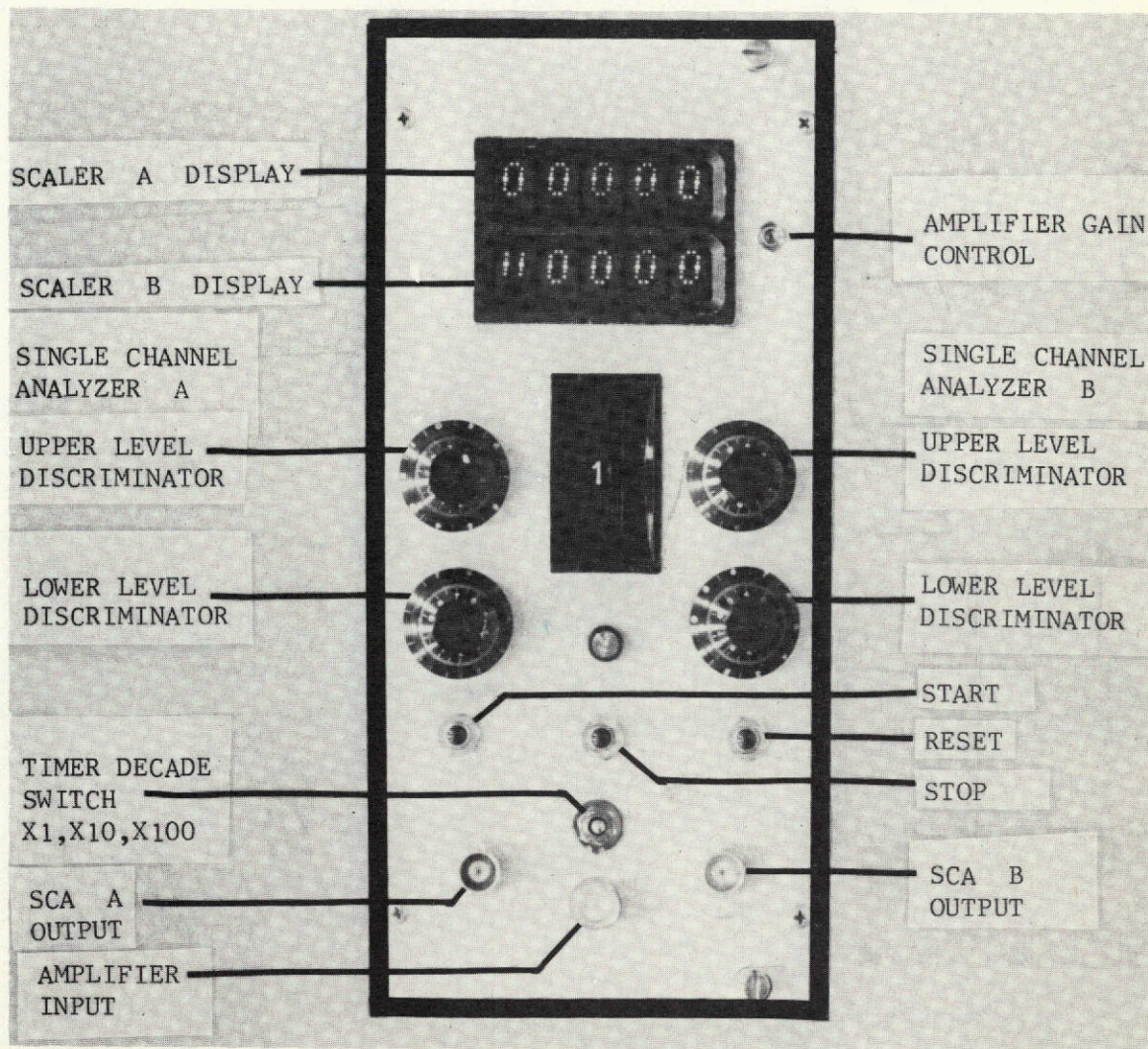


Figure 3. Front panel of dual channel system describing the various controls. The system which is mounted in a three width Nuclear Instrumentation Module contains a 60 Hz timer, two single channel analyzers, two buffered scalars, and two addressable control boards. The scalar buffers and addressed control boards are compatible with a commercial digital magnetic tape interface device.¹

¹ Harshaw Model NE-25.

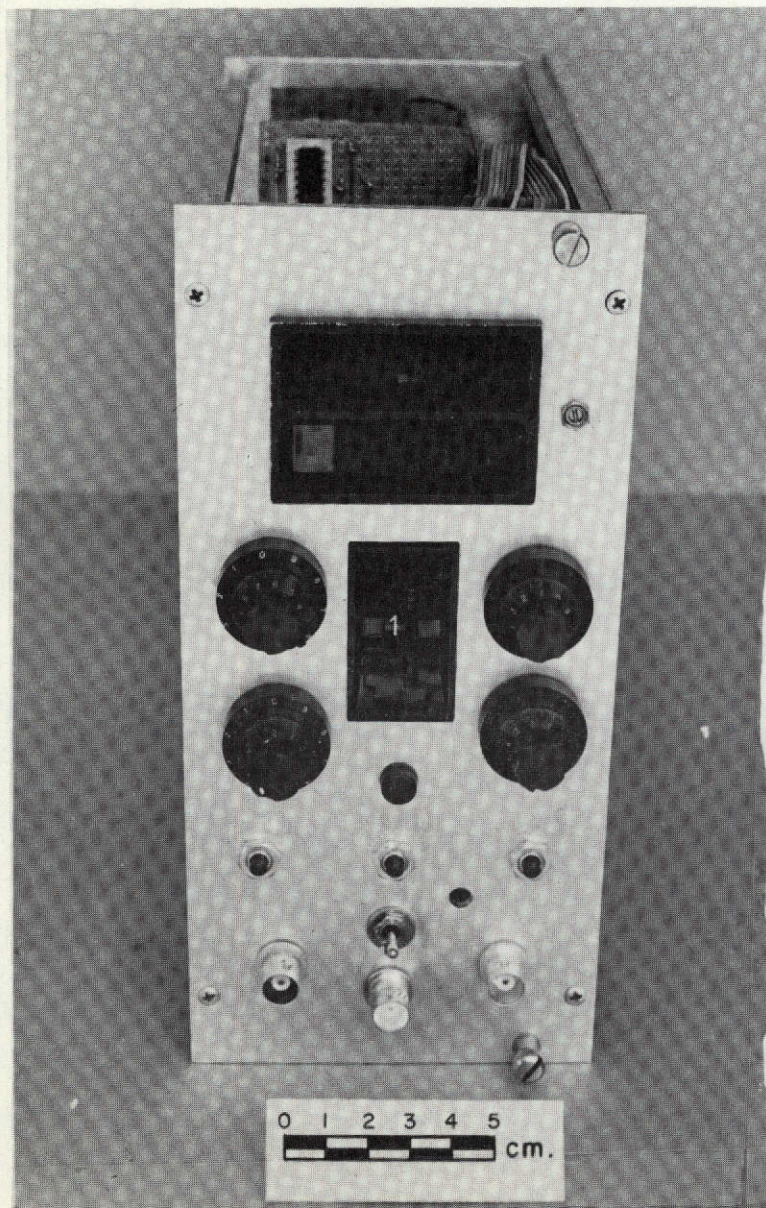


Figure 1. Front view of the dual channel system illustrating the positions of the controls necessary to operate the unit after the breadboards were mounted in a three width Nuclear Instrumentation Module.

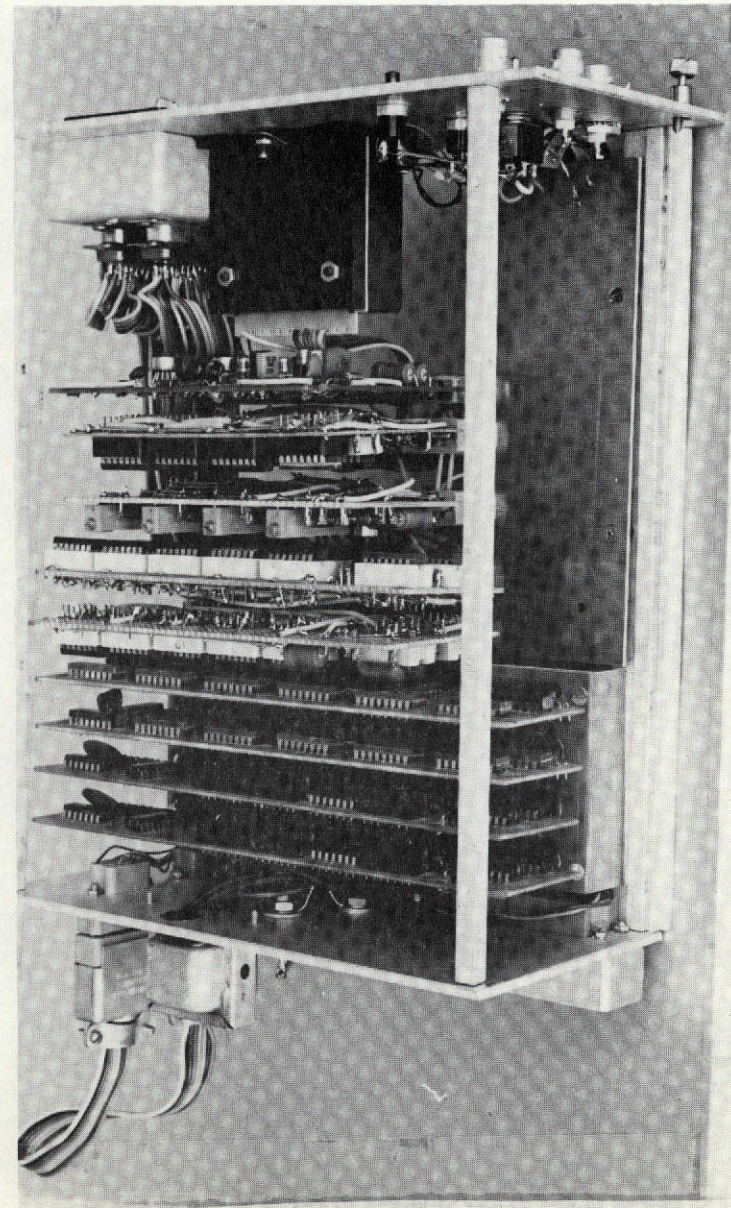


Figure 2. Side view of the dual channel system illustrating the placement of the breadboards into a three width Nuclear Instrumentation Module.

60 ~ TIMER, REMOTE CONTROL

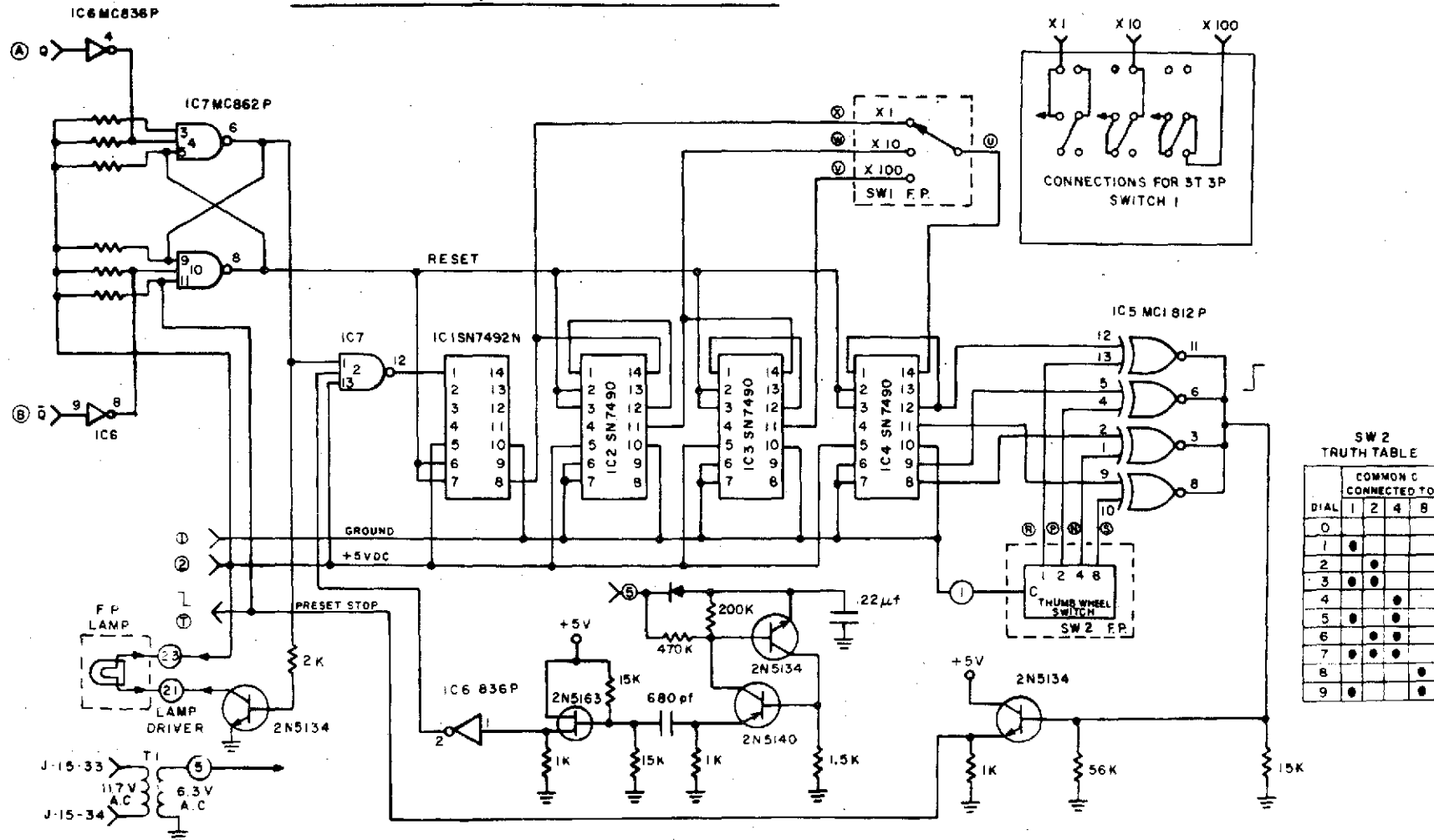


Figure 4a. Schematic of 60-Hz timer with Start-Stop flip-flop controlled by remote signals from the Address Control Board.

60~TIMER, INTERNAL CONTROL

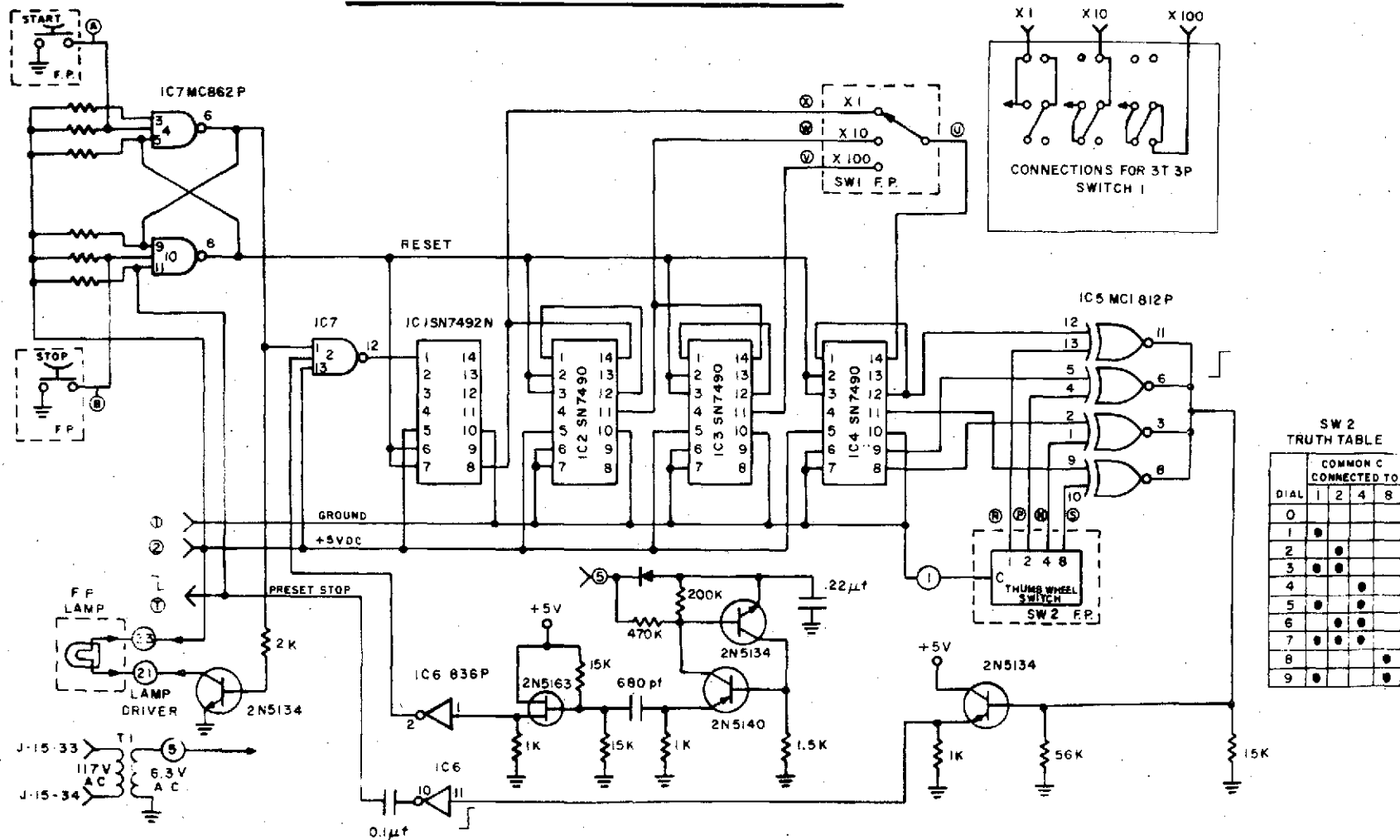


Figure 4b. Schematic of 60-Hz timer with Start-Stop flip-flop controlled by push buttons.

COMPARISON OF COMPACT SCINTILLATION DETECTORS
FOR BONE MINERAL CONTENT MEASUREMENTS

by

R. M. Witt and R. B. Mazess
Department of Radiology - Cosmic Medicine Laboratory
University of Wisconsin Medical Center
Madison, Wisconsin 53706

It appears that the best detector for counting the transmitted photons in the absorptiometric determination of bone mineral content (BMC) remains a thallium-activated sodium iodide, NaI(Tl), scintillation crystal optically coupled to a photomultiplier tube (PMT). A PMT suitable for the detector to be used with the bone scanner for space flight should be compact to minimize its volume and mass, and it should be a ruggedized type meeting the necessary shock, vibration and acceleration specifications. To serve as part of a low energy (30 keV to 60 keV) scintillation photon detector, the tube should have high current gain ($\times 10^6$) and a low anode dark current ($\sim 10^{-10}$ amperes) at the specified operating voltage and temperature.

In addition the tube should have only a small "hysteresis" instability in the anode current and a small change in the anode sensitivity after the light and the high voltage are applied. The gain should be stable ($< 1\%$ change) with time and for order of magnitude changes in the count rate. The photocathode material should have a high quantum efficiency and the spectral response should be matched to the emission spectrum of NaI(Tl) scintillator which peaks at about 410 nanometers.

The specifications for two small PMT's suitable of space flight were compared to determine if they were suitable for the new compact inflight bone mineral scanner, Table 1. Both PMT's are developmental models. Of the two tubes compared in this report, tube B appears to have the best current gain and dark current specifications while still retaining the need to be small and compact. The prototype scanner, described in another report¹, was designed to use this tube as the scintillation detector.

Reference

1. R. B. Mazess and Y. Towliati, A Compact Scanner for Measurement of Bone Mineral, USAEC Report, COO-1422-120, (1972)

TABLE 1. COMPARISON OF TWO DEVELOPMENTAL PHOTOMULTIPLIER TUBES SUITABLE FOR SPACE FLIGHT

	TUBE A C31016B			TUBE B 11J412			
	MIN	TYPICAL	MAX	MIN	TYPICAL	MAX	UNITS
ELECTRICAL SPECIFICATIONS:							
Cathode Sensitivity	47x10 ⁻⁶	67x10 ⁻⁶			70x10 ⁻⁶		A/lm
Luminous		.079 ¹		.058 ²	.070 ²		A/W
Radiant		24 ¹		17.5 ²	21 ²		%
Quantum Efficiency		1.9x10 ⁵			10 ⁵ at 1700V		
Current Amplification					10 ⁶ at 2400V		
Anode Dark Current		5x10 ⁻¹⁰	1x10 ⁻⁹		2.5x10 ⁻¹¹	1.0x10 ⁻¹⁰	A
Operating Voltage, anode to cathode			1500			3500	V
Operating Current			20			100	μA
MECHANICAL SPECIFICATIONS:							
Maximum Length		4.7			9.3 Potted		cm
Maximum Diameter		2.67			3.18 Potted		cm
Maximum Cathode Diameter		1.90			2.48		cm
Cathode Type		CsKSb			CsKSb		
Window Material		Corning #7056			Corning #7056		
Number of Dynodes		10			12		
ENVIRONMENTAL STRESS:							
Temperature		-100 to +85			-80 to +150		°C
Shock		75± 7g's, 11 ± 1msec			150g, 6msec		
Vibration		20.7g(rms) 50 to 2000Hz			30g, 20 to 2000Hz		

Notes: 1. at 400 nm
2. at 410nm

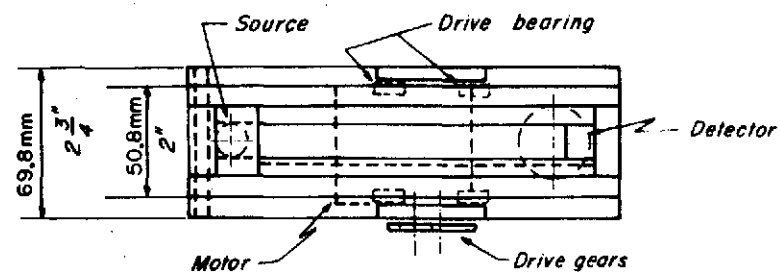
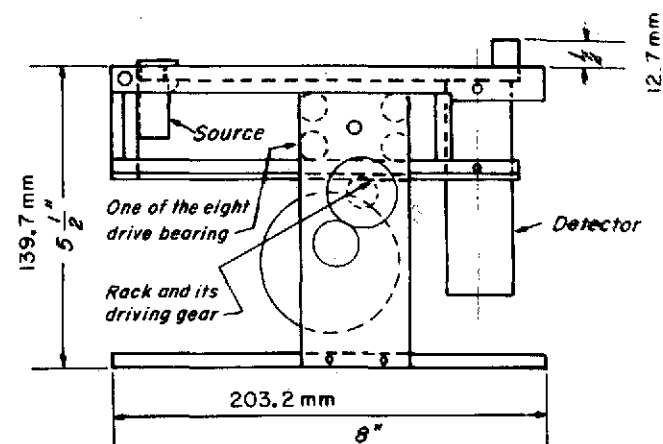
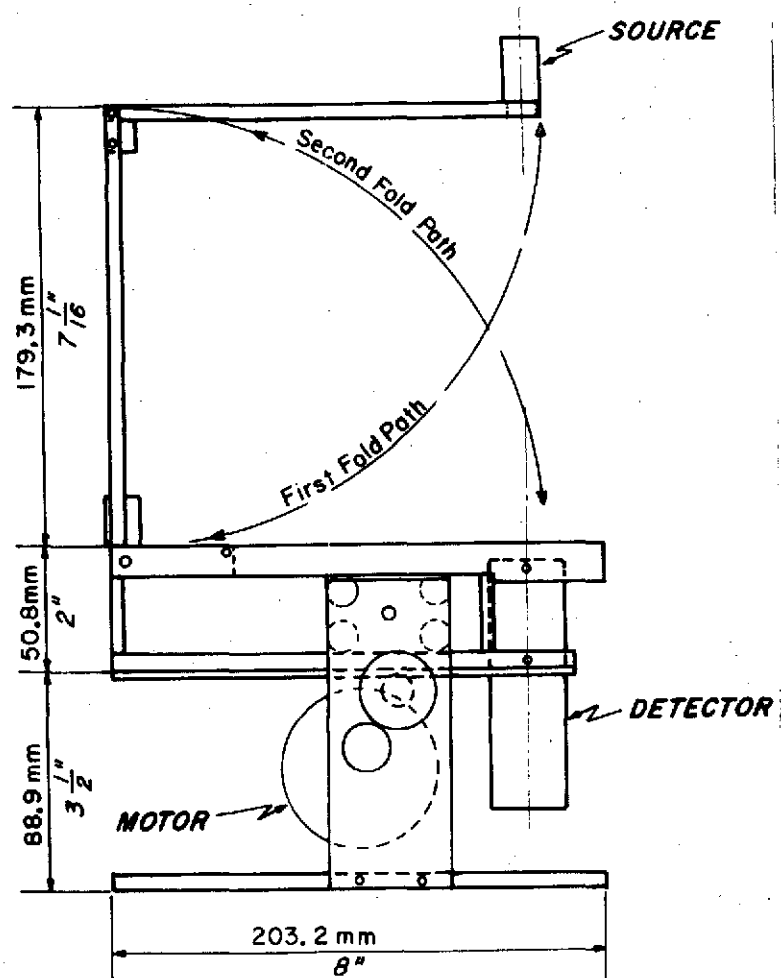
A COMPACT SCANNER FOR MEASUREMENT OF BONE MINERAL

Richard B. Mazess and Youssef Towliati

A small, light-weight mechanical scanner has been constructed as an engineering model for measurement of bone mineral content in astronauts during space flight; the scanner also may be used clinically and in field studies. The scanner was constructed to fold into a storage mode when not in use in order to conserve on space. In the storage mode the approximate dimensions are 200 x 150 x 75 mm; in operation an arm holding the radionuclide source folds out (Figure 1). The weight of the mechanical scanner is about 2000 grams, but it could be lightened considerably. This scanner is to be used with a lucite scanning platform currently under construction.

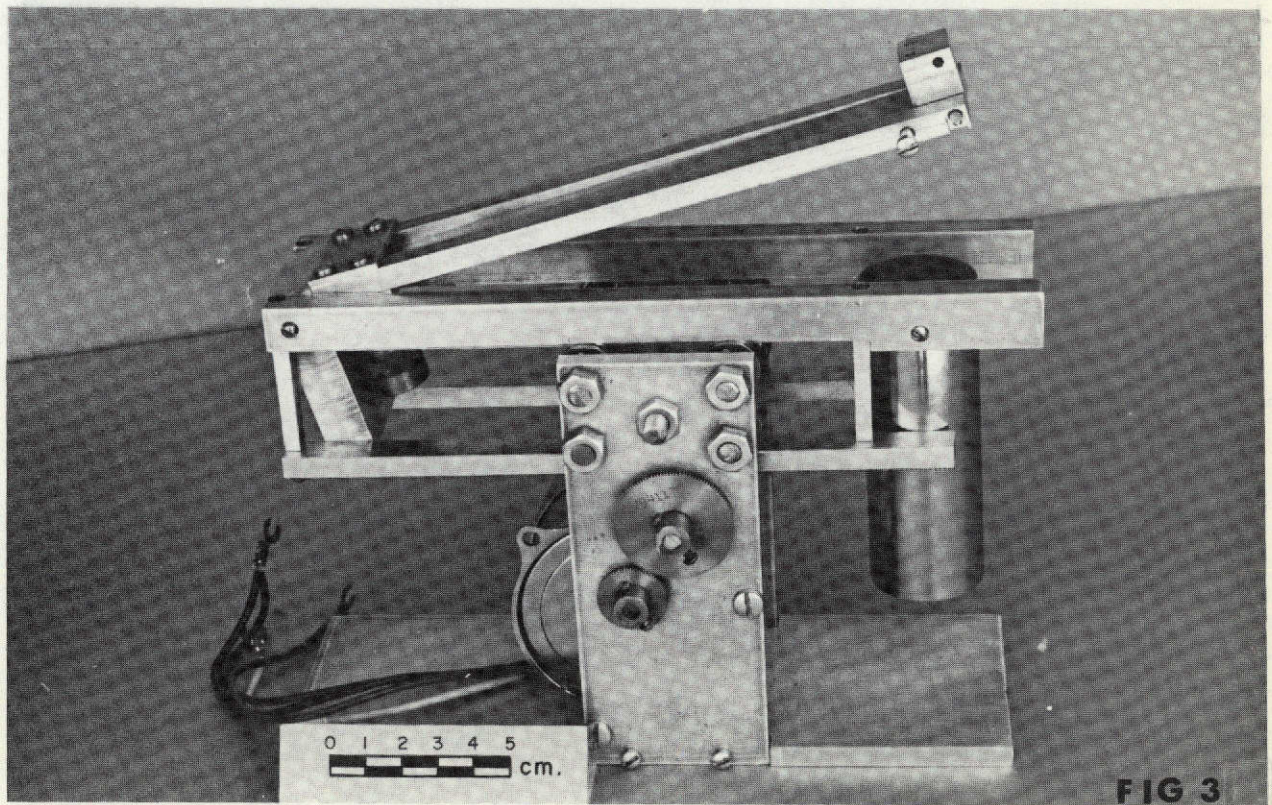
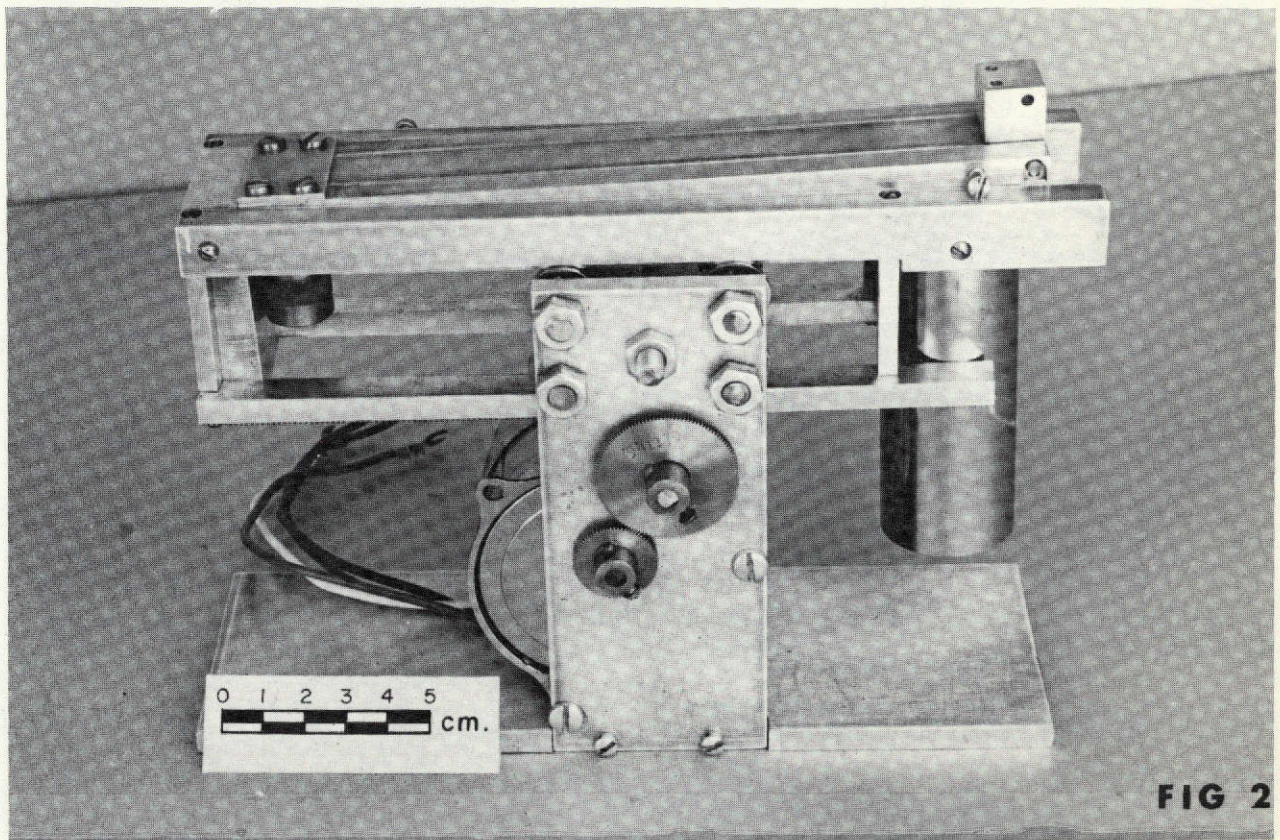
A reversible motor drives the detector-source yoke through drive gears; a rack gear is attached to the yoke. A full 10-cm path can be scanned, thereby allowing measurements across the forearm (radius and ulna). All long bones could be scanned, and it would also be possible to scan across the heel. Scan speed may be altered by changing the gears; we are currently scanning at 1.2-mm per second. A photomultiplier tube-scintillation detector is mounted on the bottom of the yoke; this protects the tube and keeps high voltage lines out of the way. In storage mode the radionuclide source is locked within the body of the yoke; a small lead disc over the source aperture prevents any of the beam from exiting through the folding arm which covers the source.

COMPACT SCANNER

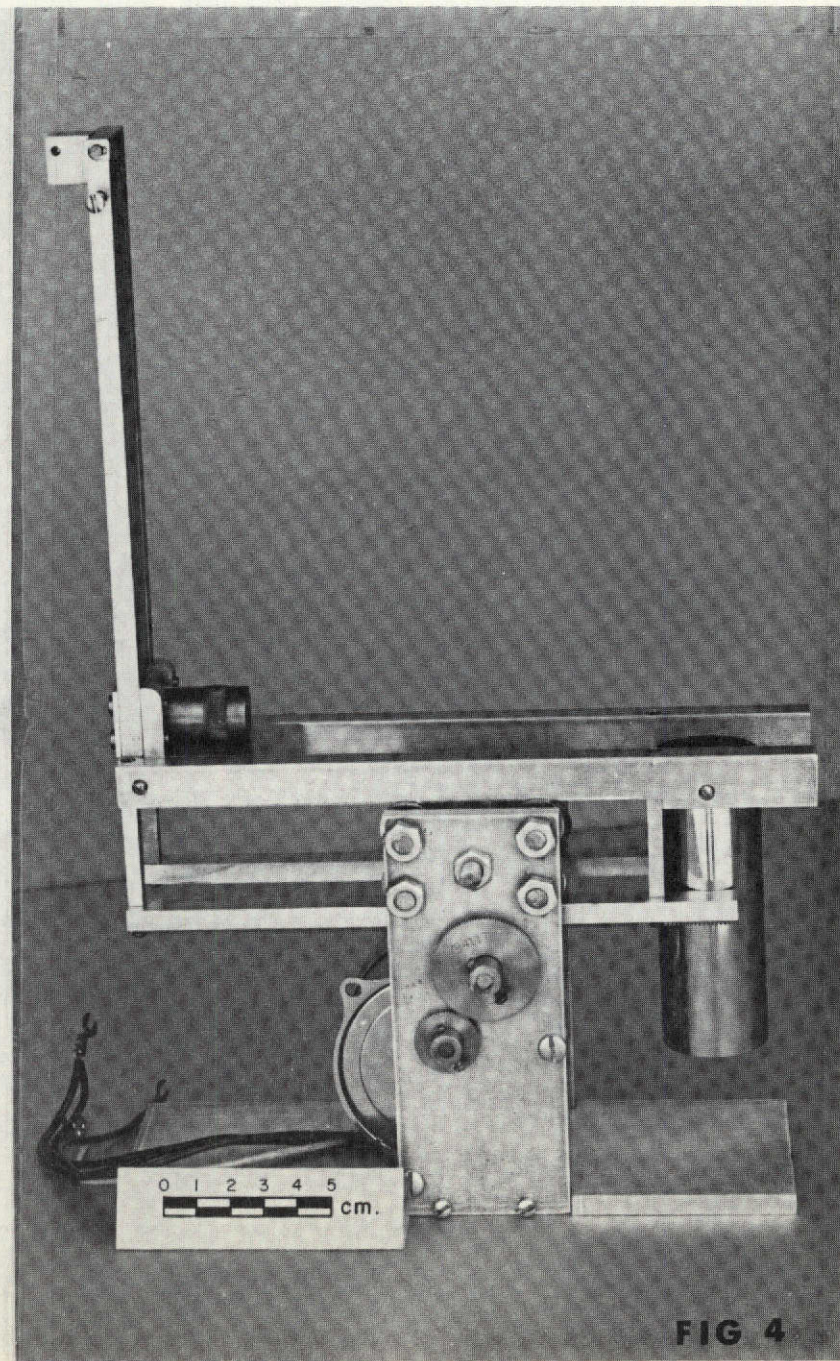
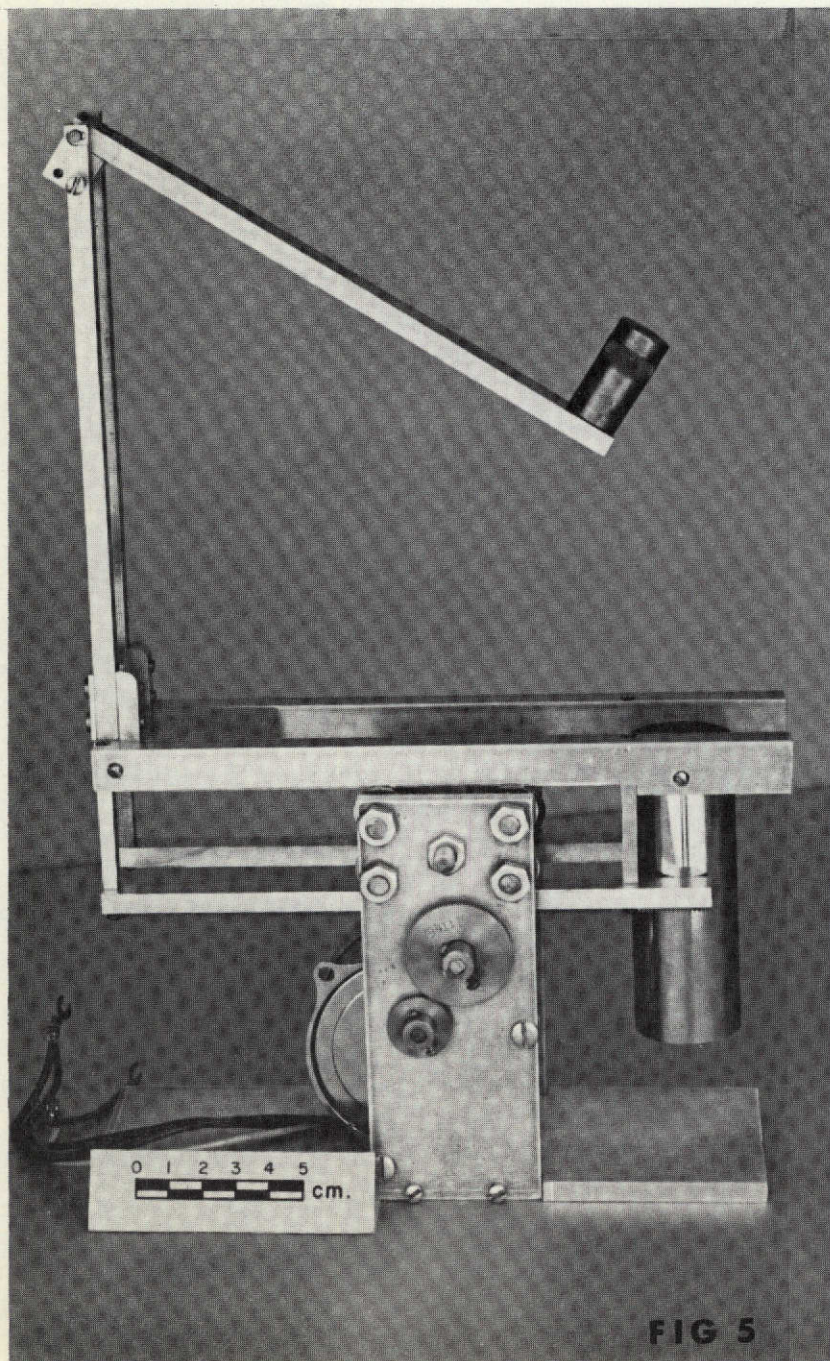


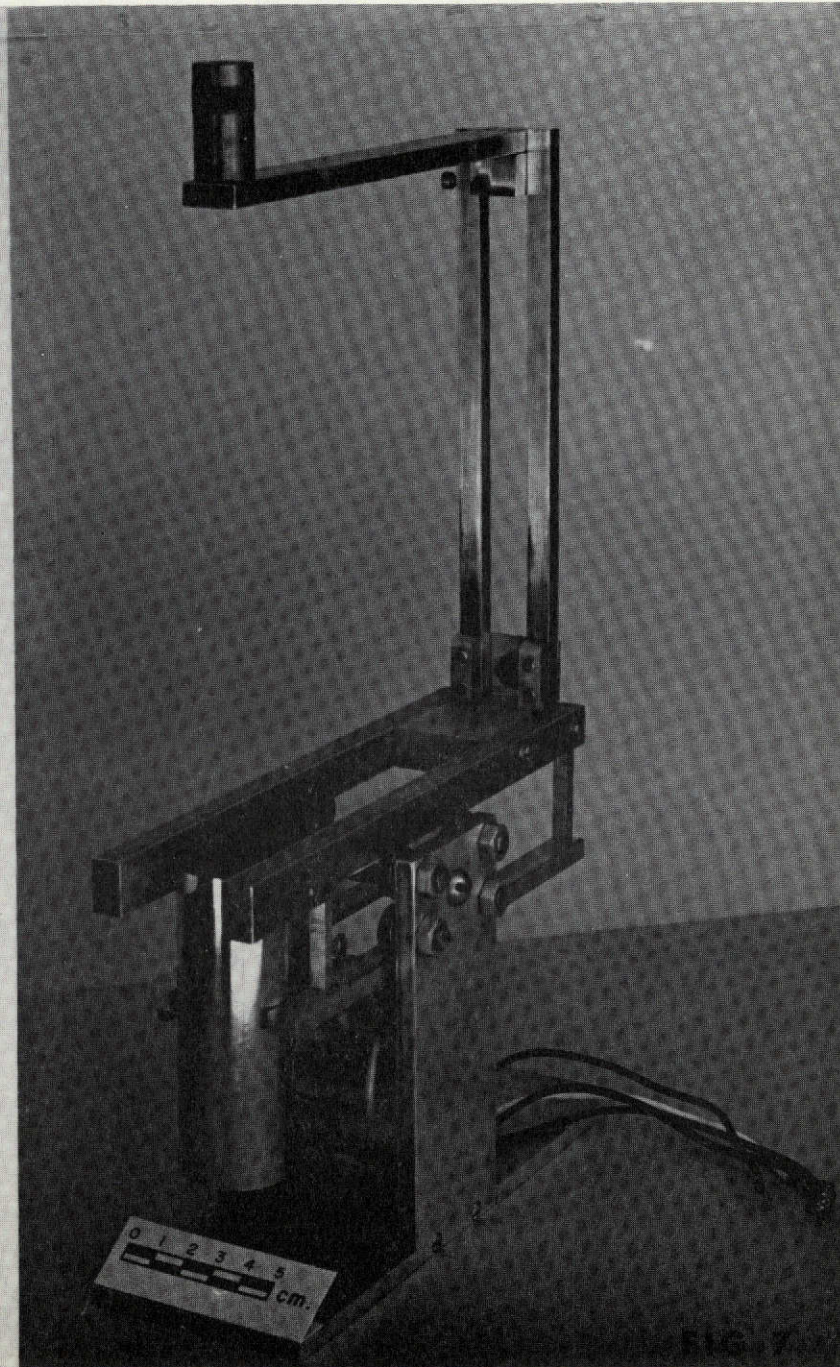
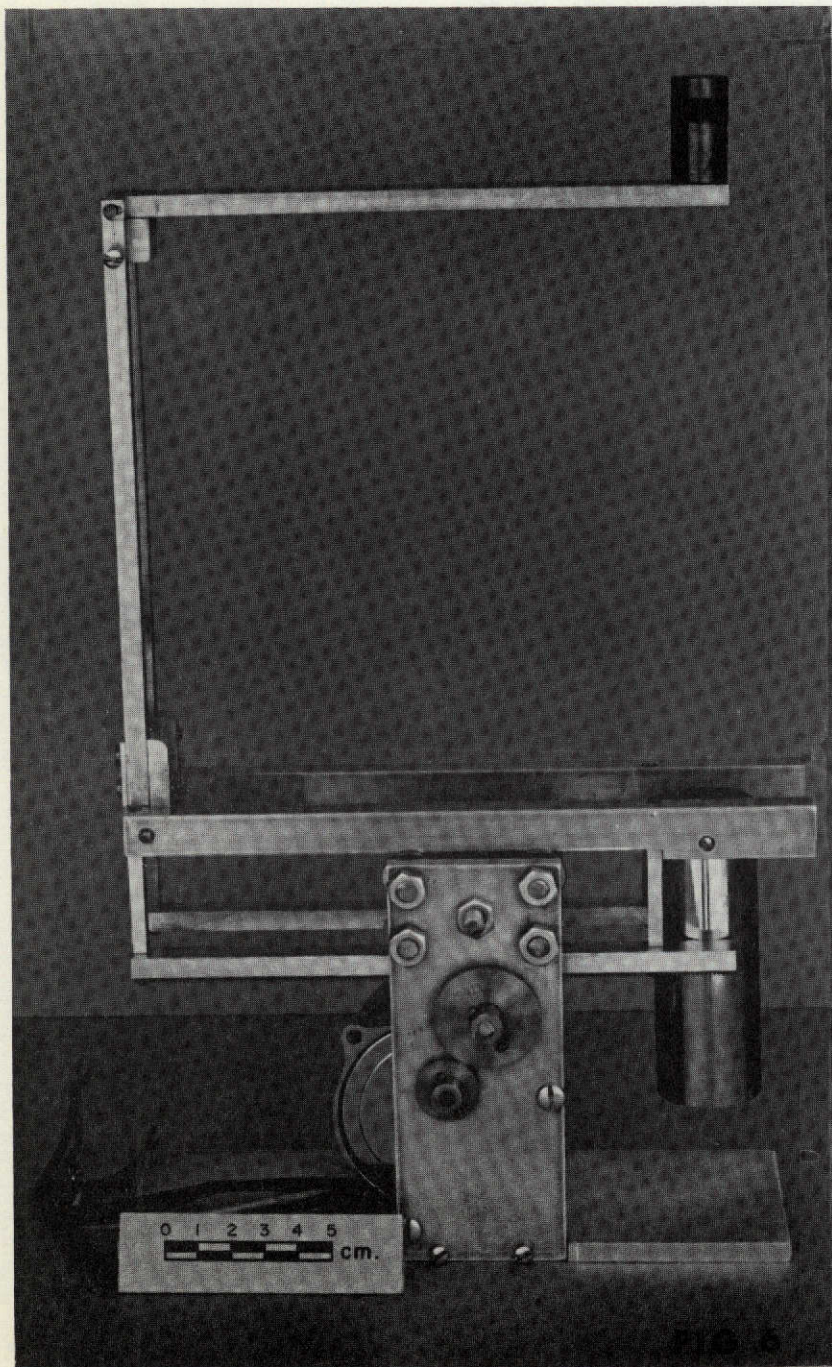
II SIDE AND TOP VIEW IN STORING MODE

Figure 1. Diagrams of the compact bone mineral scanner in operational and in storage modes.



Figures 2 - 7. Progressive views of the folding bone mineral scanner as it is unfolded from its storage position to its scanning position.





BEDREST SUBJECT MEASUREMENTS AT USPHS

by

Philip F. Judy and John R. Cameron
 Department of Radiology
 University of Wisconsin
 Madison, Wisconsin

Studies were undertaken to evaluate the accuracy of the absorptiometric measurement of bone mineral mass of the os calcis^{1,2}. This method is the proposed technique to evaluate the os calcis of the astronauts in Skylab Experiment M078.* The purpose of M078 is to determine the effects of weightlessness on bone and evaluate remedial measures. The bone mineral mass of the os calcis, radius, and ulna of each astronaut will be measured before and after the mission.

Previously x-ray densitometric methods have indicated a decrease in bone mineral mass during weightlessness³, but the poor precision of the method made the results difficult to interpret. The absorptiometric method provides a precise estimate of bone mineral mass, and the accuracy of the radius and ulna measurement is about 3%. The purpose of this study was to evaluate the accuracy of the measurement of bone mineral mass of the os calcis. The principle error of this technique is expected to be by the variation in the composition of soft tissue. The most significant factor is the large lipid content of adipose tissue inside and outside of the os calcis.

Method

The error caused by adipose tissue was estimated from the absorptiometric measurement of the os calcis with monoenergetic photons of different energies (28 keV, 44 keV, 60 keV and 100 keV). The magnitude⁴ of the error for each photon energy for each photon energy is different and is described by equation (1).

$$\text{Log } \frac{I_0^*}{I} - C_1 M_{\text{BM}} = C_2 M_{\text{lipid}} \quad (1)$$

where BM = bone mineral mass traversed.
 M_{lipid} = lipid mass transversed in excess of baseline value.
 C_1 = difference of linear attenuation coefficients of bone mineral and soft tissue divided by the density of bone mineral.
 C_2 = difference of linear attenuation coefficients of lipid and soft tissue divided by the density of lipid.

* Principal Investigator, John M. Vogel, USPHS Hospital, San Francisco, California.

Six bedrest subjects at the USPHS hospital² were scanned three times during the study at two month intervals. They were scanned using ^{125}I (28 keV), ^{241}Am (60 keV), and ^{153}Gd (44 keV and 100 keV) as radio-nuclide sources. A K_2HPO_4 standard was scanned to calibrate each photon beam. The mass attenuation coefficients for polymethyl methacrylate and aluminum were determined.

Preliminary Results

The analysis of the subjects is not finished. The mass attenuation coefficients for each beam are shown in Table I. The results are in agreement with measurements previously made with the same sources⁵.

The measured calibration constants, $1/C_1$, are shown in Figure 1. The values were compared with the theoretical values predicted by the mass attenuation coefficients of water and bone mineral. The excellent agreement indicated the contrast between polymethyl methacrylate and K_2HPO_4 saturated solution vary as function of photon energy similarly to water and bone mineral between 28 keV and 100 keV. The calibration procedure therefore was felt to be valid with respect to the effects of the variation of chemical composition of tissues.

Analysis to be Undertaken

The precision of the subject measurements at each photon energy will be determined. This will determine the precision of the bone mineral mass measurement if a correction were made using Equation (1) and photon beams of various energies were used. Since the primary consideration in M078 is the determination of small changes of bone mineral mass and each individual is his own control, the precision of a new method should be the same or better than the absorptiometric technique using ^{125}I , if it is to be recommended as a replacement.

The effect of different size beams and different energies on the "edge effect"⁵ will be determined, so differences caused by different size beams will not be interrupted as an error caused by the variation in the adipose tissue.

Table I
Mass attenuation coefficients (cm^2/g)

	28 keV		44 keV		60 keV		100 keV	
PMM*	0.3255	0.001	0.2155	0.0003	0.1842	0.0005	0.1685	0.0031
Al	nd		0.5063	0.0014	0.2823	0.0001	0.1649	0.0003

* PMM-polymethyl methacrylate

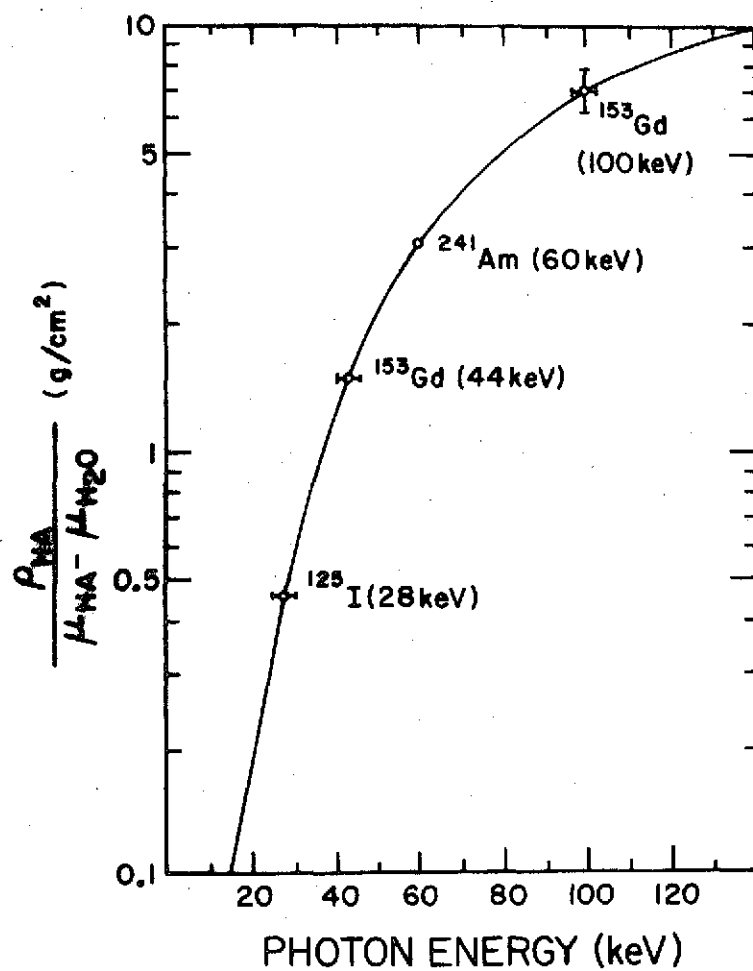


Figure 1

Comparison of the measured and theoretical values of the density of bone mineral divided by the difference of the linear attenuation coefficients of bone mineral and soft tissue ($1/C_1$)

Acknowledgments

Partial support was provided by funds from NASA grants Y-NGR-50-002-051 and NAS 9-12306.

We wish to thank F. N. Case and his colleagues at Isotopes Development Section, Oak Ridge National Laboratory who fabricated the ¹⁵³Gd source.

References

1. Cameron, J. R., and Sorenson, J. A: Measurement of Bone Mineral In Vivo; An Improved Method. Science 142:230-232 (1963)
2. Vogel, J. M., and Anderson, J. T: Rectilinear Transmission Scanning of Irregular Bones for Quantification of Mineral Content. J. of Nuclear Medicine 13:13-18,(1972)
3. Mack, P. B. and LaChance, P. A: Effects of Recumbency and Space Flight on Bone Density. Amer. J. Clin. Nutr. 20:1194-1205, (1967)
4. Wooten, W. W., Judy, P. F., and Greenfield, M. A: Analysis of the Effects of Adipose Tissue on the Absorptiometric Measurement of Bone Mineral Mass. Submitted for publication.
5. Judy, P. F: Theoretical Accuracy and Precision in Photon Attenuation Measurement of Bone Mineral. In Proc., Bone Measurement Conference, Cameron, J. R., Ed. CONF-700515, p. 1-21, (1970)

PREDICTION OF BODY COMPOSITION FROM ABSORPTIOMETRIC LIMB SCANS

by

Richard Mazess
Department of Radiology
University of Wisconsin Medical Center
Madison, Wisconsin

It has been shown that absorption measurements at two energies can be used to measure the fractional composition of a two-component absorber, and this approach has been used to determine the fat and lean cellular mass of soft tissue (Mazess et al, 1970; Sorenson and Cameron, 1964; Preuss and Schmonsees, 1972). Absorptiometric scanning with low-energy nuclides to determine fat, lean-cellular, and bone mass in vivo has been developed at the University of Wisconsin Bone Mineral Laboratory. The relationship between these local measurements, usually on the limbs, and total body composition is unknown, but a high degree of association was expected since even poor measures of local composition, such as skinfolds or limb circumferences, are fairly highly correlated with total body composition. This preliminary report describes the results obtained in normally hydrated and dehydrated subjects.

Methods

Measurements were made on ten adult males at the NASA Ames Research Center. Anthropometric determinations, including skinfolds (Harpender caliper) and circumferences, were made on each subject. Subjects ranged from 6 to 33% body fat and from 66 to 126 kg in body weight. In addition measurements were made of total body water (deuterium oxide dilution) and body density (underwater weighing, with determination of residual volume). Absorptiometric scans were made with ^{125}I and ^{241}Am across the middle of the upperarm and the forearm, and across the lower part of the calf. At least two scans were done with each radionuclide at each site. Sites on both sides of the body were measured. Four of the subjects were remeasured after several days of voluntary dehydration in which they lost 1.6 to 4.0% of body weight, or 2.4 to 5.6% of body water.

Measurements were made on standards on about eight occasions (Table 1). There was a low coefficient of variation for "tissue" mass measurements, and slightly higher variation for "bone" mass measurements. More important, however, is the low variation (less than 1%) for the $^{125}\text{I}/^{241}\text{Am}$ absorption ratio which indicates the relative amounts of lean and fat. Previous studies also showed a long-term precision of about 1% for this ratio (Mazess et al, 1970).

Table 1. Coefficients of Variation for Measurements of Standards

		n=7 <u>SMALL</u>	n=9 <u>LARGE</u>
125-I	TISSUE	.62%	.60%
	BONE	.55%	1.51%
241-Am	TISSUE	.60%	.46%
	BONE	2.88%	1.81%
RATIO	TISSUE	1.00%	.66%
	BONE	2.66%	2.53%

Results

There was only a slight difference between the right and left side determinations on the subjects (Table 2). The variation of tissue mass from ^{125}I or ^{241}Am scans was 3 to 4%, but this variability was largely anatomical as seen by the similar magnitude of variability in tissue width. The variability in $^{125}\text{I}/^{241}\text{Am}$ ratio, however, was quite low (1%) showing the relative uniformity of composition from side to side. Moreover the overall variability among the measurements of $^{125}\text{I}/^{241}\text{Am}$ ratio in these subjects was small (1%). There was little if any advantage to dividing the total mass by tissue width, nor was there any advantage to dividing the scan into peripheral or central segments. In contrast, there was a high variability in fat-fold measurement (15%).

Table 2. RMS variation between right and left sides on 14 determinations at three scan sites.

	<u>UPPERARM</u>	<u>FOREARM</u>	<u>CALF</u>
125-I	3.40%	4.02%	2.75%
241-Am	3.56%	3.87%	3.11%
Width	2.38%	2.46%	3.03%
RATIO	.64%	1.18%	.76%

Local absorptiometric measurements were highly correlated with total body fat as estimated by the formula of Siri (1956) from both density and total body water. The best estimate in the normally hydrated men was given by an average of all three scan sites; the dehydrated men tended to fall slightly below this regression line (Figure 1). The regression line itself deviated somewhat from the theoretical line. The upperarm scan was of major influence in predicting total body fat, the calf measurement was only moderately associated and the forearm measurement was even of lower degree of association (Table 3). The upperarm fatfold (average of both sides) was moderately correlated with total body fat, and the sum of eight fatfolds was very highly correlated ($r = 0.97$).

In dehydrated subjects the calf seemed most markedly affected and measurements at this site, and also at the forearm site, had a higher prediction error. Upperarm scans were not affected by dehydration and

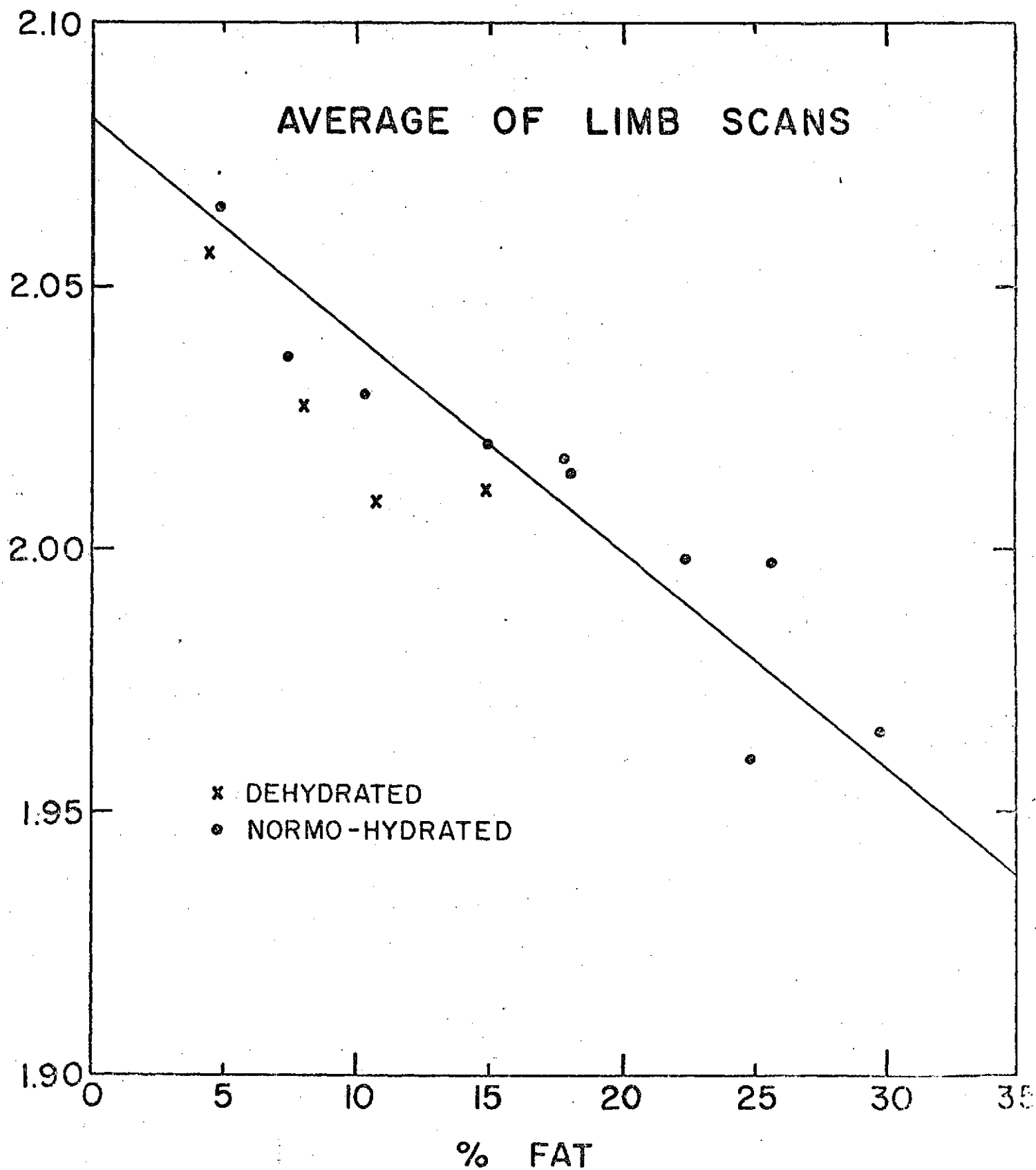


Figure 1. Relationship between average absorptiometric scan ratio and the percentage of body fat in 10 normally hydrated and in 4 dehydrated adult males.

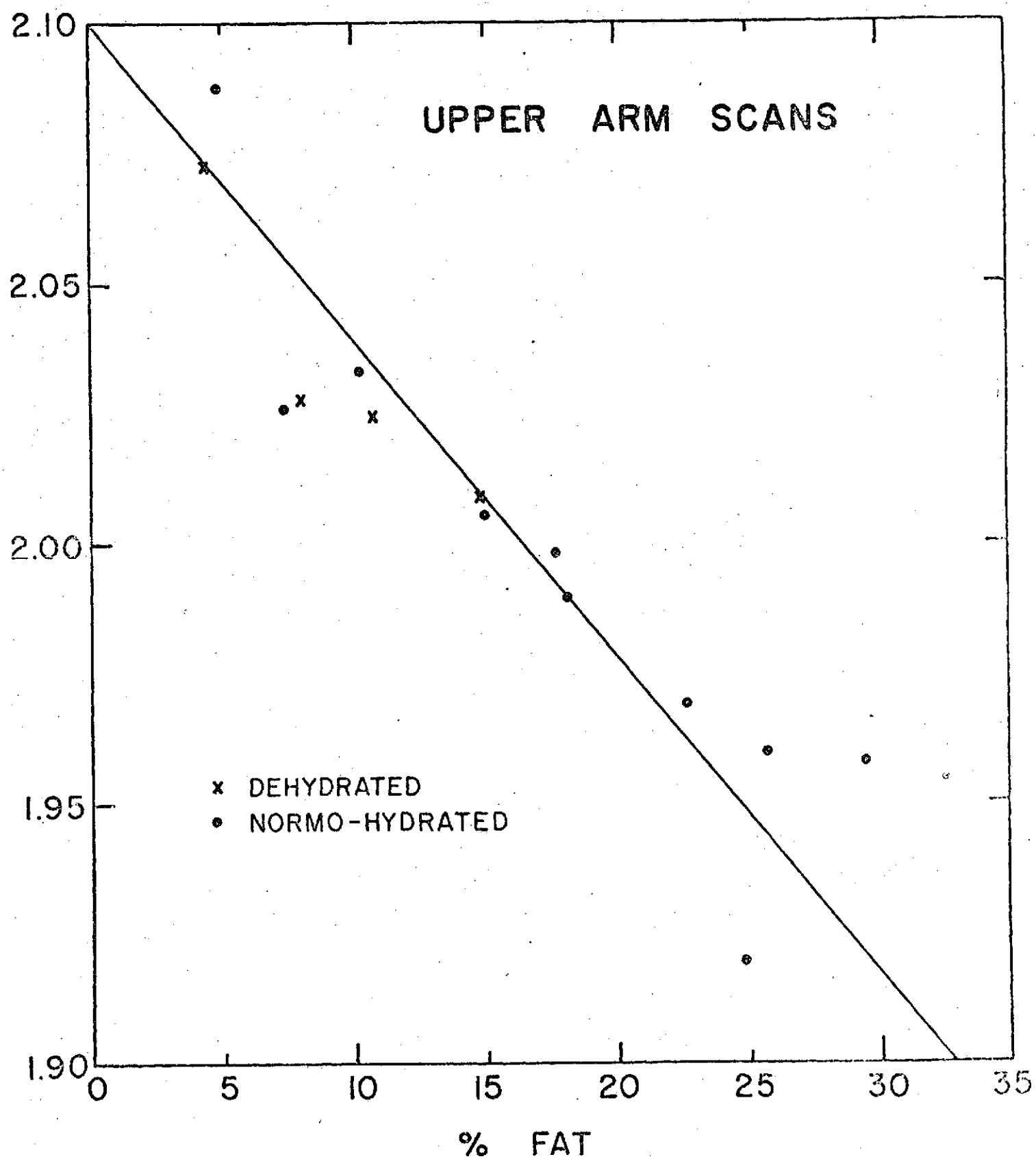


Figure 2. Relationship between the absorptiometric scan ratio on the upperarm and the percentage of body fat in 10 normally hydrated and 4 dehydrated adult males.

predictability was just as good for data from dehydrated subjects (Figure 2). The correlation for all 14 determinations for upperarm ratio and body fat was 0.93 and the standard error of estimate was 3.2%. Fatfolds were also not affected by dehydration and their prediction accuracy remained high.

Table 3. Correlations between local measurements and percent body fat (Siri 1956), and the standard error of estimates in predicting body fat; measurements in ten normally hydrated men.

		<u>r</u>	<u>SEE</u>
SCANS	UPPERARM	-0.91	3.56
	FOREARM	-0.70	6.22
	CALF	-0.85	4.56
	3 SITES	-0.93	3.24
FATFOLDS	UPPERARM	0.86	4.45
	SUM of 8	0.97	1.96

It is interesting that the regression relationship between upperarm absorptiometric ratio and body fat is close to the theoretical relationship between this ratio and fat concentration. Theoretically at 100% lean the ratio should be about 2.10 while at 100% fat the ratio should be about 1.53; the values from the regression are 2.10 and 1.49. The forearm and calf scans have a different relation to body fat as does the average ratio derived from all three sites. The upperarm site seems to be the choice in terms of ease of measurement, highest precision, best prediction of total body fat, and close approximation to theoretical expectation.

The absorptiometric scans also permitted measurement of bone mineral content, and total skeletal weight was predicted from these scans as described by Mazess (1971). Total mineral weight in these adult males averaged 2817 g; this was 3.53% of total body weight and 4.38% of lean body mass. Total mineral and body water were used to calculate lean body mass; the density of lean body mass was 1.093 versus the usually accepted value of 1.10. The lower density was a result of the lower mineral weight in these subjects. Up until the present time it has been erroneously assumed that the total mineral is a much higher proportion of total body weight and of lean body mass, and no accurate prediction of mineral mass has been possible.

Discussion and Conclusions

Absorptiometric scans on the limb, especially the upperarm, are related not only to the local composition in the scan path but to the total body composition (as determined by indirect techniques). It has already been shown that absorptiometric determinations of lean-fat composition are very accurate and precise (1% error), and the present results show that they are representative of total body composition as well. Other local measures, such as fatfolds, when used with care are also very

highly correlated with total body fat. However, fatfolds are quite variable and cannot be determined with precision. There is a 15% side to side variation in fatfolds for example, and the long-term precision is even poorer. Moreover, the compressibility of adipose tissue varies with age and sex, and this together with anatomical variability means that the relationship between fatfold and total body fat will change with age, sex, nutritional status, and other factors. On the other hand absorptiometric determinations are very precise direct measurements of lean-fat composition, and it appears unlikely that the relationship between these measures and total fat will be appreciably changed by age, sex, or hydration. An additional advantage of absorptiometry is that bone mineral content is also measured and this allows a prediction of total skeletal weight; this value can be used to correct the prediction of body fat and lean body mass.

For surveys of nutritional status the fatfolds are obviously advantageous, but for quantitative research or clinical studies the more precise absorptiometric technique is preferred.

Acknowledgements

This research was supported by NASA Y-NGR-50-002-051, NASA Y-NGR-50-002-183, and AEC-(11-1)-1422 . The work was performed while the author was on a NASA Faculty Fellowship at Ames Research Center during the summers of 1970 and 1971. The aid of John Greenleaf, Don Young, Wayne Howard, Jim Bosco, and Laszlo Juhos is gratefully acknowledged.

References

1. Mazess, R. B., Cameron, J. R. and Sorenson, J. A., 1970. Determining body composition by radiation absorption spectrometry. Nature 228:771-772.
2. Mazess, R. B., 1971. Estimation of bone and skeletal weight by direct photon absorptiometry. Invest. Radiol. 6:52-60.
3. Preuss, L. E. and Schmonsees, W., 1972. ¹⁰⁹Cd for compositional analysis of soft tissue. Int. J. Appl. Radiation Isotopes. 23:9-12
4. Siri, W. E., 1956. The gross composition of the body. In: Lawrence, J. H., and Tobias, C. A., (eds). Advances in Biological and Medical Physics, Vol. IV. Academic Press, N. Y.
5. Sorenson, J. A. and Cameron, J. R., 1964. Body composition determination by differential absorption of monochromatic x-rays. In: Symp. Low-Energy X- and Gamma Sources and Applications. Technology Research Institute, Chicago. AEC Report ORNL-11C-5: 277-289.

BONE MINERAL CONTENT OF ESKIMOS IN ALASKA AND CANADA:

PRELIMINARY REPORT

by

W. Mather and R. B. Mazess
Department of Radiology
University of Wisconsin
Madison, Wisconsin

During the past year (October, 1971 and May, 1972) measurements of the bone mineral content were made on the Eskimo inhabitants of two villages in the Foxe Basin of Canada's Northwest Territories (Hall Beach and Igloolik). This is a preliminary report of these measurements and a compilation of measurements made in 1968-1970 on the Eskimos living in the villages of Point Hope, Wainwright, and Barrow.

METHODS

Direct photon absorptiometry as developed at the University of Wisconsin was used to determine the bone mineral content at two locations on both the radius and ulna (Cameron and Sorenson, 1967). Measurements in all five villages were made with a portable system that allowed immediate digital readout of bone mineral content and bone width (Mazess et al., 1972). All scans of the radius and ulna were made with an ^{125}I source (28 keV). A three-chambered bone phantom of saturated dipotassium hydrogen phosphate solution was used for calibration (Witt et al., 1970).

In Canada bone mineral content determinations were made on 335 subjects, 164 from Hall Beach and 171 from Igloolik. There were 177 children age 5 to 19, 123 adults age 20-49, and 35 elderly age 50 and up. Males and females were equally represented in all age groups. In Alaska there were 413 subjects measured of which 63 were measured in 2 successive years (an average was taken in these cases). 217 of these were children, 88 were adults and 107 were elderly.

Four scans were made at each site in order to obtain an average value. The coefficient of variation of the determination at each site varied from 1.5 to 4%, decreasing with larger bone sizes and older subjects.

The data from the different villages was merged into Alaskan or Canadian groups after T-tests were performed. Most of the significant differences found could be attributed to the highly variable bone width at the site of the distal ulna.

RESULTS

Heights and weights of Eskimos in Canada and Alaska, and of U.S. whites,

are presented in Table 1. U. S. whites are taller and heavier than Alaskan Eskimo males and taller than Alaskan Eskimo females. Alaskan Eskimo males and females throughout growth and adulthood have greater heights, and weigh more than Eskimos in the Foxe Basin of Canada.

Tables 2 and 3 give the bone mineral content in grams/centimeter and bone mineral-to-width ratios of Eskimos and whites. During the years of growth (5-19 years) Canadian Eskimo children have lower bone mineral content than Alaskan Eskimo children who, in turn, are lower than U.S. whites.

Both groups of Eskimo adults (age 20-49) demonstrate a similar bone mineral content. Evidently the Canadian Eskimo children grow at a slower rate, but as adults reach a bone mineral content equivalent to Alaskan Eskimos. Male and female Eskimo adults, Canadian and Alaskan, are at levels 8% less than U.S. whites

In the elderly we find that Eskimos lose bone mineral at a rate greatly accelerated compared to that of whites. The loss is as much as 22% greater in both males and females from Canada age 60-69, and 27% greater in females 70 and up from Alaska.

DISCUSSION AND CONCLUSIONS

The lower bone mineral content of Eskimos is commensurate with their smaller height and weight. In Canada bone mineral content is 8% lower as is height and weight; in Alaska, height is 5% lower but bone mineral content is only 1% lower. Apparently Canadian Eskimos have a normal bone mineral content status relative to stature, and by this reference Alaskan Eskimos may even be slightly elevated. In the elderly this is not the case; both Eskimo groups lose bone mineral content, and the loss is far greater than stature differences.

Data collected on a skeletal series of Sadlermiut Eskimos from Southhampton Island show similar patterns of high bone loss in the elderly. This appears associated with increasing risk of fracture in the same population. It remains to be seen if the extensive bone loss in elderly contemporary Eskimos is associated with skeletal problems, and to isolate the factors operative in this population.

TABLE 1. AVERAGE HEIGHTS AND WEIGHTS OF ESKIMO AND WHITE SUBJECTS BY AGE

	<u>AGE</u>	<u>NUMBER</u>			<u>HEIGHT (cm)</u>			<u>WEIGHT (kg)</u>		
		Canada	Alaska	U.S.	Canada	Alaska	U.S.	Canada	Alaska	U.S.
MALES	5-7	12	23	41	116	117	125	22.5	23.3	24.5
	8-9	24	19	47	125	130	138	27.1	30.4	31.0
	10-11	20	22	55	135	140	147	32.6	35.2	37.7
	12-14	20	20	45	147	151	160	43.1	47.5	52.2
	15-16	8	9	43	163	163	175	55.3	55.1	68.1
	17-19	10	15	37	165	171	182	60.6	69.7	74.5
	20-49	61	40	68	163	168	178	65.8	68.4	77.5
	50-59	12	13	24	163	166	176	61.0	74.6	77.0
	60-69	8	27	35	156	163	175	60.1	67.7	75.4
	70+	-	13	32	-	163	175	-	69.8	71.2
FEMALES	5-7	12	26	32	113	120	126	21.5	24.5	24.3
	8-9	12	22	36	123	128	136	26.2	28.9	29.4
	10-11	17	17	43	132	140	147	30.7	37.3	38.0
	12-14	20	22	46	148	152	162	44.5	53.1	48.6
	15-16	9	10	37	153	157	166	53.4	58.7	56.2
	17-19	13	12	62	152	158	166	53.4	59.9	58.3
	20-49	62	49	121	153	155	163	55.3	63.3	62.5
	50-59	11	23	37	150	153	162	61.6	62.4	64.9
	60-69	4	20	43	146	153	160	62.1	65.5	61.5
	70+	-	11	103	-	141	160	-	48.6	57.7

TABLE 2. BONE MINERAL CONTENT IN CANADIAN AND ALASKAN ESKIMOS AND IN
UNITED STATES WHITES (gram/centimeter)

AGE	<u>MALES</u>			<u>FEMALES</u>		
	Canada	Alaska	U.S.	Canada	Alaska	U.S.
5-7	.44	.46	.50	.38	.44	.45
8-9	.48	.54	.57	.43	.48	.52
10-11	.57	.63	.67	.49	.56	.61
12-14	.71	.76	.81	.67	.76	.78
15-16	.88	.93	1.08	.81	.85	.87
17-19	1.06	1.16	1.20	.82	.88	.92
20-49	1.21	1.21	1.31	.88	.90	.97
50-59	1.06	1.13	1.33	.78	.78	.86
60-69	.99	1.02	1.24	.65	.69	.80
70+	-	1.06	1.23	-	.51	.71

TABLE 3. BONE MINERAL/WIDTH IN CANADIAN AND ALASKAN ESKIMOS AND IN
UNITED STATES WHITES (gram/centimeter²)

AGE	<u>MALES</u>			<u>FEMALES</u>		
	Canada	Alaska	U.S.	Canada	Alaska	U.S.
5-7	.47	.47	.50	.44	.48	.49
8-9	.51	.53	.55	.48	.50	.55
10-11	.54	.57	.60	.52	.58	.59
12-14	.60	.64	.65	.62	.68	.67
15-16	.68	.72	.76	.68	.72	.73
17-19	.75	.82	.82	.69	.74	.75
20-49	.78	.82	.88	.69	.73	.76
50-59	.68	.75	.88	.60	.61	.70
60-69	.62	.68	.79	.49	.54	.63
70+	-	.69	.79	-	.40	.55

References

1. Cameron, J. R. and Sorenson, J. A. Measurement of bone mineral in vivo: an improved method. Science 142:230-232, 1963
2. Cameron, J. R., Mazess, R. B., and Sorenson, J. A. Precision and accuracy of bone mineral determination by direct photon absorptiometry. Invest. Radiol. 3:141-150, 1968
3. Mazess, R. B., Cameron, J. R., and Miller, H. Direct readout of bone mineral content using radionuclide absorptiometry. Int. J. Appl. Radiation (in press) 1972
4. Sorenson, J. A. and Cameron, J. R. A reliable in vivo measurement of bone mineral content. J. Bone Jt. Surg. 49A: 491-497, 1967
5. Witt, R. M., Mazess, R. B., and Cameron, J. R. Standardization of bone mineral measurements. ASAEC Report COO-1422-70, 1970

Acknowledgement

This work is supported in part by NASA-Y-NGR-50-002-051 and by AEC-(11-1)-1422. The studies were part of the Canadian and Alaskan International Biological Program, Human Adaptability Section.

PROGRESS IN CLINICAL USE OF PHOTON ABSORPTIOMETRY*

R.B. Mazess, P.F. Judy, C. Wilson, and J.R. Cameron
Department of Radiology (Medical Physics Section)
University of Wisconsin Hospital, Madison 53706
Proc. Int. Symp. Clinical Aspects of Metabolic Bone
Disease (Detroit, June 1972) Excerpta Medica Press
(in press)

INTRODUCTION

Direct photon absorptiometry by low energy (20- to 100-keV) radionuclide transmission scanning provides a precise and accurate (less than 2% error) indication of bone mineral content. This method, since its introduction a decade ago, has achieved widespread acceptance by researchers and clinicians concerned with measurement of the skeleton. Details of the method, experimental results, and varied applications have been described in numerous publications, and have been dealt with in a recent symposium volume (Cameron, 1970). The essence of the absorptiometric method consists of passing a mono-energetic well-collimated beam of radiation, typically from a several hundred mCi source of ^{125}I (27.4keV) across a limb; the changes of beam attenuation due to the bone mineral are recorded and analyzed. In the past decade considerable sophistication has been gained relating to instrumentation, data interpretation, and biomedical application. This report describes some of the technical progress made in our laboratory, particularly those innovations with direct bearing on medical applications. In addition, some of the biomedical applications of absorptiometry and clinical findings are discussed.

TECHNICAL INNOVATIONS

(a) Direct Readout System: For the past decade most systems for photon absorptiometry have used scaler-timers and digital output. Over the past several years our laboratory has developed an analog system, using a precision linear-ratemeter and logarithmic conversion of the ratemeter signal, to provide immediate digital readout of bone mineral content and bone width (Mazess et al., in press). The direct readout system has several advantages over digital handling of scan data including: (1) lower operational and equipment costs, (2) immediate availability of results, and (3) smaller size and weight, allowing greater mobility. These advantages have lead one company (Norland Instruments) to produce a commercially-available direct readout system. Complete plans for construction of such a system are available from the University of Wisconsin Instrumentation System Center (Engineering Research Bldg.)

* Supported by NASA - Y - NGR - 50 - 002 - 051 and AEC-(11-1)-1422

Table 1. Precision of measurement of a three-chambered standard over a 20-month period of clinical use; figures are coeff. of variation.

CHAMBER	AMONG MEASUREMENTS			AMONG 7 SOURCES	
	Mineral	Width	n	Mineral	Width
SMALL	1.91%	0.96%	275	1.58%	0.41%
MEDIUM	1.19%	0.96%	969	0.72%	0.30%
LARGE	1.04%	0.45%	275	0.84%	0.23%

The direct readout system is as accurate and precise as earlier digital systems. Over a 20-month period the coefficient of variation for hundreds of measurements on standards was about 1% (Table 1); the error in predicting the ash weight of bone sections was about 1.5%. Clinical measurements were done on about 100 patients using both digital and analog systems simultaneously; the results from both systems were highly correlated ($r=0.99$) and the standard error of estimate in predicting from one system to the other was about 3%.

(b) Analysis of Sources of Error: A variety of technical factors, excluding gross errors in setting-up instrumentation, can effect absorptiometric scans. These factors are associated chiefly with the nature of the photon beam; the source, its geometry and filtration, are quite important, as is detector geometry. P.F. Judy has investigated and evaluated the sources of error in his doctoral dissertation ("A Dichromatic Attenuation Technique for the In Vivo Determination of Bone Mineral Content") including:

- (1) finite counting intervals
- (2) beam profile
- (3) beam hardening and filtration
- (4) edge effects
- (5) scattered radiation
- (6) counting statistics
- (7) variation of bone mineral composition
- (8) variation in the composition of the soft-tissue surrounding the bone or in the marrow cavity.

These technical factors can be controlled so that precision and accuracy is maintained. Deviations can be ascertained by making determinations on suitable standards, or through other appropriate calibration procedures. R.M. Witt has developed standards consisting of annuli of dipotassium phosphate solution in a lucite block; these permit assessment of precision over time, and allow calibration. Variation among seven laboratories in values reported for these standards was within about 2% indicating the small errors involved in absorptiometry even in completely different laboratories.

The largest single source of error in making serial measurements on an individual, or in comparing individuals, does not involve the method itself but only the location of the correct scan site. The magnitude of this error is inversely proportional to the care taken in positioning the

subject. For linear scans in the clinic routine precision is on the order of 2%, but it can be improved to 1% by making individualized casts of the subject's limb. In field surveys the precision is reduced to about 5%.

(c) Area Scanning: One way to minimize repositioning and location errors is to scan a larger area of the limb in order to average out anatomical irregularities, or any peculiar local anomalies. J. Sandrick has developed a small light-weight scanner for rectilinear area scanning. Plans of this scanner, and its controls, are available from the AEC Technical Information Service.

We evaluated the increased precision achieved by area scanning over conventional linear scans by measuring 5 subjects, using both approaches, on 5 occasions over a 6-week period. The variation in mineral content is reduced by about 40% while the variation in width over time is reduced by only 10% on the forearm bones (Table 2). The absolute magnitude of the error, however, is quite important; area scanning on the radius gives a precision of 0.8% which permits sensitive assessment of changes in mineral content.

Table 2. Comparison of the precision of area scanning versus linear scanning on the forearm bones at midshaft. The data are averages from 5 subjects done on 5 occasions over a 6-week period; 10 repeat scans were done on each subject on each occasion.

		COEFF. VARIATION		AREA/ LINEAR	AREA- LINEAR
		area	linear		
<u>ULNA</u>	MINERAL WIDTH	1.58%	2.37%	0.67	0.79%
		2.08%	2.31%	0.90	0.23%
<u>RADIUS</u>	MINERAL WIDTH	0.80%	1.46%	0.55	0.66%
		1.63%	1.90%	0.86	0.27%

(d) Dichromatic (Dual-Photon) Absorptiometry: In the past several years we have concentrated on developing absorption measurements at two energies, rather than at a single energy, in order to measure bone embedded in soft-tissue, or to measure the relative amounts of lean and lipid components of soft-tissue. A combination of radionuclides, such as ^{125}I and ^{241}Am (27- and 60-keV), are used, or a single source with two emissions, such as ^{109}Cd (22- and 88-keV) or ^{153}Gd (43- and 100-keV) may be used. New sources, such as $^{123\text{m}}\text{Te}$ and $^{125\text{m}}\text{Te}$ are being investigated. The dual photon approach permits measurements of bone without the necessity for a constant thickness of tissue-equivalent material surrounding the limb. In practical terms, this eliminates the need for limb immersion in water baths, or for preparation and use of Super-Stuff. More important, however, is the new potential for dichromatic scanning of locations impossible to measure with the single-photon method, such as the spine and hip.

Preliminary dual-photon scans of the spine have shown a long-term precision of 4.6% using ^{153}Gd on a spine phantom. Comparable precision can

be achieved on humans in vivo provided there is careful relocation. In a less controlled situation we have found variation from 7 to 20% over time depending on the subject. Area scanning is now being used to enhance reproducibility.

(e) Validation Studies: Over the past decade it has been shown that absorptiometry is a very accurate indicator of local bone mineral content. Under simulated in vivo conditions the ash weight of bone sections is predicted with an error of only 1 to 3%. The accuracy of measurement on uniform standards is even higher (less than 0.5% error). Absorptiometric determinations are related not only to the weight of the bone mineral in the scan path, but to the weight of the total long bone, and also to the total skeletal weight. In series of excised bones, both Wilson and Mazess (1971) have shown that a scan on any long bone is highly correlated with scans on any other long bone. Apparently there is relative uniformity in the mineral content, and in changes of mineral content, throughout the appendicular skeleton. This finding indicates the usefulness of scans in indicating mineral status. Recent results by C. Wilson, however, show that the mineral content on appendicular bones is only moderately correlated with spinal bone mineral strength ($r=0.7$). However, even scans on adjacent vertebra do not give much information about their neighbors ($r=0.8$). Scans on appendicular bones, however, are well-correlated ($r=0.87$) with the mineral content of the femoral neck; this important relationship indicates that a radius scan may be of diagnostic aid in relation to hip fractures.

SUBSTANTIVE APPLICATIONS

(a) Normative Data: We have measured the bones, typically the shaft of the radius and the ulna, on over 1000 U.S. white adults, and on over 400 white school-age children. In addition, measurements have been made, as part of the International Biological Program, on several hundred Eskimo children and adults from both northern Alaska and northern Canada. Similar normative data has been collected by other laboratories (Kaiser Research Foundation, Jefferson Medical Center, Mayo Clinic, Univ. of Rochester, Univ. of Indiana) and the pattern of bone growth and bone loss has been outlined in white, Negro, and Oriental populations. In the elderly whites, bone loss occurs earlier and to a greater extent in females at ages 40 to 50, and continues at about 10% per decade thereafter. Bone loss does not occur in males until age 50, and the loss amounts to only about 3% per decade. Even more rapid bone changes occur in children; their bones grow at a rate of about 8% per year. Accumulation of such data by different laboratories will not only better define the normal pattern of age changes, but will allow more exact discrimination and interpretation of skeletal deviancy.

(b) Patient Data Bank: We have measured the bones in over 1000 patients exhibiting a variety of diseases. J.M. Jurist has devised a standard medical history and coding system; uniform data is collected from all patients, then coded and put on magnetic tape. This clinical data bank is updated about every 6 months. Copies of this system are available on request.

Use of the data bank allows convenient sorting of clinical data with respect to any of the variables (subject description, disease diagnosis,

treatment). M. Mueller, who supervises clinical measurement of bone mineral, has studied several hundred patients with rheumatoid arthritis using the data bank. In 144 women it was found that the loss of bone mineral was associated with the severity and duration of the disease. In steroid-treated patients the mineral loss was seen after a shorter disease duration and lesser severity; the extent of demineralization seemed related to the total steroid dose received. Similar studies are being done in other disease categories.

(c) Discrimination of Skeletal Abnormality: Mere deviancy of bone mineral content for a particular age-sex category does not necessarily indicate skeletal abnormality or pathology. Bone size and body size affect the amount of bone. On the other hand, there appear to be some minimal thresholds below which the bone is architecturally unsound regardless of other factors.

E. Smith and J. Jurist found that a bone mineral content of 0.68 g/cm on the radius shaft discriminated between 50 white females free of disease and 50 osteoporotic (defined by spontaneous fractures of the femoral neck, vertebrae, or radius) females. Bone mineral content below this value indicates osteoporosis and the danger of fracture regardless of the subject's body size or age. In a series of 24 cadavers examined by C. Wilson the femoral necks were broken in all cases where the radius mineral content was below 0.68 g/cm. Discrimination of abnormality might be improved by use of height, weight, limb circumferences and lengths, and biochemical information; we are examining this possibility.

In school-age children indices of skeletal abnormality are difficult to develop since bone grows at 8% per year and also varies with body size. We have used regression relationships observed in a sample of 322 white children to formulate indices of abnormality; deviancy from the expected bone mineral content is examined using prediction equations for age, bone width, and height and weight. In a sample of normal children about 5% fall more than two standard deviations below the mean, but it is not clear if these children really evidence marginal skeletal status or if this is merely the nature of the "normal" distribution. These deviant children average only 6% (7 months) retardation in skeletal age, and there is no association between degree of demineralization and maturational delay.

(d) Serial Observations of Skeletal Abnormality and Treatment: The high precision of absorptiometry makes it especially useful for observing the small changes occurring with skeletal disease, or measuring those small changes resulting from therapy or alterations of bone stress. P.F. Judy has collaborated with J. Vogel (U.S. P.H.S. Hospital, San Francisco) in monitoring changes during bed rest. Judy has also monitored bone mineral in 5 chronic hemodialysis patients using precise relocation made possible through casts. All patients were in end-stage renal failure with a creatinine clearance less than 3 ml/min; none received vitamin D and all were free from apparent skeletal involvement as seen radiographically. Over a period of from 20 to 72 weeks the coefficient of variation in the patients was less than 1%; the variation in the standard was only 0.2% and in the normal control subject it was 0.3%. Use of the ultra-precise method permitted confirmation of the absence of onset of renal osteodystrophy in these patients.

We have cooperated with Hugh Hickey (Marquette Medical School) in following the bone changes in elderly nuns receiving fluoride supplementation (75 mg/day). Both treated and untreated controls lost bone over the two-year follow-up period, but there were no apparent differences between the groups.

E. Smith followed bone changes in elderly subjects during an exercise program and also with physical rehabilitation. Control subjects lost 0.5% bone mineral over 9 months; the exercise group gained 1.7% over their control value of bone mineral, while the physical rehabilitation group, which apparently were demineralized as a result of previous bedrest, gained almost 8%. Studies of the effects of exercise on bone are in progress.

DISCUSSION AND CONCLUSIONS

The development of any novel biomedical method, such as absorptiometry, requires both technical and applied research efforts. Many laboratories and researchers are involved in this work, and the present report outlines some of the recent contributions of the Wisconsin laboratory. In order to aid communication in this expanding field we have tried to institute regular research meetings (in the fall of even-numbered years) and instructional workshops (in the fall of odd-numbered years). As the body of technical and substantive information dealing with absorptiometry increases we expect to find increasing clinical utilization and understanding of this method.

ACKNOWLEDGMENTS

We gratefully acknowledge the help of J. Jurst, M. Mueller, E. Smith, J. Sandrick, K. Kianian, and R.M. Witt in this research; J. Fischer and S. Kennedy have collected our clinical data with care and interest.

REFERENCES

- Cameron, J.R. (1970): Proceedings of Bone Measurement Conference. Atomic Energy Commission Conference 700515 (available CFSTI, Springfield, Va.).
- Mazess, R.B. (1971): Estimation of bone and skeletal weight by direct photon absorptiometry. Investigative Radiology 6:52-60.
- Mazess, R.B., Cameron, J.R., and Miller, H. (in press): Direct readout of bone mineral content using radionuclide absorptiometry. International Journal of Applied Radiation and Isotopes.

THE BONE MINERAL CONTENT AND PHYSICAL STRENGTH OF
AVASCULARIZED FEMORAL HEADS. AN EXPERIMENTAL STUDY ON ADULT RABBITS

A Proposed Experiment

Robert M. Witt
Department of Radiology

INTRODUCTION

As many as two-thirds of the patients with fractures of the femoral neck develop either partial or total bone necrosis of the femoral head. In particular, those patients who begin weight-bearing soon after bony union of the original fracture and who have either a partially or totally dead femoral head, often experience degenerative changes and collapse of the femoral head. The collapse, which has been called late segmental collapse, may appear from six months to two years after the initial femoral neck fracture. The collapse, which is apparent on radiographs and often appears in the upper quadrant or weight-bearing region of the femoral head, usually is the first diagnostic sign indicating that a patient has necrosis of the femoral head.

Two causes of this late segmental collapse have been proposed. Some investigators have observed collapsed bone at the interface between the dead and living bone in the repair zone of creeping substitution. These investigators have suggested that both the resorption of the old dead bone and the deposition of new, not fully mineralized living bone to replace the resorbed bone weaken the femoral head so that it can not withstand the forces of weight-bearing. Other investigators have observed fractures within the dead trabeculae in the subchondral bone. They have suggested that the gross collapse of the femoral head after weight-bearing is resumed is the result of the accumulation of many unrepaired physical fatigue fractures in the dead trabeculae.

EXPERIMENTAL PURPOSE

The purpose of the experiment is to determine the location of the greatest mechanical weakness in femoral heads with partial or total bone necrosis. The two hypotheses to be tested are: 1. the collapse of the femoral head initiates in the interface between the dead and living bone at the zone of creeping substitution; and 2. the collapse initiates entirely within the dead trabecular bone. The experiment will also determine if there is an absolute increase in the bone mass of the femoral head during the creeping substitution repair of bone tissue.

METHODS AND MATERIALS

The experimental animal will be adult New Zealand White rabbits (age

1 year). A total of twenty animals will be used in the experiment. They will be divided into four groups of five animals each. One hip will be the experimental and the other one the control. The blood supply to the experimental femoral head will be temporarily disrupted with a surgical procedure. The surgical procedure will be a capsulotomy with division of the ligamentum teres, temporary dislocation of the femoral head, and tight ligation of the neck of the femur with a stainless steel wire. To force the animal to use both hind limbs equally, a sham operation will be performed on the opposite side. The surgery will be performed in the facilities of Experimental Animal Surgery by Dr. Salamon, an orthopaedic resident. The four groups of animals will be killed at 3, 6, 12, and 24 weeks after the operation since only after three weeks following the interference of the blood supply to bone can one easily confirm from histological sections that the bone tissue is dead. The other times were chosen to obtain groups of animals with femoral heads in various stages of repair. The experiment will terminate after 24 weeks since in the rabbit most femoral heads will be totally repaired.

Radiographs will be taken at surgery and immediately after death. Radiographs will also be taken of both femurs in air and in a water bath after they are removed. The femurs will be fixed to preserve them for the histological studies. After the femurs are fixed, the bone mineral content determinations will be made. Rectilinear bone mineral scans will be made of the whole femoral heads and additional linear scans will be made on the femoral shaft at the 25%, 50% and 75% sites measured from the distal end. After all 40 femurs are recovered, the physical strength and mechanical properties of the intact femoral heads will be determined. The physical test will be the test of two elastic bodies in contact. The femoral head of the rabbit will be assumed to be an elastic sphere and will be placed in contact with a steel ball bearing. A force will be applied until the femoral head yields.

Two elastic spheres pressed against each other by a force, P , will have an approximately circular area of contact of radius, a , and their centers will be displaced by a distance, Z . The maximum pressure, P_{MAX} , between the two spheres will be at the center of the area of contact. These three quantities are related by the following equations:

$$P_{MAX} = 0.616 \sqrt[3]{\frac{P}{R_e^2} E_e^2}$$

$$a = 0.88 \sqrt[3]{\frac{PR_e}{E_e}}$$

$$Z = \frac{a^2}{R_e}$$

where, $\frac{1}{R_e} = \frac{1}{R_1} + \frac{1}{R_2}$, R_1, R_2 = radii of two spheres

$$\frac{1}{E_e} = \frac{1}{E_1} + \frac{1}{E_2} , \quad E_1, E_2 = \text{moduli of elasticity of the two materials}$$

After the physical tests are completed, decalcified, hematoxylin and eosin stained sections of the whole femoral heads will be prepared for the histological studies. The histological studies will include a quantification of the different stages of damage and/or repair, and possibly a quantification of the ratio of bone area to the total area of the femoral head. The latter would be compared to the BMC measurements.

RESULTS

The results of the experiment will be organized into three areas:
1. bone mineral mass determinations, 2. physical strength determinations, and 3. histological observations.

The bone mineral mass measurements should determine whether or not the apparent increase in bone mass observed on radiographs, and the increase in bone tissue volume observed on the histological sections represents a real increase in bone mass. If the femoral heads composed of dead trabeculae cocooned within a sheath of living bone have a real increase in bone mass, the bone mineral content of the experimental femoral heads should be greater than the controls. The increase should appear after the repair phase begins. The bone mineral content will also be compared to the radiographs, the physical strength of the whole femoral heads, and the microscopic changes in the bone tissue.

The physical tests of the avascularized femoral heads should determine which mode of collapse occurs. The tests will determine the ultimate strength of the femoral heads and the maximum pressure at the yield point. A comparison of the maximum pressure of the experimental and control femoral heads should demonstrate if femoral heads partially or almost totally composed of dead bone are weaker than femoral heads entirely composed of normal living bone. If the head fails due to an accumulation of unrepaired fatigue microfractures in the dead bone, those femoral heads tested later after the operation should accumulate more microfractures, and therefore, should have a lower ultimate strength. The physical tests should also show if those heads composed of dead bone cocooned in a sheath of living bone are mechanically weaker than those heads composed entirely of normal living bone.

The histological sections will show the location of the fractures in the trabeculae and in those femoral heads undergoing repair they will possibly reveal whether or not the cement line between the dead and living bone tissue is a point of mechanical weakness and fracture initiation. The histological studies are also necessary to determine when the tissues are dead and to describe and follow the progress of their recovery and repair. These descriptions of the microscopically observable tissue changes will be used to classify the animals according to the amount and degree of tissue damage and repair present in the femoral heads at the time the animals are killed.

The results of the experiment are intended to yield statistically significant differences in the BMC and the maximum pressure at mechanical failure between the experimental and the control femoral heads. Relationships should also be demonstrated to exist between the time after the operation and the following: bone mineral content; physical strength; histological observations; and the radiological observations. These latter results will most probably be presented as correlations between the various parameters.

For the proposed experiment, one can estimate the smallest difference detectable between experimental groups. Given an estimate for the experimental standard deviation, s_0 , this difference can be calculated from the following equation,

$$d = \frac{(Q_{a,f})(s_0) \sqrt{F_{f,f_0}}}{\sqrt{n}}$$

where, s_0 = estimated standard deviation with f_0 degrees of freedom
 a = number of groups or treatments
 n = number of individuals per group
 f = $a(n - 1)$ new degree of freedom
 Q = upper 5% percentage points in the studentized range
 F = upper 5% percentage points in the F-distribution

or in relative terms,

$$\frac{d}{D} = \frac{(Q_{a,f})(CV) \sqrt{F_{f,f_0}}}{\sqrt{n}}$$

where, D = mean value of the measurement
 CV = coefficient of variation of the experiment

Bone Mineral Content Measurements

For the BMC measurements the estimate for the CV is 0.02, and since this estimate has been obtained from many measurements, one can assume that $f_0 = \infty$. For the proposed experiment, $a = 4$, $n = 5$, and $f = 16$ and from the tables in SNEDECOR*, $Q_{4,16} = 4.05$ and $F_{16,\infty} = 1.214$. From these values $d/D = 0.04$ (4%). Therefore, if the estimated $CV = 0.02$, the experiment should be able to detect differences of 4 percent between groups with a 25 percent chance of failing to detect a difference this size should it exist. Since the control group will be composed of twenty individuals instead of the assumed five, the experiment will be able to detect slightly smaller differences.

Physical Tests Determinations

A similar calculation can be made for the physical tests measurements if one assumes that the CV from WILSON (Ph.D. Thesis, 1972) is typical for physical tests made on cancellous bone. His CV was 0.20 for $f \sim 72$.

* George W. Snedecor, Statistical Methods, 5th ed., 1961.

From the tables $F_{16,72} = 1.260$, and for these values $d/D = 0.407$ (41%). Thus for the physical tests with an assumed CV of 20 percent, the experiment should be able to detect differences of 41 percent between the groups with a 1 in 4 chance of failing to detect a difference this size should it exist. Additional calculations show that it would take about 30 individuals per group or a total of 120 animals to detect differences on the order of 10 percent with the same 20 percent coefficient of variation.

DESCRIPTION OF SUPPORT FACILITIES

Animal Care Unit

The animals will be purchased and housed by the Animal Care Unit of the University of Wisconsin Medical Center. The animals will be placed in nonmetabolic cages and fed the standard diet as provided by Animal Care.

Experimental Surgery

The surgery will be performed in the facilities of Experimental Surgery with the cooperation of Dr. Gilboe. Experimental Surgery will provide the necessary sterile environment, the instruments to perform the operation, and two experienced technicians to assist with the administration of the anesthetic and the immediate post-operative care of the animals.

Bone Mineral Laboratory

The bone mineral content determinations will be made in the University of Wisconsin Bone Mineral Laboratory with the absorptiometric technique developed by Drs. Cameron and Sorenson. This technique has been used previously to determine the bone mineral content, BMC, of small animal bones including both in vivo measurements on anesthetized rats, chickens, and rabbits; and in vitro measurements on excised bones from rats, turkeys, and rabbits.

Scans of the whole femoral head will be made with a rectilinear scanner. The transmission count data will be recorded on digital magnetic tape and processed by the Madison Academic Computing Center, MACC, on their UNIVAC 1108 digital computer. The BMC measurements at the other sites on the femur (e.g. distal epiphysis and the mid-diaphysis) will be made with the UWBML analogue system which gives the results immediately and will save time and computer funds.

Engineering Mechanics Experimental Testing Laboratory

The two elastic spheres in contact tests will be performed in the Department of Engineering Mechanics Experimental Testing Laboratory by John Dreger. The test machine is a MB Electronics, Model TM 6 Universal Testing Machine. The proximal portion of the femur will be placed between the jaws of the machine and the femoral head will be loaded with a steel sphere until failure. The static test will be made at a constant strain or displacement rate.

The ultimate load at failure will be measured with a commercially manufactured force transducer which has a maximum load capacity of 1000.

pounds and a resolution of 0.25 percent (2.5 pounds). The calibration of the load cell is traceable to the National Bureau of Standards. The displacement between the centers of the two bodies will be determined by measuring the displacement between the jaws of the machine with a linear differential transformer, LDT, displacement transducer. Since the ultimate loads are expected to be less than 200 pounds, deflections and bending of the machine stand, jaws, etc. will be neglected.

The machine is equipped with a XY recording device and plots of loading force versus displacement will be obtained for each specimen.

Department of Pathology Laboratory

The University of Wisconsin Department of Pathology has the facilities to provide standard decalcified sections of bone tissue. The sections will be stained with hematoxylin and eosin.

Topical Bibliography

Definition and etiology

Johnson, L. C., Histogenesis of avascular necrosis, pp. 55-79, In Proceedings of the Conference on Aseptic Necrosis of the Femoral Head, U.S.P.H.S., N.I.H., 1964.

Phemister, D. B., Bone growth and repair, *Annals of Surgery*, 102:261- ,1935.

_____, Changes in bones and joints resulting from interruptions of the circulation. 1. General considerations and changes resulting from injuries, *Arch. Surg.*, 41:436-472, 1940.

_____, Circulatory disturbances in the head of the femur, *American Academy of Orthopaedic Surgeons Lectures*, 1:129- ,1943.

Coleman, S. S., and Compere, C.L., Femoral neck fractures: Pathogenesis of avascular necrosis, Nonunion and late degenerative changes, *Clinical Orthopaedics*, 20:247-265, 1961.

Hulth, A., Necrosis of the head of the femur, *Acta chirurgica Scand.*, 122:75-84, 1961.

Sevitt, S., Avascular necrosis and revascularisation of the femoral head after intracapsular fractures. A combined arteriographic and histological necropsy study, *J. Bone Joint Surg.*, 46B: 270-296, 1964.

Trueta, J., and Harrison, M.H.M., The normal vascular anatomy of the femoral head in adult man, *J. Bone Joint Surg.*, 35B: 442-461, 1953.

Crock, H.V., A revision of the anatomy of the arteries supplying the upper end of the human femur, *J. Anat.*, 99: 77-88, 1965.

Mussbichler, H., Arterial supply to the head of the femur. An arteriographic study in vivo of lesions attending fracture of the femoral neck, *Acta radiol.*, 46: 533- , 1956.

Claffey, T.J., Avascular necrosis of the femoral head. An anatomical study, *J. Bone Joint Surg.*, 42B: 802-809, 1960.

Holmquist, B. and Alffram, P.A., Prediction of avascular necrosis following cervical fracture of the femur based on clearance of radioactive iodine from the head of the femur, *Acta orthop. Scand.*, 36: 62-69, 1965.

Wisham, L.H., Katz, J.F., and Dworecka, F.F., The effect of changes in position on the clearance of radioactive sodium from the head of the femur of immature dogs, *Amer. J. Orthop.*, 8: 132-135, 1966.

Woodhouse, C.F., Anoxia of the femur head, Surgery, 52: 55-63, 1962.

_____, The prevention of avascular necrosis, pp. 225-238, In Proceedings of the Conference on Aseptic Necrosis of the Femoral Head, U.S.P.H.S., N.I.H., 1964.

De Haas, W., and MacNab, I., Fractures of the neck of the femur, South African Medical Journal, 30: 1005-1010, 1956.

Jones, J. P., Jr., and Engleman, E. P., Osseous avascular necrosis associated with systemic abnormalities, Arthritis Rheum 9: 728-736, 1966.

Banks, S. W., Aseptic necrosis of the femoral head following traumatic dislocation of the hip, J. Bone Joint Surg., 23: 753-781, 1941.

Boettcher, W. G., Bonfiglio, M., Hamilton, H. H., Sheets, R. F., and Smith, K., Non-traumatic necrosis of the femoral head. Part I. Relation of altered hemostasis to etiology, J. Bone Joint Surg., 52A: 312-321, 1970.

_____, Non-traumatic necrosis of the femoral head. Part II. Experiences in treatment, J. Bone Joint Surg., 52A: 322-329, 1970.

Frost, H. M., the etiodynamics of aseptic necrosis of the femoral head, pp. 393-413, In Proceedings of the Conference on Aseptic Necrosis of the Femoral Head, U.S.P.H.S., N.I.H., 1964.

Phemister, D. B., Changes in bones and joints resulting from interruption of circulation. II. Nontraumatic lesions in adults with bone infarction; arthritis deformans, Archives of Surgery 41: 1455-1482, 1940.

Histological Description

Johnson, L.C., Histogenesis of avascular necrosis, pp. 55-79, In Proceedings of the Conference on Aseptic Necrosis of the femoral Head, U.S.P.H.S., N.I.H., 1964.

Catto, M., A histological study of avascular necrosis of the femoral head after transcervical fracture, J. Bone Joint Surg., 47B: 749-776, 1965.

_____, The histological appearance of late segmental collapse of the femoral head after transcervical fracture, J. Bone Joint Surg., 47B: 777-791, 1965.

Coleman S.S., and Compere, C.L., Femoral neck fractures: Pathogenesis of avascular necrosis, Nonunion and late degenerative changes, Clinical Orthopaedics, 20: 247-265, 1961.

Bonfiglio, M., Aseptic necrosis of the femoral head intact blood supply is of prognostic significance, pp. 155-175, In Proceedings of the Conference on Aseptic Necrosis of the Femoral Head, U.S.P.H.S., N.I.H., 1964.

Sevitt, S., Avascular necrosis and revascularization of the femoral head after intracapsular fractures. A combined arteriographic and histological necropsy study, J. Bone Joint Surg., 46B: 270-296, 1964.

Hulth, A., Necrosis of the head of the femur, Acta chirurgica Scand., 122: 75-84, 1961.

Brown, J.T., and Abrami, G., Transcervical femoral fracture, J. Bone Joint Surg., 46B: 648-663, 1964.

Phemister, D.B., Bone growth and repair, Annals of Surgery, 102: 261- , 1935.

_____, The pathology of ununited fractures of the neck of the femur with special reference to the head, J. Bone Joint Surg., 21: 681- , 1939.

Sherman M.S., and Phemister, D.B., The pathology of ununited fractures of the neck of the femur, J. Bone Joint Surg., 29: 19-40, 1947.

Radiographic Appearance

Norman, A., and Bullough, P., The radiolucent crescent line - An early diagnostic sign of avascular necrosis of the femoral head, J. Hospital for Joint Diseases 24: 99-104, 1963.

Brown, J. T., and Abrami, G., Transcervical femoral fracture, J. Bone Joint Surg., 46B: 648-663, 1964.

Catto, M., The histological appearance of late segmental collapse of the femoral head after transcervical fracture, J. Bone Joint Surg., 47B: 777-791, 1965.

Johnson, L. C., Histogenesis of avascular necrosis, pp. 55-79, In Proceedings of the Conference on Aseptic Necrosis of the Femoral Head, U.S.P.H.S., N.I.H., 1964.

Coleman, S. S., and Compere, C. L., Femoral neck fractures: Pathogenesis of avascular necrosis, Nonunion and late degenerative changes, Clin. Orthop., 20: 247-265, 1961.

Phemister, D. B., Changes in bones and joints resulting from interruptions of circulation. I. General considerations and changes resulting from injuries, Arch. Surg., 41: 436-472, 1940.

Animal Experiments - Rabbits

Rokkanen, P., Role of surgical interventions of the hip joint in the aetiology of aseptic necrosis of the femoral head, Acta Orthop. Scand. Suppl. 58: 1-107, 1962.

"
Rosingh, G. E., Steendijk, R., and Van den Hooff, A., Consequences of avascular necrosis of the femoral head in rabbits. A histological and radiological study, J. Bone Joint Surg., 51B: 551-562, 1969.

"
Rosingh, G. E., and James, J., Early phases of avascular necrosis of the femoral head in rabbits, J. Bone Joint Surg., 51B: 165-174, 1969.

Bobechko, W. P., and Harris, W. R., The radiographic density of avascular bone, J. Bone Joint Surg., 42B: 626-632, 1960.

Stewart, W. S., Aseptic necrosis of the head of the femur following traumatic dislocation of the hip joint; case report and experimental studies, J. Bone Joint Surg., 15: 413-438, 1933.

Miltner, L. J., and Hu, C. H., Osteochondritis of head of femur; experimental study, Arch. Surg. (Chicago) 27: 645-657, 1933.

"
Rokkanen, P., and Slatis, P., Effect of compression on the healing of subcapital osteotomies of the femoral neck and on the avascularized femoral head. An experimental study on adult rabbits.

Scheck, M., and Sakovich, L., Subchondral trabecular compression of the femoral head in the etiology of aseptic necrosis. Experimental study in rabbits, J. Surg. Res. 9: 61-71, 1969.

DETERMINATION OF VERTEBRAL BONE MINERAL MASS BY
TRANSMISSION MEASUREMENTS*

3 P. F. Judy, J. R. Cameron, K. M. Jones and M. G. Ort
Department of Radiology
University of Wisconsin
Madison, Wisconsin

ABSTRACT

A dichromatic photon attenuation technique for the precise determination of lumbar vertebral bone mineral mass in vivo has been developed. A 100 mCi source of ^{153}Gd was used as a source of 44 keV and 100 keV photons. The collimation of the NaI(Tl) detection defined a 2.5 cm by 1 cm beam at the vertebra. The average of three scans at 2.5 cm intervals along the vertebral column was determined. The lower edge of the beam of the first scan was positioned coincident with the transtuberular plane and the position of the scanner relative to the top of the patient's head was recorded for repositioning purposes. No radiographs were taken. The total radiation exposure was measured with TLD for the three scans and was 2 mR to the dorsal surface of the trunk. The measurement took 25 minutes.

The precision of 7 measurements in vivo over a period of 3 months was 5%. The measurement of 8 excised vertebral columns under 15 cm of water was compared with their ashed mass per unit length (400°C for 48 hours). The ashed mass could be estimated from the scan measurements with a standard error of 3%. These experiments suggest, if the measurement system is properly calibrated, the dichromatic photon attenuation technique provides an accurate and precise measurement of vertebral bone mineral mass.

* To be presented at the 3rd International Conference on Medical Physics, Goteborg, Sweden, July 30-August 4, 1972.

INTRODUCTION

A dichromatic photon attenuation technique for the precise and accurate determination of lumbar vertebral bone mineral mass in vivo was developed because changes in the vertebrae have been assumed to larger and happen sooner than in the rest of the skeleton. Roos¹ described a method using the radiations from ^{137}Cs and ^{241}Am for which the gamma-ray beam at the vertebra was circular with a diameter of at least 2 cm. The technique developed utilizes 100 Ci of ^{153}Gd ^{9,2}, a newly developed source,* which emits two essentially monoenergetic photon beams of 44 keV and 100 keV. The NaI(Tl) scintillation detector separates the radiation into two photopeaks. The 44 keV photopeak is the Eu K x-rays and the 100 keV photopeak is two gamma-rays of 97 keV and 103 keV. The collimation defined a beam of 2.5 cm by 1 cm at the vertebra. The length of the slot was aligned with the axis of the vertebral column. In order to reduce the day-to-day variation caused by repositioning errors, the average of three scans along the lumbar vertebral column at 2.5 cm intervals was determined.

METHOD

The bone mineral mass along any path in the body can be estimated from the transmission of two monoenergetic photon beams along that path using Equation (1).

$$\text{Mass}_{\text{BM}} = C \left(A - \ln I(44 \text{ keV}) + R \ln I(100 \text{ keV}) \right) \quad (1)$$

$$C = \frac{\mu_{\text{ST}}(100 \text{ keV})}{\mu_{\text{BM}}(43 \text{ keV}) \mu_{\text{ST}}(100 \text{ keV}) - \mu_{\text{BM}}(100 \text{ keV}) \mu_{\text{ST}}(43 \text{ keV})}$$

$$A = \log I_0(44 \text{ keV}) - R \log I_0(100 \text{ keV})$$

$$R = \mu_{\text{ST}}(44 \text{ keV}) / \mu_{\text{ST}}(100 \text{ keV})$$

the derivation of Equation (1) is described in detail in the appendix. This particular formula was chosen to permit easy and accurate extraction of the bone mineral mass information from the data. The use of a baseline, A, eliminates the need to determine the unattenuated intensities of the two x-ray beams, which is required in some dichromatic attenuation techniques. The ratio of mass attenuation coefficients for soft tissue, R, can be accurately and easily determined from the measurement of the mass attenuation for each beam in water. For the ^{153}Gd beams, R determined from compilations⁴ for water is 1.536 compared with the value for lean muscle which is 1.541. The value of K was determined from an ash study in the same manner single monoenergetic photon technique was calibrated. The ash study also estimated the magnitude of various errors, particularly the error caused by the large photon beam.

* Obtained from Isotopes Development Section, Oak Ridge National Laboratory, Oak Ridge, Tennessee

For the measurement the patient layed on a table. The ^{153}Gd source was 38 cm below the table top rigidly coupled to a 5 cm x 1.3 cm NaI(Tl) scintillation detector, 34 cm above the table top. In normal operation the apparatus was moved across the torso by a screw drive.

For the first scan the position of the lower edge of beam was coincident with the transtubercular plane. Three scans cephalic along the lumbar vertebral column at 2.5 cm intervals were performed. During the first set of measurements the position of the scanner relative to the top of the patient's head was recorded to permit repositioning of the patient when the measurements were repeated. No radiographs were used to reposition the patient.

The electronic components of the equipment are shown in Figure 1. The system was assembled from modules built to the Nuclear Instrument Module (NIM) standards. The two photopeaks from ^{153}Gd were separated by a dual channel analyzer. The analyzer settings for the lower energy photopeak (44 keV) were a lower level of 28 keV with a window of 32 keV, and for the higher energy photopeak (100 keV) a lower level of 91 keV with a window of 31 keV. Both of these settings included essentially all of their respective photopeaks of the pulse height spectrum shown in Figure 2 while avoiding the small photopeak due to the 69 keV gamma-ray.

The mass attenuation coefficients of aluminum for the 100 keV photopeak were independent of window size. The mass attenuation coefficients for the 44 keV decreased 0.06% per 1 keV increase in window for windows centered on the photopeak. This dependence of the measured attenuation coefficient on window was probably caused by the poly-energetic character of the Eu K x-rays ($E_K = 41 \text{ keV}$ and $E_K = 48 \text{ keV}$).

The number of count from each analyzer were counted for a fixed time, typically 10 seconds, determined by the timer. The data was then recorded on a magnetic tape. Other digital information was recorded on the magnetic tape by setting the thumb switches of the parametric recorder. The magnetic tape was transferred to the UNIVAC 1108 computer, for which computer programs were written to estimate the bone mineral mass.

The entrance exposure during a lumbar vertebral mass measurement was measured with TLD and was less than the sensitivity of the method (3 mR). The exposure rate from a 50 mCi source of ^{153}Gd at the table top was 3.5 mR/hr. The measurements took typically less than one half hour.

RESULTS

The method was calibrated and the accuracy was evaluated from the measurement of 8 excised vertebral columns under 15 cm of water. The columns were ashed at 400°C for 48 hours. The majority of the processes were removed for the vertebrae. The ash mass per unit length is plotted as a function of the absorptiometric measurement in Figure 3. The standard error of estimate from a linear regression was 3% indicating the absorptiometric measurement was a good estimator of vertebral bone mineral mass. The large value of the intercept in the regression equation was the effect of a large beam.

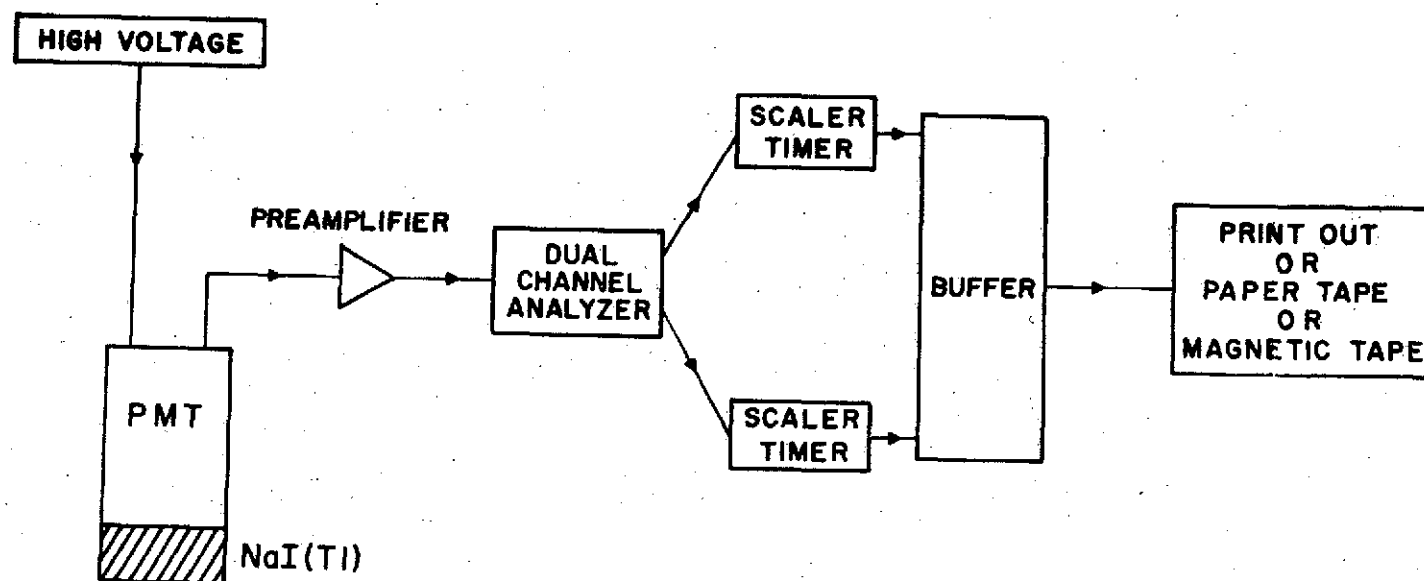


Figure 1
Electronic components of the vertebral bone
mineral mass analyzer.

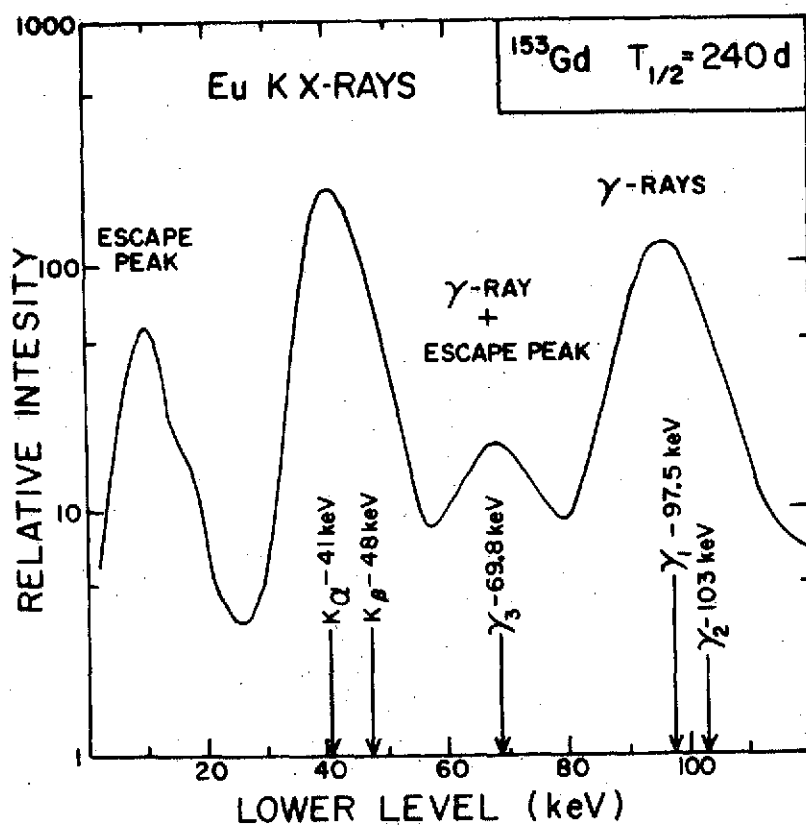


Figure 2
Pulse height spectrum for ^{153}Gd . Window = 2.6 keV

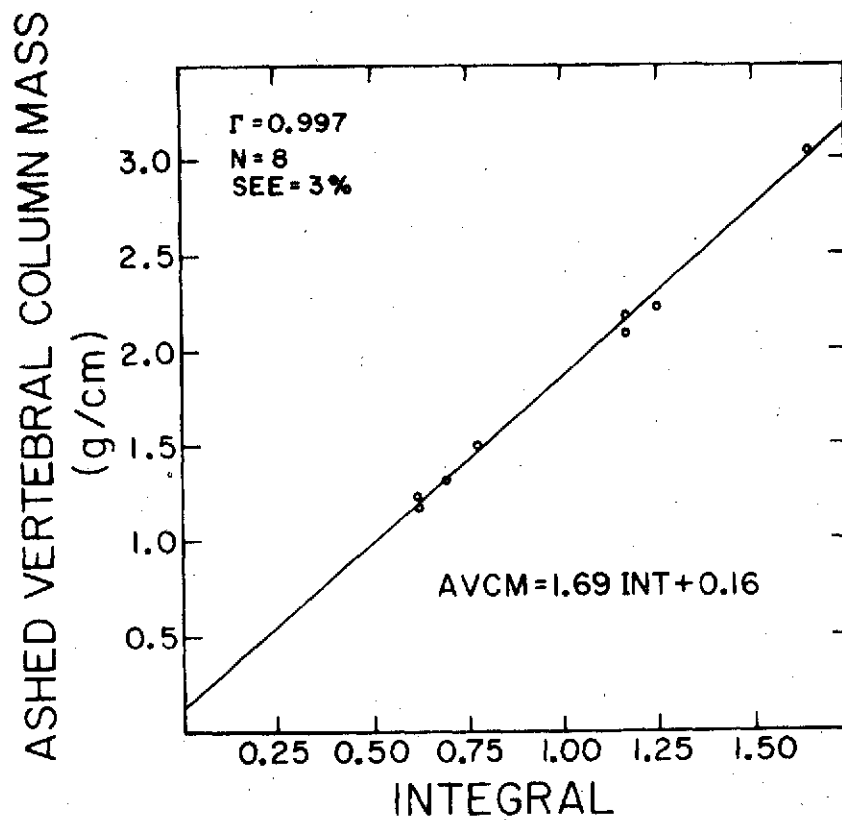


Figure 3
Regression of the absorptiometric estimate of bone mineral mass and the actual ashed vertebral bone mineral mass.

The variation of the vertebral bone mineral mass along a lumbar spine that was in a torso phantom of Mix D⁸ was estimated by scanning the phantom at 0.5 cm intervals from L3 to L5. The results are illustrated in Figure 4. All values are within 3% on the mean value.

A precision of 5% for measurements in vivo was determined for seven measurements on one subject made at 0.5 cm scan intervals (the distance between point measurement). Each measurement took about 50 minutes. The precision on excised columns under water was unchanged if the scan intervals were 1 cm. This permitted a reduction of the measurement time to 25 minutes. With this scan interval the precision for ten measurements each on five subjects averaged 13%. An inspection of the results suggested the major source of error was the determination of the baseline, A, because some scans were started or ended too close to the vertebrae. The precision of one subject was reduced from 17% to 7% by correction of this error. A prospective study is underway to evaluate the precision at 0.5 cm scan intervals with particular consideration given to the determination of the baseline.

ANALYSIS OF ERROR

The largest error of this absorptiometric measurement of vertebral bone mineral mass was caused by the variation of the determination of the baseline, A. One can expect, if finer intervals and more measurements outside of the bone are made, this error can be reduced to values determined by Poisson statistics of counting photons. In principle this type of variation can be reduced to any value by increasing the source activity or increasing the measurement time. For the subject measurements reported this variation was less than 5%. The ultimate limitations on the precision are the ability to measure the same portion of the skeleton and patient movement.

The accuracy of the method was determined by:

- (1) the size of the photon beam
- (2) the variation of the soft tissue composition across the vertebrae
- (3) the monochromaticity of the beams
- (4) the amount of scatter detected

Contrary to one's expectation the large beam (0.5 cm by 2.5 cm) cause a rather small error of less than 3% for technique calibrated by an ash study.

The soft tissues, which for this technique include the organic component of bone, vary in composition. The most significant factor is the larger lipid content of adipose tissue. If the composition of soft tissue has changed, the value of the ratio of mass attenuation coefficients for soft tissue, R, is incorrect for that path of the body. The magnitude of this error was estimated by comparing the baseline values on each side of the vertebrae and the variation in the baseline values. The analysis suggested the variation of soft tissue composition outside the vertebrae should cause an insignificant error, less than 3%. The magnitude of the error caused by adipose tissue inside the vertebral bodies can be as large

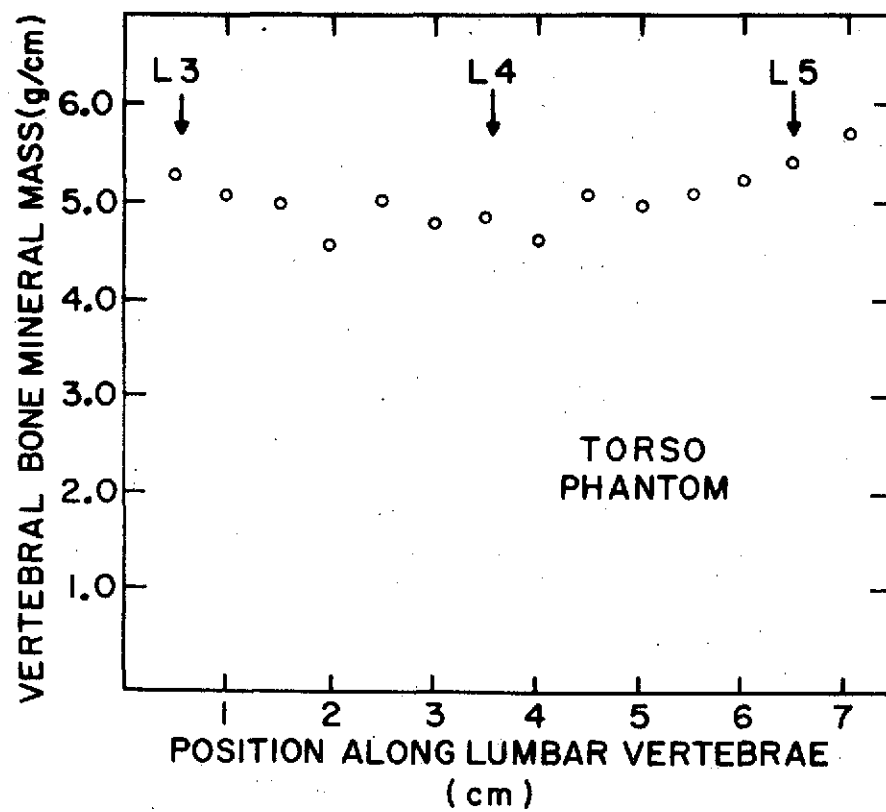


Figure 4
The measurement of vertebral bone mineral mass along
the lumbar spine of a phantom.

as 8%.⁷ This error would be reduced, if the calibration formula were obtained from an ash study made on fresh bones. The effects on the monochromaticity of the beams and the scatter also will have little effect, if the measurement is compared with ashed mass of vertebral column.

CONCLUSIONS

The absorptiometric determination of vertebral bone mineral mass using ¹⁵³Gd provided an accurate technique, if the measurement was calibrated by an ash study. The precision of the technique was 5% to 7%. The small variation (3%) of vertebral bone mineral mass along the lumbar spine suggest the variation caused by the processes and gaps from intervertebral discs are defocused with the large photon beam. The maximum change of vertebral bone mineral mass between L3 and L5 was 5% per cm, which implies if the patient can be repositioned with an accuracy of 0.5 cm, the error of repositioning can be reduced to less than 3%.

The purpose of this research was to develop a precise method to evaluate changes of bone mineral mass where each individual could be his own control. For this type of application the concern would be to control the factors that affect accuracy. The presence of adipose tissue inside the vertebral body causes the largest error with a maximum of 8%. During a study this error should not change and the precision of the measurement of vertebral bone mineral mass would be unaffected. The effects caused by crushed vertebrae being examined, the more mineral mass might enter the scan path resulting in apparent increase of bone mineral mass.

Appendix

The bone mineral mass along a path in the body can be estimated from the transmission of two mono-energetic photon beams along the line using the following equation.

$$mass_{BM} = \frac{\mu_{ST}(100\text{ KeV}) \log \frac{I_0(44\text{ KeV})}{I(44\text{ KeV})} - \mu_{ST}(44\text{ KeV}) \log \frac{I_0(100\text{ KeV})}{I(100\text{ KeV})}}{\mu_{BM}(44\text{ KeV}) \mu_{ST}(100\text{ KeV}) - \mu_{ST}(44\text{ KeV}) \mu_{BM}(100\text{ KeV})} \quad (A1)$$

μ = mass attenuation coefficient

m_{BM} = mass of bone mineral along the path in the bone having units of g/cm^2 .

ST = subscript referring to soft tissue

BM = subscript referring to bone mineral

I = transmitted intensity

I_0 = unattenuated intensity

The technique developed scans the ^{153}Gd beam across the vertebral column integrating Equation (A1) across the vertebrae to obtain the mass in section of the column.

Equation (A1) has been rearranged to permit easily and accurate extraction of the information from the data.

$$mass_{BM} = C \left[\log I_0(44\text{ KeV}) - R \log I_0(100\text{ KeV}) - \log I(44\text{ KeV}) + R \log I(100\text{ KeV}) \right] \quad (A2)$$

where

$$C = \frac{\mu_{ST}(44\text{ KeV})}{\mu_{BM}(44\text{ KeV}) \mu_{ST}(100\text{ KeV}) - \mu_{BM}(100\text{ KeV}) \mu_{ST}(44\text{ KeV})}$$

$$R = \mu_{ST}(44\text{ KeV}) / \mu_{ST}(100\text{ KeV})$$

In the situation with no bone mineral mass in the photon beam path the terms of Equation (A2) that are functions of the unattenuated intensity can be determined from Equation (A3) which was derived from Equation (A2) by setting m_{BM} to zero.

$$A = \log I_0(44\text{ KeV}) - R \log I_0(100\text{ KeV}) = (\log I(44\text{ KeV}) - R \log I(100\text{ KeV})) \Big|_{mass_{BM}=0} \quad (A3)$$

References

1. B. Roos, B. Rosengren, and H. Skoldborn: Determination of Bone Mineral Content in Lumbar Vertebrae by a Double Gamma-Ray technique. In Proc., Bone Measurement Conference, J. R. Cameron, Ed. AEC CONF-700515, 1970, p. 243.
2. R. M. Mazess, M. G. Ort, P. F. Judy, and W. Mather: Absorptiometric Bone Mineral Determination Using ^{153}Gd . In Proc., Bone Measurement Conference, J. R. Cameron, Ed. AEC CONF-700515, 1970, p. 308.
3. P. F. Judy: A Dichromatic Attenuation Technique for the In Vivo Determination of Bone Mineral Content, Ph.D. Thesis, University of Wisconsin, Madison, Wisconsin, 1970.
4. J. H. Hubbell: Photon Cross Sections, Attenuation Coefficients, and Energy Absorption Coefficients from 10 keV to 100 GeV. U.S. Department of Commerce, National Bureau of Standards, NSRDS-NBS 29, 1969.
5. J. A. Sorenson and J. R. Cameron: A Reliable In Vivo Measurement of Bone Mineral Content. Journal of Bone and Joint Surgery 49:481, 1967.
6. P. F. Judy: Theoretical Accuracy and Precision in the Photon Attenuation Measurement of Bone Mineral. In Proc., Bone Measurement Conference, J. R. Cameron, Ed. AEC CONF-700515, 1970, p. 1.
7. W. Wooten: Private Communication.
8. D. E. A. Jones: Water-Equivalence of "Mix D". Brit. J. Radiology, 25:272, 1952.
9. M. G. Ort and J. R. Cameron: Determination of Vertebral Bone Mineral In Vivo. USAEC Report COO-1422-79, 1970.

Acknowledgements

Partial support was provided by funds from NASA grants Y-NGR-50-002-051 and NAS 9-12306.

We wish to thank F. N. Case and his colleagues at Isotopes Development Section, Oak Ridge National Laboratory who fabricated the ^{153}Gd source.

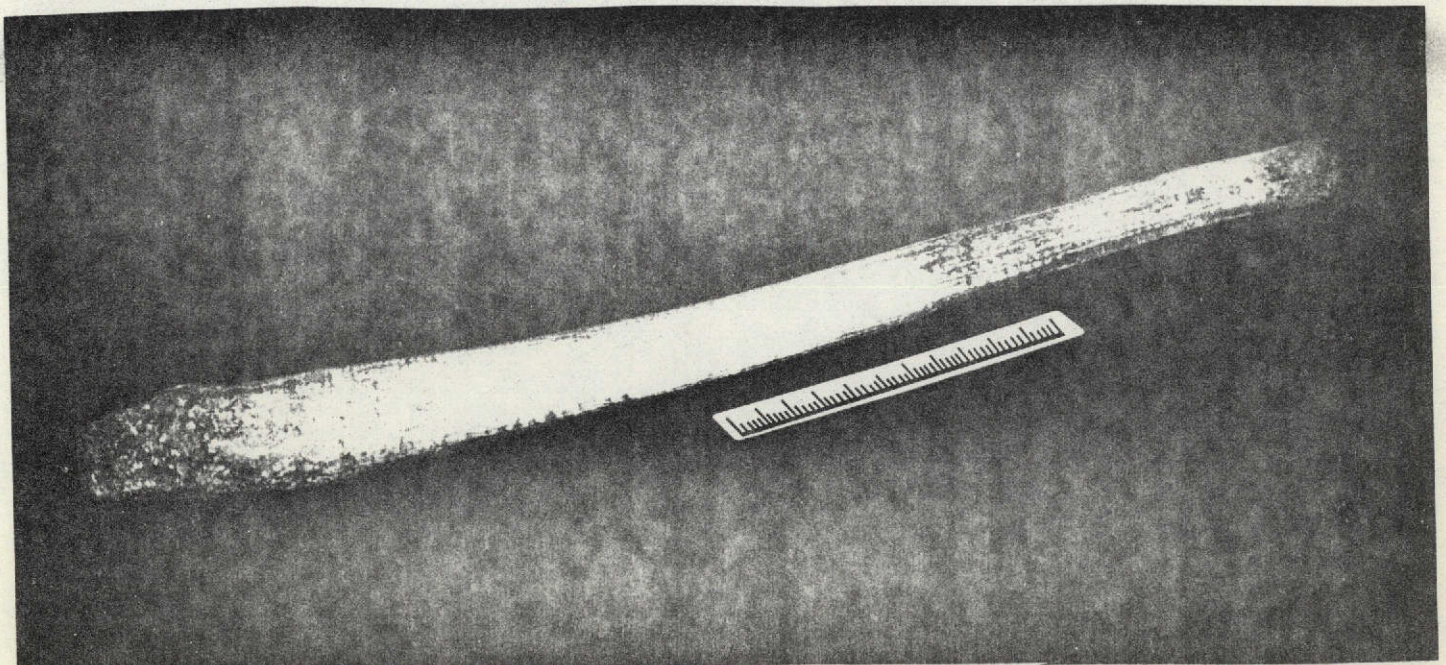
A NEW MATERIAL FOR THE INTERNATIONAL BONE MINERAL STANDARD

A. Kabluna, R.B. Mazess, and W. Mather

In the course of field surveys of bone mineral content in northern-Alaskan and northern-Canadian Eskimo communities we encountered bone specimens of unusually uniform composition. These bones are 50 to 70-cm in length and could be readily fabricated to simulate bones of different sizes for a bone mineral standard. These are called usuk in Eskimo; they are the walrus penis bone. The Eskimos themselves could make standards from the usuk thereby stimulating the depressed local economy.

We are currently investigating the distribution of bone mineral in this unusual bone. Previous studies in primates have shown that the bone mineral distribution corresponds to the stress distribution on a bone (Koch, 1917), and by evaluating the bone distribution in the usuk we may gain interesting insights and hitherto unavailable data on the physical stresses of intercourse in the walrus.

Koch, J.D. 1917. Laws of bone architecture. Am. J. Anat. 21: 177.



EXPERIENCES WITH THE USE OF VIBRATIONAL TECHNIQUES FOR THE DETERMINATION OF THE RESONANT FREQUENCY OF BONE IN VIVO

by

Charles R. Wilson
Department of Radiology
University of Wisconsin
Madison, Wisconsin

INTRODUCTION

It has been proposed that the resonant frequency of bone in vivo may be empirically useful for the clinical evaluation of bone.¹ While the formulation of a precise mathematical description of a bone vibrating in vivo is difficult, under certain simplifying assumptions concerning the ulna it can be shown that the product of its resonant frequency (F_0) of transverse vibration and length (L) is proportional to the square root of the ratio of Young's Modulus and the linear density of the ulna.² Jurist³ found that the product $F_0 \times L$ of the ulna in osteoporotic women was significantly lower than normal individuals of similar age and physique. An investigation of the relationships between the resonant frequency and various physical parameters of bone such as bone mineral content, density, Young's Modulus, and ultimate strength was planned. A number of experimental conditions such as arm and wrist orientation, etc. affect the measurement of the resonant frequency³ and preliminary measurements in vivo were made to gain familiarity with the technique and to establish suitably controlled experimental procedures. However, difficulties were encountered which prevented the completion of the original investigation. This report describes some of these difficulties and a number of observations on the effects changes in the experimental instrumentation have on the measured frequencies.

METHODS

Two techniques were used for the determination in vivo of the resonant frequency of bone. In the first technique, the vibrational response technique (VRT) of Jurist², an oscillatory force is applied to the ulna at the olecranon process by an electromagnetic driver. The frequency of the force is swept through the range of about 50 to 400 Hz. A small piezo-electric accelerometer strapped to the wrist at the styloid process detects the transverse vibration set up in the bone by the driver. This signal is amplified and rectified to provide a DC voltage which is recorded as a function of the frequency of the driving force on a chart recorder. This record is the vibrational response of the bone and the resonant frequency is taken at the frequency of the maximum amplitude response. In the cases where there are several resonances in the curve, the frequency is taken at the first or lowest frequency. Figure 3 shows a typical ulnar response curve.

In the second technique, the feedback technique (FBT), the bone is the frequency controlling element, a mechanical vibration filter, in a physical

oscillator.⁴ Figure 1 is a block diagram of the method. A transient vibration which should include the resonant frequency of the ulna is started by either tapping the bone or by random motions of the driver due to circuit noise. This vibration is detected by the accelerometer at the styloid process, and the amplified accelerometer signal powers the driver which is in contact with the olecranon process. The ulna responds preferentially at its resonant frequency, with the relative magnitude of vibration at resonance being greater than at other frequencies. Thus the predominate frequency of the vibration now detected by the accelerometer and hence that of the driving force which is reintroduced into the ulna is the ulna's resonant frequency. As this cycle is repeated a progressively stronger signal at the resonant frequency of the ulna is fed back resulting in steady state oscillations in the circuit with the ulna vibrating at its resonance. A frequency meter is then used to determine the resonant frequency of the ulna.

OBSERVATIONS

In both techniques the frequencies assigned to the resonances found in vivo were dependent upon the orientation of the arm, the position and orientation of the accelerometer and driver, muscle tension, etc. The vibrational response curves obtained using the VRT usually contained several resonant peaks whose frequencies and relative amplitudes could be varied by changing any of the above factors. In a similar fashion the frequencies at which oscillations occurred in the FBT were also dependent upon these factors. However for any particular set of measurement conditions in either technique discrete resonant frequency could be found. The standard deviation was typically 5% and it was slightly better, about 3%, for trained subjects. The reasons for this effect was not known and it was assumed that the discrete resonances obtained were due to preferential excitation of different vibrational modes or non-harmonic overtones of the fundamental. It was believed that comparisons of the resonant frequencies obtained at different times would be possible by rigidly constraining the measurement conditions so that the same mode was always excited.

The resonant frequencies determined by the two techniques were expected to be related due to the similarity in the methods used to excite and detect the vibrations in vivo. However no correlation was found between the resonant frequencies of 131 subjects determined by the two techniques. The driver and accelerometer were positioned to the subject's arm in approximately the same position for both techniques and the two measurements were performed within 10 or 20 minutes of each other. Figure 2 is a scattergram of these measurements. It appeared that one or both of the techniques were not accurately measuring the vibrations of the bone, although the instrumentation seemed to be operating properly. Since the frequencies of oscillation in the FBT seemed to be more sensitive to the contact pressure between the bone and accelerometer than the VRT, the elastic nature of the skin and soft tissue was suspected as modifying the detection of the vibration of the bone. It was thought that the skin might be more important in determining the frequency of oscillation than the elastic properties of the bone. An arm phantom for use with the FBT was constructed to investigate this hypothesis.

The phantom consisted of a rod ("bone") supported on a pad of stiff spongy material ("tissue") with small pieces (~ 1 mm thick) of turkey skin ("skin") placed between the "bone" and the accelerometer and driver. Rods of lucite, steel, aluminum, wood, and an excised fibula were used to simulate "bones" of different elastic moduli. The vibrational properties of the phantoms were similar to those of the bone in vivo; the range of frequencies was about the same, i.e. about 300-750 Hz; the frequency was dependent upon contact pressure and/or orientation between the accelerometer, driver and the "bone"; and the coefficients of variation were typically 5-7%. There was no obvious relation between the different "bones" and the frequency at which oscillations were excited and it appeared that transverse vibrations in the "bones" were ineffective in governing the frequencies of oscillation. It could not be determined whether transverse vibrations were occurring and were masked by the effect of the "skin" or whether they were not occurring in the "bone" at all.

Since the manner in which vibrations are excited and detected is the same in both techniques, the question regarding the actual presence of transverse vibration in the bone or whether these are measured is also applicable to the VRT. VRT measurements on the ulna in vivo were performed using different accelerometers, drivers, and oscillators. It was felt that if the measured vibrational response curves and resonant frequencies were relatively independent of different instrumentation, it would at least indicate that a quantity related to the bone's vibrations was being measured. Table 1 contains a list of the various components used, the accelerometers are listed in order of decreasing mass and sensitivity (mv per cm/sec^2). The frequency responses of the accelerometers were uniform in the frequency range of interest, i.e. less than 1000 Hz. The orientation of the limb, position of the accelerometer and driver, and other measurement factors were maintained as constant as possible for the various components used.

Different Accelerometers: Figure 3 shows the ulnar response curves obtained using accelerometers A-1 and A-2 with oscillator 0-1 and driver D-1. While there is fair agreement between the curves above 500 Hz, there is evidence that these peaks are due to variation in the driver output rather than vibrations in the bone.² However, it is frequencies below 500 Hz that are of interest because the technique assumes that the ulnar resonance in vivo occurs in this region. The differences in the recorded responses are apparent; in the case of A-1 the ulnar resonant frequency could be anywhere from 290 Hz to 400 Hz, while for A-2 it would be taken to be about 400 Hz.

Different Oscillators: The ulnar response curve shown in Figure 4 was obtained using accelerometer A-2 with driver D-1 and oscillator 0-2 on the same individual whose responses are shown in Figure 3. The response in Figure 4 should be the same as that labelled A-2 in Figure 3. The only difference in the methods used to obtain these curves is the oscillators used; this is the reason for the different abscissas in the figures. However, there is no correspondence between the curves at those frequencies which overlap. In Figure 3 the resonant frequency would be nearly 400 Hz while if determined from Figure 4 it would be either ~ 125 Hz or ~ 250 Hz. Although the range below 200 Hz is not shown in Figure 3, there was no response corresponding to the one at ~ 125 Hz seen in Figure 4.

Different Bones: Since the anterior surface of the medial tibia is readily accessible and relatively flat it was felt that measurements here might reduce the variations due to changes in orientation of the driver and accelerometer seen with the ulna, and tibial vibrational response curves in vivo were obtained. The position of the leg, points of contact between the accelerometer and driver, and the leg, and contact pressure were maintained constant. Figure 5 shows the response of the tibia obtained using oscillator O-2 and driver D-1 with accelerometers A1, A2, and A-3. While the apparent resonances at 125 Hz are not greatly shifted in frequency for the different accelerometers, there are slight differences in the shapes of these peaks. There is a shift of about 50 Hz, ~ 200 Hz to ~ 250 Hz, between the frequencies at which the maximum response occurs for accelerometers A-2 and A-3 respectively. Also the corresponding peak is missing in the response obtained using A-1. It is interesting to note that the tibial response obtained using A-2 and the ulnar response (Figure 4) also obtained with A-2 and the same oscillator and driver are remarkably similar for such dissimilar bones.

Different Drivers: Tibial responses were measured using oscillator O-2 and either accelerometer A-1 or A-2 with drivers D-1 and D-2. These curves are shown in Figure 6. The response curves obtained using A-1 with drivers D-1 and D-2 are similar with resonances at about 125 Hz. However, the curves obtained for the different drivers with A-2 are quite different, there is a shift of about 60 Hz between the frequencies at which the higher resonance appears and the resonance at ~ 100 Hz is not present in the curve obtained using D-2. It could be argued that these differences seen with A-2 are caused by the excitation of different vibrational modes, but it is difficult to see why similar changes are not found in the response curves obtained using accelerometer A-1 with the two drivers.

CONCLUSIONS

The above observations provide a basis for reasonable doubt concerning the validity of the basic premise of the vibrational techniques, i.e. that transverse vibrations are excited in the bone in vivo and that the accelerometer accurately detects this motion. In the phantom studies the resonances appeared to have no dependence on the elastic moduli of the various "bones" used, indicating that transverse vibrations are either not occurring in the "bone" or that the vibrations do not determine the frequency of oscillation. The vibrational response curves which presumably were proportional to the bone's transverse vibrations in vivo change with different excitation and detection instrumentation. The absence or presence of resonant peaks in the response curves or shifts in their frequencies caused by using different accelerometers, drivers, and oscillators make it difficult to believe that the bone's vibration is accurately represented in the response curves. The curves are clearly more complex than first assumed and probably represent motions other than the bone alone. It is doubtful that the true resonant frequency or even a measure of it can be determined by this technique in its present state. Investigators at three other laboratories have also indicated that they have encountered difficulties in the practical use of this technique.⁵ While it is recognized that a complete investigation is necessary to resolve these questions and that the observations presented do not entirely meet this need, they are of value in alerting other investigators to some of the uncertainties not discussed in the initial references concerning the vibrational techniques.

References

1. Jurist, J. M. and W. Selle, "Acoustical Detection of Osteoporosis", The Physiologist, 8:203, 1965.
2. Jurist, J. M., "In Vivo Determination of the Elastic Response of Bone: I. Method of Ulnar Resonant Frequency Determination", Physics in Medicine and Biology, 15:417-426, 1970.
3. Jurist, J. M., "In Vivo Determination of the Elastic Response of Bone: II. Ulnar Resonant Frequency in Osteoporotic, Diabetic, and Normal Subjects", Physics in Medicine and Biology, 15:427-434, 1970.
4. Wilson, C. R., C. E. Vought, and J. R. Cameron, "Bone as the Resonant Element in a Feedback Oscillator", USAEC Progress Report, COO-1422-54, 1969.
5. Private Communications

Table 1: Instrumentation

	<u>Code Number</u>	<u>Manufacturer</u>	<u>Comments</u>
PIEZOELECTRIC ACCELEROMETERS	A-1	Endevco Corp.	78 gms; Most Sensitive
	A-2	Glenite	20 gms; Intermediate
	A-3		2 gms; Least Sensitive
DRIVERS	D-1	Atlas Electric Device Co.	Atlas PD-4V; Modified with Lucite Driver Piston
	D-2	Reliance Electric Mfg. Co.	Modified Ashworth Sound Reproducer
OSCILLATORS	O-1	Heath Co.	Kit.
	O-2	Home Built	From RCA Design Manual

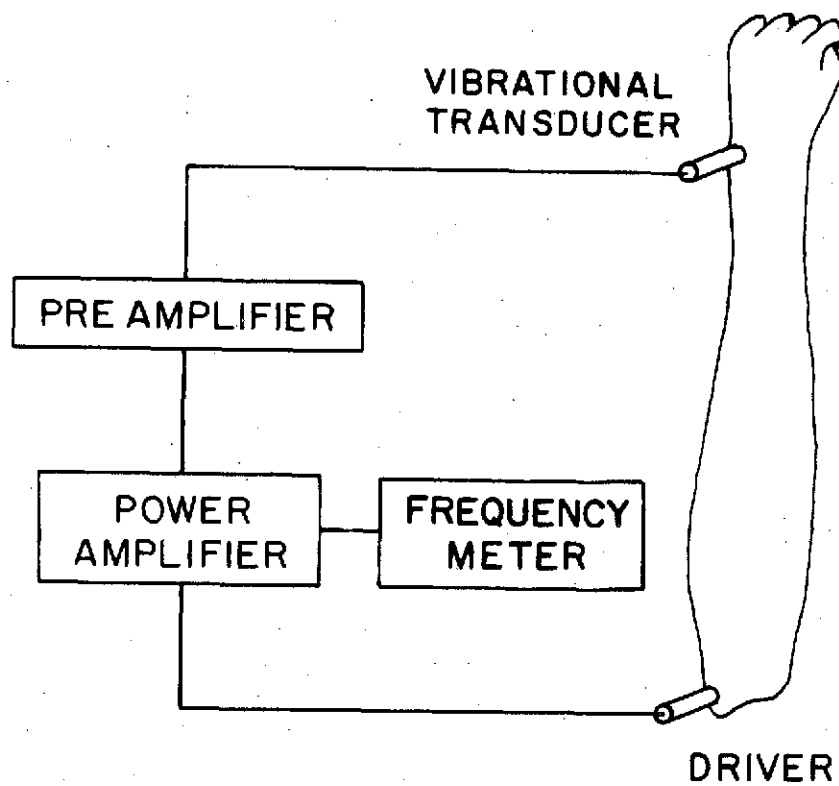


Figure 1. Block diagram of the feedback technique for determining the ulnar resonant frequency in vivo.

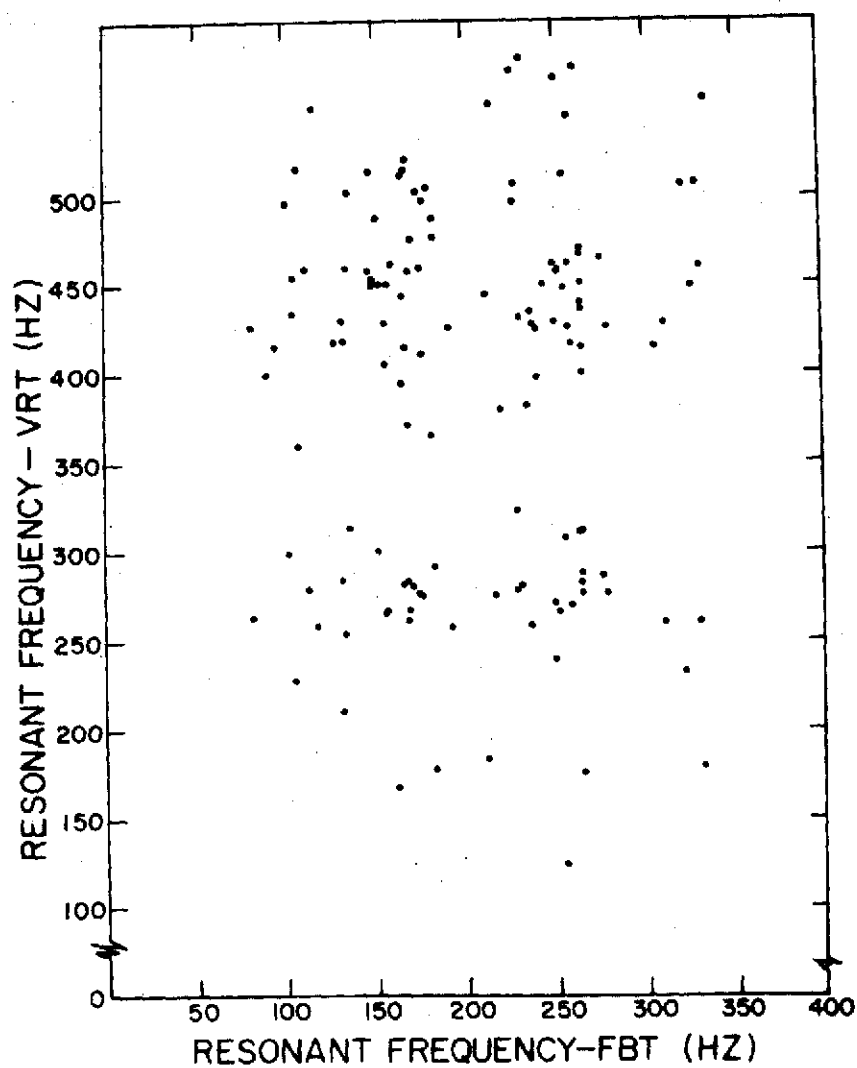


Figure 2. Scattergram of ulnar resonant frequency determined in vivo using the FBT and VRT (Number of subjects = 131).

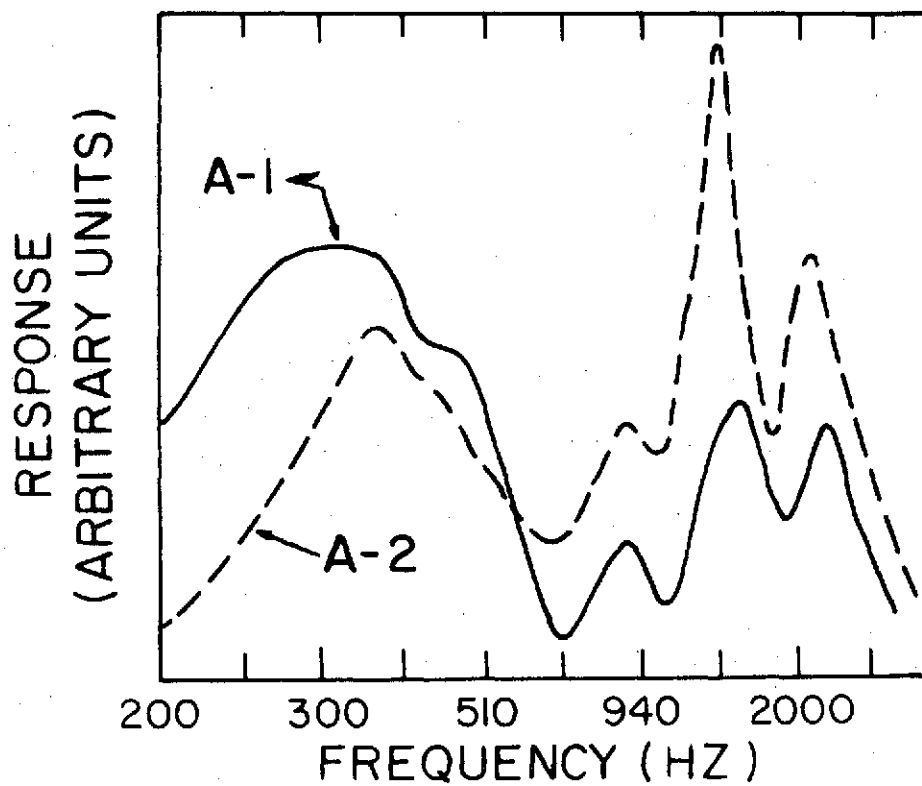


Figure 3. Ulnar response curves obtained in vivo using oscillator 0-1 and driver D-1 with accelerometers A-1 and A-2.

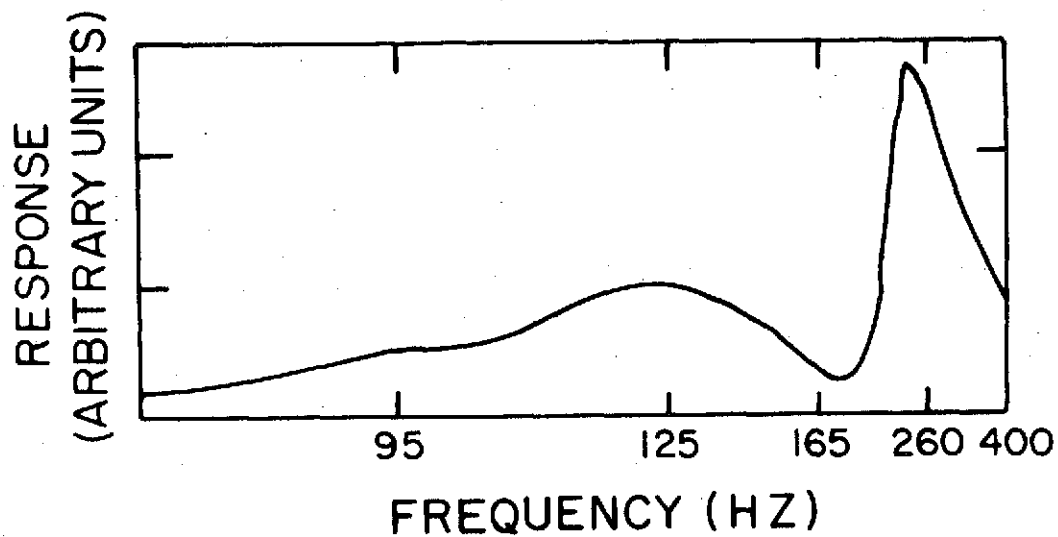


Figure 4. Ulnar response curve obtained in vivo using oscillator 0-2, driver D-1, and accelerometer A-2.

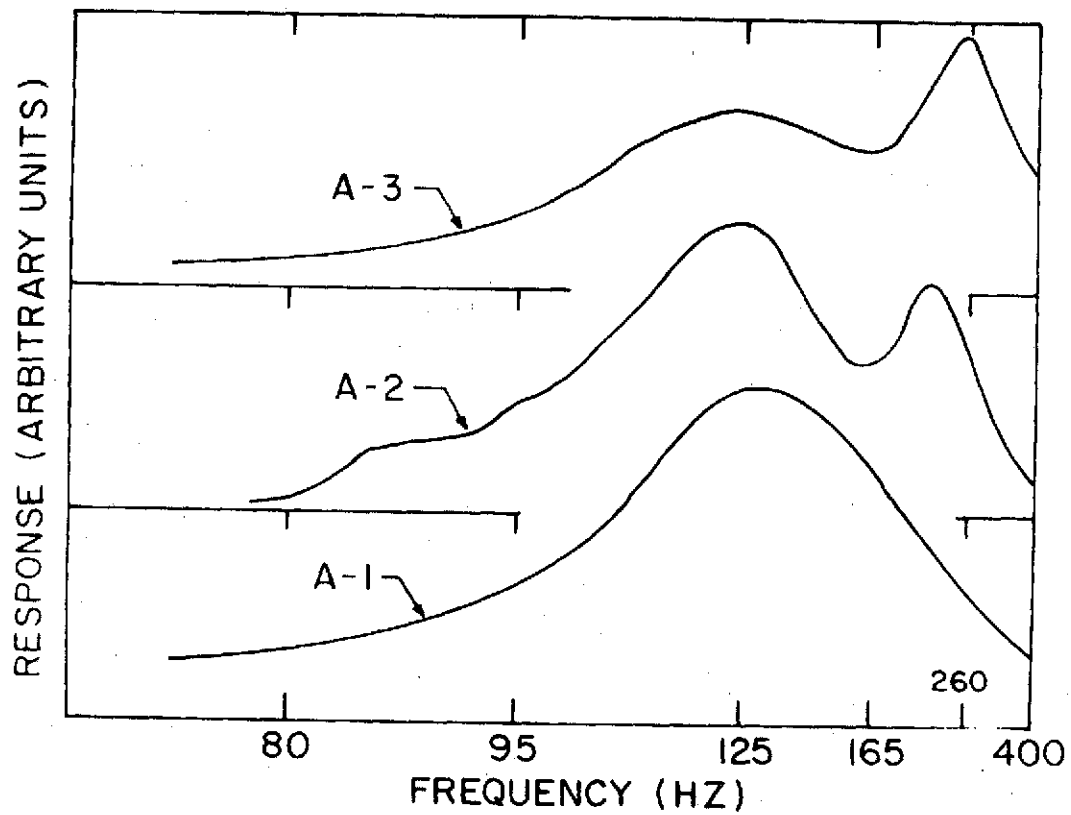


Figure 5. Tibial response curves obtained in vivo using oscillator 0-2 and driver D-1 with accelerometers A-1, A-2, and A-3.

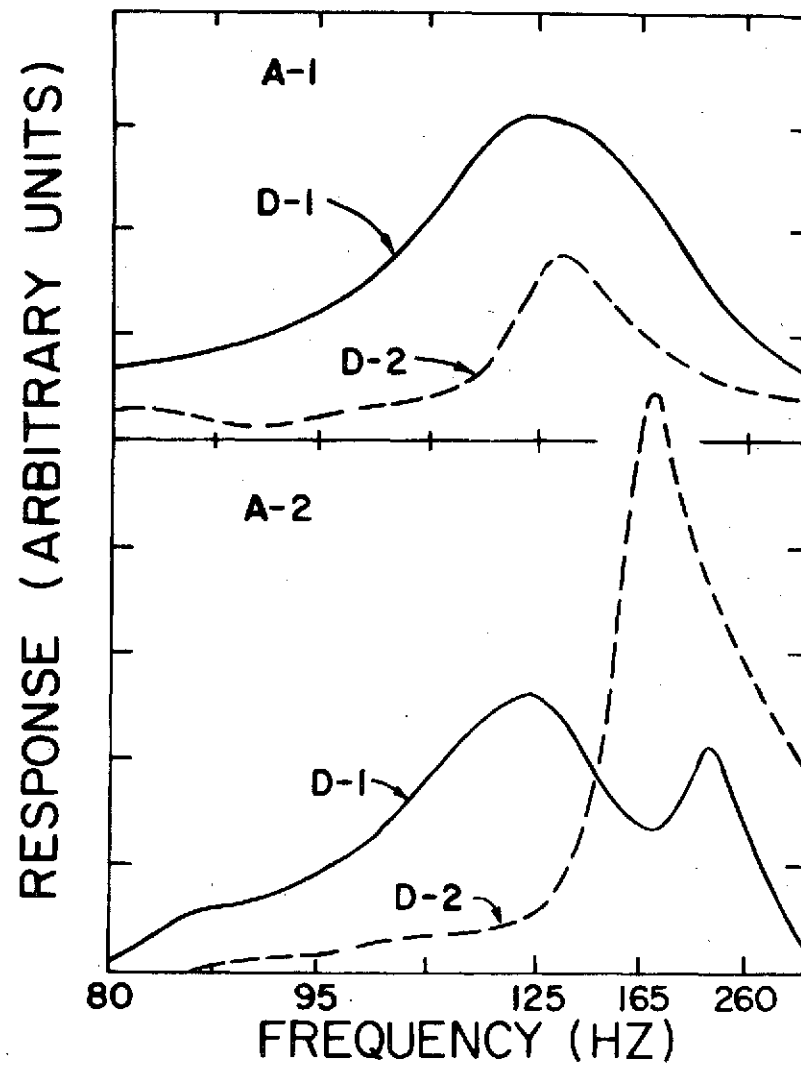


Figure 6. Tibial response curves obtained in vivo using oscillator 0-2 and accelerometers A-1 and A-2 with drivers D-1 and D-2.

REPORT ON THE FIRST BONE MINERAL WORKSHOP-1971

by

Richard Mazess
Department of Radiology
University of Wisconsin Medical Center
Madison, Wisconsin

The availability of a commercial unit for the measurement of bone mineral mass and the widespread interest in this measurement lead to the organization of a three day workshop held at the University of Wisconsin from September 30 to October 2, 1971. The workshop faculty consisted of J. R. Cameron, J. Fischer, P. F. Judy, R. B. Mazess and C. R. Wilson. The main emphasis of the workshop was on the principles of the instrumentation and the use of ^{125}I for scans on humans. It was intended for individuals who were using or were considering using the photon absorptiometric technique, and was oriented toward aiding these individuals in recognizing and dealing with practical problems associated with the method.

An outline of the topics covered in the workshop is given along with a list of the participants. A workbook containing a brief discussion of each of these topics was prepared and given to the participants.* While the majority of the time was spent in presentations or discussions there were opportunities for the participants to work with a number of bone mineral analyzers constructed at the University of Wisconsin, and a commercial unit manufactured by Norland Associates.

Because of the favorable comments received from this workshop another workshop probably will be held in the fall of 1973.

* Copies of the workbook are available upon request.

OUTLINE

- I. Measurement of Bone Mineral Content
 - A. Historical comment
 - B. Attenuation of radiation in tissue
- II. Detailed Description of Bone Mineral Instrumentation
 - A. Description of University of Wisconsin equipment
 - B. Description of University of Wisconsin procedures
 - C. Commercial scanning equipment
 - D. Commercial radionuclide sources
- III. Informal Discussion of Technical Problems
- IV. Evaluation of Sources of Error in Bone Measurement
 - A. Fundamental aspects
 - B. Technical variation
 - C. Empirical evaluation of errors
- V. Data Collection and Interpretation
 - A. Clinical measurement of bone mineral content
 - B. Collection of data for clinical history
 - C. Data interpretation
- VI. Open Session
- VII. Demonstration Lectures and Experiments

BONE MINERAL WORKSHOP PARTICIPANTS

September 30 - October 2, 1971

John Bevan
Miami Valley Labs
Procter & Gamble
Cincinnati, Ohio 45239

Lawrence Blau
The Hospital for Special Surgery
535 East 70th Street
New York, New York 10021

Joseph Dicka
General Electric Medical Systems
6719 Seybold Rd.
Madison, Wisconsin 53719

Linda Hofschulte
Mayo Clinic
Rochester, Minnesota 55901

B. G. Oltman
Argonne National Labs
9700 So. Cass Avenue
Argonne, Illinois 60439

J. Thomas Payne
Box 382 Mayo
University Hospital
Minneapolis, Minnesota 55455

Robert R. Recker
2305 So. 10th St.
Omaha, Nebraska 68144

Fred Rose
Norland Instruments
1009 Janesville Dr.
Box 47
Fort Atkinson, Wisconsin 53538

Paul D. Saville
Creighton University
Department of Medicine
Omaha, Nebraska 68144

Robert A. Schlenker
Argonne National Labs
9700 So. Cass Avenue
Argonne, Illinois 60439

Stuart Starr
950 E. 59th St.
Room ESB-9
Chicago, Illinois 60637

John Ullmann
USPHS Hospital
15th Avenue at Lake Street
San Francisco, California 94118

Chet Varns
Procter & Gamble
Miami Valley Labs
Research Division
Cincinnati, Ohio 45239

Edith Weinberg
Orthopedic Research Lab
Massachusetts General Hospital
Boston, Massachusetts 02114

Jon Vergedal
Mineral Metabolism
VA Hospital
Seattle, Washington 98108

Michael E. Wise
Atomic Energy of Canada Limited
Commercial Products
P.O. Box 6300
Ottawa, Ontario, Canada

Wesley Wooten
Medical Physics
Department of Radiology
UCLA Center for Health Sciences
Los Angeles, California 90024

Louis Zeitz
Department of Biophysics
Sloan-Kettering
New York, New York 10021

Interpretation of Fracture Index Charts

by: E. Smith, Ph.D. and J. R. Cameron, Ph.D.

University of Wisconsin Bone Mineral Laboratory

A. Introduction

The spontaneous fracture index graphs, bone mineral (g/cm) and bone mineral/width (gm/cm^2), were derived from data collected at the University of Wisconsin Bone Mineral Laboratory over more than five years (1965-1971). All measurements were obtained using the ^{125}I monoenergetic photon absorption technique developed at the University of Wisconsin. The site measured was at a point $1/3$ the distance from the distal end of the radius (standard site). This region of the radius is quite uniform, and a slight error in repositioning has little effect on the measurement. The data collected agree with the findings of other investigators.

Many investigators^(1, 2, 3, 4, 5, 6, 7) report bone mineral decreases in women by twenty to thirty percent between the ages of thirty and seventy. This decrease in bone mineral is cited as part of the normal aging process. The aging process results in bone which is chemically normal in mineral structure^(8, 9) but reduced in bone mineral mass.⁽³⁾ Reduction in bone mineral mass makes the bone more susceptible to fracture.⁽¹⁰⁾ While not all elderly people with large bone loss develop clinical symptoms of osteoporosis, such as spontaneous fractures, the probability of fracture significantly increases. While the quantity of bone mineral does not account for total bone strength, it provides a good indication of the resistance of bone to fracture. Therefore, a bone mineral index reflects when bone is more susceptible to fracture.

Smith⁽¹¹⁾ determined a discriminant value for high probability of bone fractures from a three year study of elderly women. Fifty control Caucasian females and fifty osteoporotic Caucasian females (as determined by spontaneous fracture of the hip, vertebrae and distal radius) were compared to each other. A discriminant bone mineral value of 0.68 g/cm was determined between the control and osteoporotic group. Whenever a patient has a bone mineral value of less than 0.68 g/cm the patient is suspect of clinical osteoporosis. For successful patient therapy, it would be helpful to select the population prior to spontaneous fracture. Smith and Cameron⁽¹²⁾ propose the following definition of osteoporosis in adult Caucasian females.

- 1) Any individual whose bone mineral mass at the standard measurement site of the radius is more than two standard deviations below the mean for individuals of that same age, sex, and bone size, or;
- 2) Any adult female whose bone mineral at the standard site of the radius is less than 0.68 gm/cm, or;
- 3) Any individual who has a spontaneous fracture (who has not been diagnosed as having a bone disease which would cause the fracture).

These criteria give an objective starting point for determining osteoporosis prior to spontaneous fractures. They do not negate the physician's diagnostic responsibility for determining the patient's bone mineral status in relation to her past history and/or the use of other laboratory reports to make the final diagnosis of clinical osteoporosis.

B. Spontaneous Fracture Index Graph Interpretations

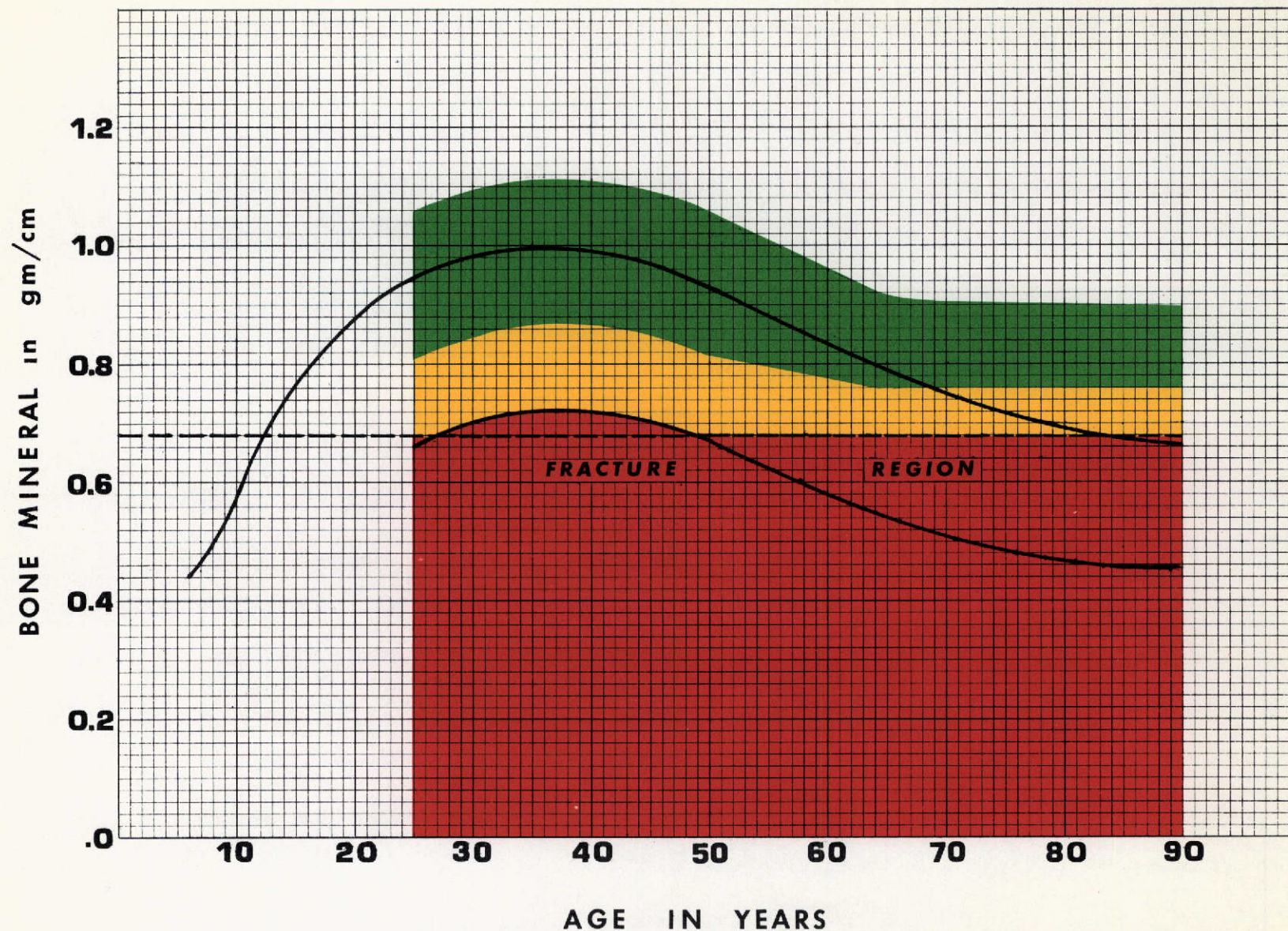
- 1) The curved, upper solid black line represents the mean values obtained from the Wisconsin Bone Mineral Laboratory population studies.
- 2) The lower solid black line is 30% or about 2 standard deviations below the mean value.
- 3) The dashed line is the discriminant analysis value determined by Smith. (11)
- 4) Between 25 to 50 years the green region represents approximately one standard deviation.
- 5) GREEN REGION - Patient has adequate bone mineral.
- 6) YELLOW REGION - Patient may be developing tendency to fracture and should be measured at regular intervals. Therapy should be considered.
- 7) RED REGION - Spontaneous fracture probability is high. Patient should be placed on therapy programs and should be measured at regular intervals.

When instigating therapy, measure the patient three or four times in the first month to establish good baseline values and to measure the patient's progress at one to two month intervals thereafter. When making serial measurements, the physician should expect a patient's data to exhibit a scatter with a standard deviation of two to three percent.

C. Bone Mineral Measurement Guidelines

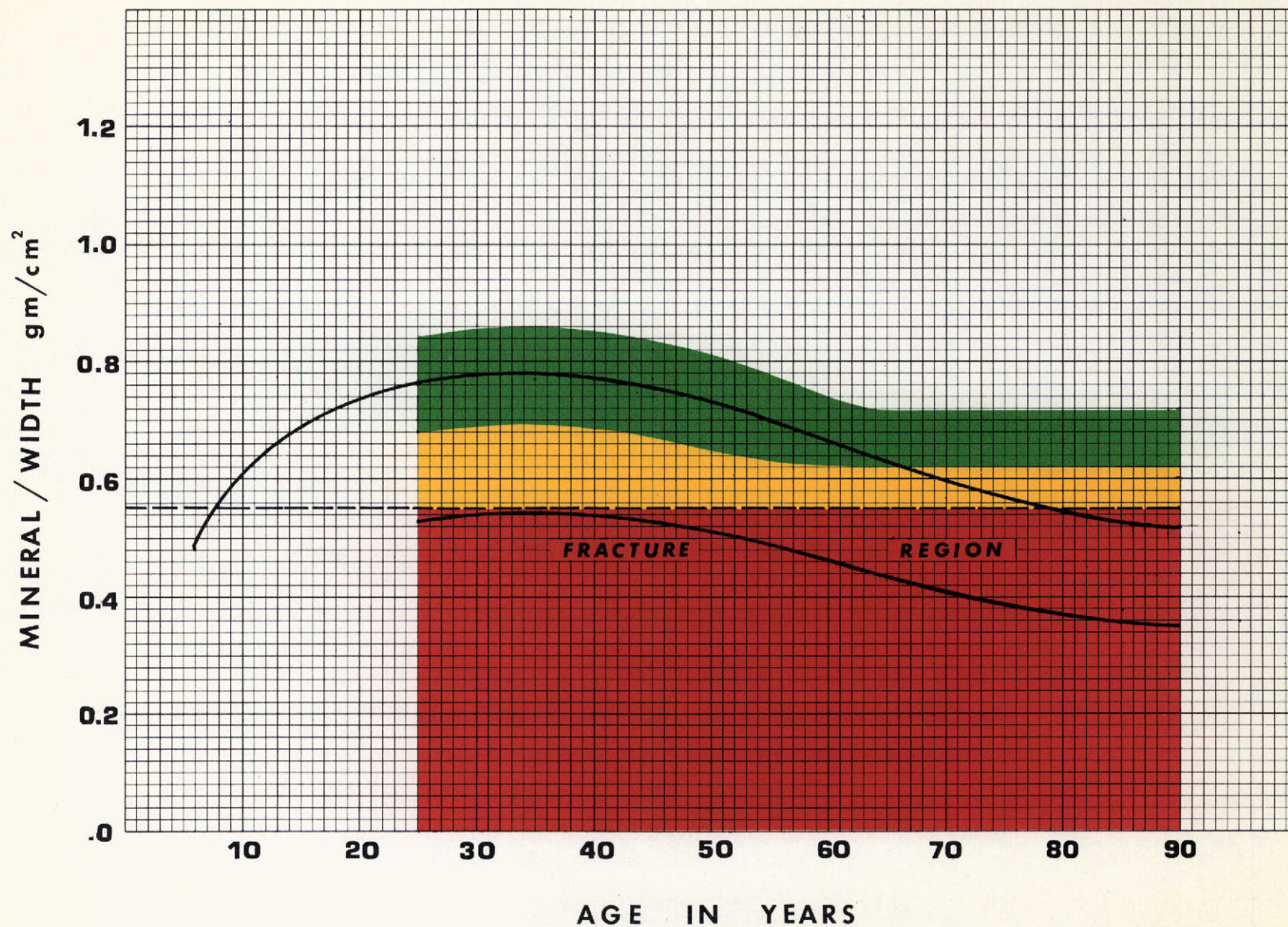
Women over forty-five years old should be measured annually and the values obtained should be graphed. If a patient's values are in the yellow region of the fracture index charts, they should be measured and graphed at three month intervals. If the trend of the data is downward, therapy is indicated. The criticality of the therapy

SPONTANEOUS FRACTURE INDEX FEMALE CAUCASIAN



Everett L. Smith, Jr., Ph.D.
and John R. Cameron, Ph.D.
University of Wisconsin
Bone Mineral Laboratory

SPONTANEOUS FRACTURE INDEX FEMALE CAUCASIAN



Everett L. Smith, Jr., Ph.D.
and John R. Cameron, Ph.D.
University of Wisconsin
Bone Mineral Laboratory

depends upon the rate of bone mineral decline and on how close the patient's values are to the red region. Long term rates of mineral loss greater than one percent per year are serious, regardless of the region of the fracture index chart. Trend conclusions must be based on at least four data points taken at minimum intervals of three months.

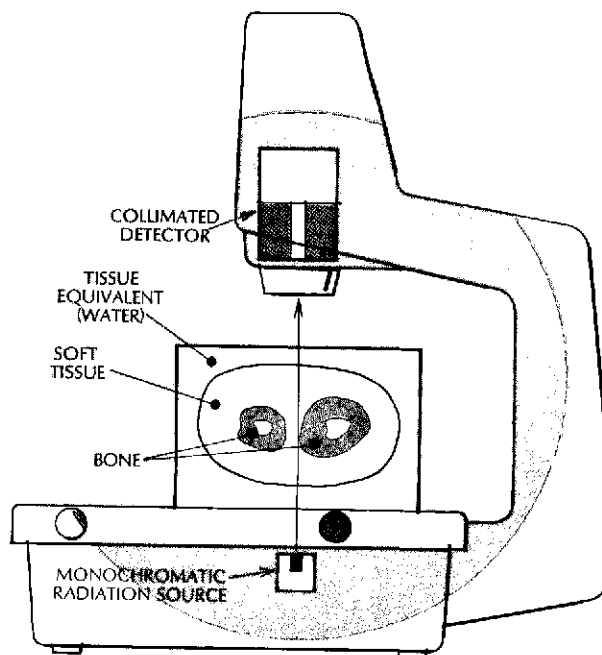
D. Bone Mineral Vs. Bone Divided by Width

In the majority of cases the total mineral content alone is a reliable indicator of an individual's propensity to fracture. However, in cases of very slight build or exceptionally heavy build it is sometimes helpful to also compare the mineral divided by the width to values derived from average individuals. The results of both comparisons must then be considered, together with other clinical data, in reaching a final interpretation.

REFERENCES

1. Arnold, J.S. The quantitation of bone mineralization as an organ and tissue in osteoporosis. In Dynamic Studies of Metabolic Bone Disease. Pearson, O.H. & Joplin, G.F. (Eds.). Blackwell, Oxford, pp. 59, 1964.
2. Atkinson, P.J. Changes in resorption spaces in femoral cortical bone with age. *Journal of Path. and Bacteriology*, Vol. 89, No. 1, pp. 173, 1965.
3. Caldwell, R.A. Observations on the incidence, etiology, and pathology of senile osteoporosis. *Journal of Clin. Path.* 15: pp. 421, 1962.
4. Cameron, J.R. and Sorenson, J.A. Measurement of bone mineral in vivo: An improved method. *Science*, 142, pp. 230, 1963.
5. Garn, S.M., Rohmann, C.G., and Wagner, B. Bone loss as a general phenomenon in man. *Fed. Proc.*, Vol. 26, pp. 1729, Nov.-Dec., 1967.
6. Saville, P.E. Changes in bone mass with age and alcoholism. *Journal Bone and Joint Surgery*, Vol. 47: pp. 492, 1965.
7. Trotter, M., Broman, G.E. and Peterson, R.R. Densities of bones of white and negro skeletons. *Journal Bone & Joint Surgery*, 42-A, pp. 50, 1960.
8. Barnett, E. and Nordin, B.E.C. The clinical and radiological problem of thin bones. *Brit. J. Radiol.* 34: pp. 683, 1961.
9. Casuccio, C. Concerning osteoporosis. *Journal of Bone and Joint Surgery*, Vol. 44-B, No. 3, pp. 453, Aug. 1962.
10. Wilson, Charles R. Relationship of photon absorption measurements of bone mineral content to bone strength. Doctoral Thesis, University of Wisconsin, 1971.
11. Smith, Everett L., Jr., Bone changes with age and physical activity. Doctoral Thesis, University of Wisconsin, 1971.
12. Smith, E.L. and Cameron, J.R. A proposed quantitation definition of osteoporosis (in preparation).

Automatic, non-invasive technic for diagnosing bone disease



Complete scanning procedure in 5 minutes or less

Accurate, precise method.

No biopsy. No radiographs.

Portable, safe, simple operation.

NORLAND · CAMERON BONE MINERAL ANALYZER

RELATIONSHIP BETWEEN BONE MINERAL CONTENTS OF THE RADIUS

FEMORAL NECK, THORACIC VERTEBRAE AND OTHER SITES*

by

C.R. Wilson and J.R. Cameron
Department of Radiology
University of Wisconsin
Madison, Wisconsin

ABSTRACT

The loss of bone and the increased incidence of spontaneous fractures in the femoral neck and spine during aging is a serious medical problem. However, osteoporosis is not usually diagnosed prior to the occurrence of a spontaneous fracture due to the difficulty in accurately determining in vivo the amount of bone in these areas. The monoenergetic x-ray photon absorptiometric technique for determining bone mineral content provides an accurate and precise measurement, but the method is usually limited to the appendicular bones. The relationships between the mineral contents at various sites on the radius, femoral neck and lower thoracic vertebrae of twenty-four skeletons (ages from 35 to 89 years) were examined to evaluate the ability of the radius mineral content to reflect the mineral content of the femoral neck and the spine. It was found that the radius bone mineral content was highly related to that of the femoral neck, $r = 0.87$, and moderately related to the mineral content of the thoracic vertebrae with the majority of the correlation coefficients between 0.60 and 0.70. Also regression analyses indicated that the radius mineral content and age provides a moderately accurate estimate (standard error of estimate of about 17%) of the mineral contents of the femoral neck and spine.

INTRODUCTION

The importance of the structural function of bone to the health of the individual is well known. However, in many instances there is a failure of the skeleton to provide adequate structural function throughout life. A progressive deterioration in skeletal integrity begins after maturity with the most serious loss of strength occurring in the femoral neck and spine. Fractures in these areas, associated with minimal trauma and called "spontaneous" increase markedly with age. The incidence of fracture of the femoral neck in women doubles for every five years of age after the fifth decade.¹ It has been estimated that over four million persons in the United States over 50 years old have suffered vertebral fracture or collapse.²

The load bearing capacity of a bone in vivo, whether it is a vertebra, radius, femur, etc., is dependent on the bone's form or architecture, the intrinsic strength of the bone tissue, and the amount of bone present. Aging in general produces changes in these factors which lead to a deterior -

* To be presented at the Third International Conference on Medical Physics, Including Medical Engineering, Göteborg, Sweden, July 30-August 4, 1972.

ation in the strength of the skeleton. However, the primary factor in the increased skeletal fragility in old age is the reduction in the total amount of bone present in the skeleton resulting from cortical thinning, increased porosity and loss of trabecular bone. It has been demonstrated in vitro that the strength of the femoral neck³ and vertebrae^{4,5} are highly related to the amount of bone present, with the deterioration in strength in these areas paralleling or even exceeding the loss of bone with age. A "spontaneous fracture resulting from the loss of bone in these areas is often defined as clinical osteoporosis. Estimates have been made that the probability of "spontaneous" failure of the spine increases greatly when the mass of bone in the vertebra is reduced to fifty percent or less than present at maturity.⁶ However the recognition of the potential osteoporotic or individual at risk is not usually possible because of the difficulty in accurately determining the amount of bone in either the femoral neck or spine in vivo.

Attempts to measure bone mass in vivo in these areas using x-ray photodensitometry of radiographic images⁷ have not been very successful. Difficulties related to the polyenergetic nature of the photon beam, the ill-defined amount of scattered radiation reaching the film, etc. contribute to a sizeable uncertainty in the measurement of bone mass using this technique. The photon absorptiometric technique developed by Cameron⁸ circumvents many of these difficulties. The amount of bone mineral is determined by measuring the transmission of a narrow monoenergetic photon beam from a radioactive source (typically ¹²⁵I) through the bone. This technique provides an accurate and precise measurement of the mineral content either in vitro or in vivo.

Although the absorptiometric technique is usually limited to the peripheral bones of the skeleton, i.e. radius, ulna, os calcis, etc., the bone mineral content of the appendicular skeleton reflects the status of the clinically significant areas of the axial skeleton. It is evident that the bone of the appendicular and axial skeleton are related since the majority of factors which influence bone such as diet, age, genetic heritage, hormonal levels, etc., are systemic. The mass of individual bones of both the axial and appendicular skeleton are interrelated and empirical formulae for estimating the masses of axial or the entire skeleton from the mass(es) of one or more of the appendicular bones have been reported.^{9, 10, 11} Smith¹² found that the radius mineral content is significantly lower in women with "spontaneous" fracture of the hip than age-matched normals of similar physique. Also Goldsmith¹³ reported that the radius mineral content was sufficiently related to standard radiographic criteria for assessing the spine to be of diagnostic value in separating normal and osteoporotic individuals. Therefore the feasibility of quantitatively estimating the amount of bone in the femoral neck and spine from the mineral content of a single or combination of locations on the appendicular skeleton and age was investigated.

The bone mineral content at sites on the radii, ulnae, humeri, fibulae, tibiae, femurs, and thoracic vertebrae of 24 skeletons were measured using the photon absorptiometric technique. Single and multiple regressions were calculated to evaluate the accuracy of estimating the mineral content of the femoral neck and thoracic vertebrae from the bone mineral content of the radius, the bone mineral content of the radius and age, and the bone

mineral contents of the radius with other scan sites and age. Correlation coefficients between the mineral contents at sites on the same bone and between different long bones were also calculated.

METHODS AND MATERIALS

Partial skeletal remains consisting of the radii, ulnae, humeri, tibiae, fibulae, femurs, and the eighth through eleventh thoracic vertebrae of 24 cadavers were obtained from the University of Wisconsin Department of Anatomy. The cadavers, 17 males and 7 females ranging in age from 35 to 89 years, were acquired by the University of Wisconsin from hospitals and nursing homes around the state and information as to the cause of death, race, and length of confinement to bed prior to death was lacking. Prior to scanning, most of the soft tissue adhering to the long bones was removed. The eighth through eleventh vertebrae were separated and the intervertebral discs were removed. The lumbar vertebrae could not be obtained because the dissection techniques used by the anatomy students destroyed these vertebrae. All bones were stored at 0° C and measures were taken to prevent dehydration.

The BMC* of the long bones were measured at positions corresponding to 25, 50, and 75 percent of the total length of the bone measured from its distal end using the photon absorptiometric technique. These scan sites will be referred to as D, M, and P, corresponding to distal, midshaft, and proximal, respectively. In addition to these sites the radius and ulna were also scanned at 33 percent of the length from the distal end, the distal third site or DT. The BMC of the femoral neck was measured at the narrowest portion of the neck. The size and shape of the neck varies in the region between the trochanter and the femoral head and there are differences in the shape of the femoral neck between individuals. Thus it is difficult to measure the corresponding anatomical site on different femurs. Sets of four or five consecutive scans across the femoral neck were repeated three or more times with the femur repositioned after each set in order to reduce anatomical variations. The coefficient of variation in the BMC of the four or five scans in a set was typically less than one percent, and the coefficient of variation of the mean BMC on the femoral neck was about five percent. The mineral content, width and height of the individual thoracic vertebrae were obtained by scanning each vertebra through its maximum width with the vertebra in positions. Both scans were made in the coronal plane through the maximum width. The beam was perpendicular to the disc along the first scan path; for the second path the vertebra was rotated 90° about an axis perpendicular to the plane of the first scan path. The portion of the vertebral body scanned in both paths was the same and the BMC in the two cases agreed to within less than five percent.

The BMC at each site on the long bone and vertebrae was obtained by averaging four or five consecutive scans. The coefficients of variation in the BMC and the sites were between one and two percent. The "mineral" of an Al bar standard was measured at various times each day to monitor the performance of the equipment. Table 1 gives the mean coefficients of variation of the BMC of the midshaft site of some long bones, the ninth thoracic vertebra, and the Al standard.

*Bone Mineral Content

RESULTS

The correlation coefficients (r) between the bone mineral content (BMC) at sites on the same bone and between different bones were calculated. Table 2 illustrates the magnitude of the coefficients between sites on the same bone; $p \leq 0.001$ in all cases. Coefficients of similar magnitude were found between sites on contra-lateral pairs of bones. The interrelation between the BMC at scan sites on different long bones were also high, with r typically greater than 0.85. Table 3 gives the coefficients between the BMC at sites on the radius and sites on the ulna, humerus, tibia, fibula, and femur. The coefficients between the BMC at sites on the radius and sites on the lower extremities are slightly lower than those between the former and sites on the humerus and ulna. This is due probably to the greater difficulty in scanning the corresponding anatomical sites on each of the lower bones. The magnitude of the correlation coefficients between the mineral contents of the eighth through eleventh thoracic vertebrae were slightly less than those found between scan sites on the long bones (Table 4). There is a fair degree of correlation between the vertebral bodies with r -values typically greater than 0.80 and p -levels less than or equal to 0.005.

The ability to estimate the BMC of the femoral neck from the BMC at sites on the long bones was investigated by calculating the regression relations between the BMC of the femoral neck and the BMC of sites on the radius or femur and a combination of sites on the radius and femur. These regressions were also calculated with age included as another independent variable. In all cases there was no significant gain in predictive accuracy using the multiple regressions over the single regression with only the radius bone mineral as the independent variable. There were also no marked differences in the predictive accuracy of single regressions between different sites on radius or femur and the BMC of the femoral neck. Figure 1 is a scattergram between the BMC of the DT site on the radius and the femoral neck. The regression equation, standard error of estimate (SEE), and correlation coefficients are given in the figure. The open dots represent females.

The correlation coefficients between the BMC at scan sites on the radius and the thoracic vertebrae are given in Table 5. There is a weak correlation between the radius sites and the mineral content of the individual vertebrae. Most coefficients are significantly different from zero at a p -level less than 0.005. Figure 2A is a scattergram of the mineral content of the ninth thoracic vertebra versus the BMC at the distal third (DT) site on the radius, $r = 0.68$; this scattergram is typical of those between the radial BMC and the thoracic vertebrae. Averaging the mineral contents of the four vertebrae, however, increased the interrelation between the BMC of the radius and the axial skeleton. Figure 2B is the scattergram of the BMC at the DT site on the radius and the average mineral content of the four thoracic vertebrae. The regression line and the standard error of estimate are shown. In comparison to Figure 2A the scatter appears to have been reduced and while the correlation coefficient, $r = 0.69$, is not significantly greater than that between the BMC of the DT site on the radius and the mineral content of the individual thoracic vertebrae, most of the variation is due to the two cadavers which lie approximately two standard deviations above the line. When these were omitted this correlation coefficient was considerably increased, i.e. $r = 0.85$.

Single regression equations were calculated between the average thoracic mineral content (dependent variable) and the BMC at different sites on the radius of ulna. Multiple regressions were calculated between the average thoracic mineral content and the following: the BMC at sites on the radius and the ulna; the BMC at sites on the radius and age, and the BMC at sites on the ulna and age. The latter two were also calculated with another site on the radius or ulna included as a third independent variable. There was no significant difference between the predictive accuracy of the regression equation, either single or with age, using different sites on the same bone or on different bones. Any radial scan site was as good as any other radius or ulna scan site. Also multiple regressions using the BMC at two scan sites were not statistically better than regressions using a single scan site. This was expected due to the high interrelation between the BMC at sites on the long bone. There was, however, a slight increase in predictive accuracy when age was included as a second independent variable with the BMC at a radius or ulna scan site. For example, the SEE in the predicted average vertebral mineral (PVMC) from the BMC of the radial midshaft alone was 18.6 percent while it was 16.8 percent when the radial BMC and age were used in the regression. Figure 3 is the scattergram of the predicted versus observed vertebral mineral content, the predictive equation is given on the figure.

CONCLUSIONS

While it is evident that the bone of the appendicular and axial skeleton are related the degree of relationship is not clear, and the question of whether the BMC at a scan site on the radius or ulna could be used to estimate the BMC at other appendicular locations, the femoral neck, and spine was investigated.

The high degree of correlation between the BMC at scan sites on the same long bone and on different long bones indicates the possibility of predicting the BMC at a site on the same or different bones. Regression equations between the BMC on the radius and other locations on the appendicular skeleton, although not given, were calculated. The standard error of estimates were typically less than 10 percent indicating a fair degree of uniformity in the mineral content throughout the appendicular skeleton. These results are in agreement to those previously reported by Mazess.¹⁰

Of greater interest is the relatively high correlation ($r = 0.87$) between the radius and femur mineral content and the possibility of using the radius bone mineral for assessing the likelihood of hip fractures. As was mentioned before, Smith⁹ reported that the mean radius BMC of women with hip fractures is significantly lower than age-matched controls with no fractures. Using a discriminant value of 0.68 gm/cm he found that about 80% of the fracture group had a radial mineral content below and 80% of the normals had a mineral content above 0.68 gm/cm. Substituting this discriminant value, 0.68 gm/cm, into the predictive equation in Figure 1 indicates that a femoral neck with a BMC of less than 1.55 gm/cm would have a high risk of fracture. Five of the skeletons present in the investigation (four females and one male) had a radial BMC, DT scan site of less than 0.68 gm/cm. Of these five, two showed evidence of past

femoral fracture, i.e. one had a healed fracture and the other had an orthopaedic pin in the femoral neck. The third showed no past hip fracture, however there was radiographic evidence of abnormal bone growth in the neck region. The femoral necks of the remaining two were broken and the heads of the femurs were missing. It was not possible to ascertain whether these breaks had occurred before death or during removal of the femurs from the cadavers and subsequent handling. The femoral necks of these two skeletons were clearly weaker than normal, since none of the skeletons with radial BMC greater than 0.68 gm/cm possess femurs broken in this fashion. Of all the intact femurs which could be measured only one was found to have a femoral neck BMC less than 1.55 gm/cm and in this case the contra-lateral femur had been fractured in vivo. Also only one of the skeletons (a 61 year old male) which had a radial BMC greater than 0.68 gm/cm had evidence of a hip fracture. Due to the lack of medical histories it was not known if any of the fractures were "spontaneous" or the result of major trauma. Therefore it appears that the radial BMC is a fair predictor of the femoral neck BMC and that it may be of use in the identification of individuals in danger of suffering spontaneous hip collapse.

In the case of the estimation of the vertebral mineral content from the age and BMC of the radius, the relationships between these factors does not allow a precise estimation of the vertebral mineral content. However, the degree of relationship would appear to be sufficient to be of use in assigning individuals to one of several broad classes related to the amount of their vertebral mineral content.

References

1. Bauer, G. C., "Epidemiology of Fracture in Age Persons," Clinical Orthopedics, 17:219-225 (1960)
2. Lutwak, L. and Whedon, G. D., "Osteoporosis," Disease-a-Month, (1963)
3. Vose, G. P. and Mack, P. B., "Roentgenologic Assessment of Femoral Neck Density as Related to Fracturing," American Journal of Roentgenology, 89:1296-1301 (1963)
4. Bartley, M. H., Arnold, J. S., Haslam, R. K. and Lee, W. S., "The Relationship of Bone Strength and Bone Quality in Health, Disease and Aging," Journal of Gerontology, 21:517-521 (1966)
5. Bell, G. H., Dunbar, O. and Beck, J. S., "Variations in Strength of Vertebrae with Age and their Relation to Osteoporosis," Calcified Tissue Research, 1:75-86 (1967)
6. Urist, M. R., MacDonald, N. S., Moss, M. J. and Koog, W. A. S., "Rarefying Disease of the Skeleton: Observations Dealing with Aged and Dead Bone in Patients with Osteoporosis," Mechanism of Hard Tissue Destruction, ed. Sognnaes, R. F., Washington, D. C. AAAS (1963)
7. Whedon, G. D. and Cameron, J. R., eds "Progress in Methods of Bone Mineral Measurements," U.S. Dept. of H.E.W., (1968)
8. Cameron, J. R. and Sorenson, J. A., "Measurement of Bone Mineral In Vivo: An Improved Method," Science, 142:230 (1963)
9. Trotter, M. A., "A Preliminary Study of Estimation of Weight of the Skeleton," American Journal of Physical Anthropology, 12:537 (1954)
10. Mazess, R. B., "Estimation of Bone and Skeletal Weight by the Direct Photon Absorptiometric Method," American Journal of Physical Anthropology 29:133 (1968)
11. Horseman, A., Bulvso, L., Bently, H. B., and Nordin, B. E. C., "Internal Relationships Between Skeletal Parameters in Twenty-three Male Skeletons," ed. Cameron, J. R., Proceedings of Bone Measurement Conference. AEC Conf-700515 (1970)
12. Smith, E. L., Bone, changes with Age and Physical Activity. Doctoral Thesis, Univ. of Wisconsin (1971)
13. Goldsmith, N. F., Johnston, J. O., Ury, H., Vose, G., and Colbert, C., "Bone-Mineral Estimation in Normal and Osteoporotic Women," Journal of Bone and Joint Surgery 55-A:83-100 (1971)

TABLE 1. MEAN COEFFICIENTS OF VARIATION IN BMC.

<u>Location</u>	<u>Coefficient of Variation (%)</u>	<u>Number of Observations</u>
Radius	1.25	24
Ulna	1.53	24
Femur	1.33	24
Ninth Thoracic Vertebra	1.40	18
Aluminum Bar Standard	1.38	125

TABLE 2. CORRELATION COEFFICIENTS BETWEEN BMC AT SCAN SITES ON THE
SAME BONE (n = 24)

Radius					Ulna				
	D	DT	M	P		D	DT	M	P
D	-				D	-			
DT	.99	-			DT	.98	-		
M	.97	.96	-		M	.96	.98	-	
P	.97	.98	.96	-	P	.93	.94	.96	-

Humerus				Tibia			
	D	M	P		D	M	P
D	-			D	-		
M	.97	-		M	.90	-	
P	.94	.97	-	P	.94	.90	-

Fibula				Femur			
	D	M	P		D	M	P
D	-			D	-		
M	.94	-		M	.94	-	
P	.90	.88	-	P	.86	.94	-

TABLE 3. CORRELATION COEFFICIENTS BETWEEN BMC AT SCAN SITES ON THE RADIUS AND OTHER LONG BONES

		Ulna				Humerus			Tibia			Fibula			Femur		
		D	DT	M	P	D	M	P	D	M	P	D	M	P	D	M	P
Radius	D	.91	.93	.94	.91	.94	.95	.94	.88	.85	.89	.90	.87	.78	.89	.83	.72
	DT	.93	.93	.95	.93	.95	.95	.95	.90	.86	.91	.91	.88	.80	.91	.84	.73
	M	.91	.92	.94	.93	.95	.91	.90	.84	.84	.88	.89	.88	.76	.84	.81	.71
	P	.94	.95	.95	.90	.96	.94	.94	.88	.85	.91	.85	.85	.78	.88	.83	.73

TABLE 4. CORRELATION COEFFICIENTS BETWEEN THE BMC OF THE THORACIC VERTEBRAE. (n = 18 - 20)

	Eighth	Ninth	Tenth	Eleventh
Eighth	-			
Ninth	.92	-		
Tenth	.78	.92	-	
Eleventh	.76	.78	.84	-

TABLE 5. CORRELATION COEFFICIENTS BETWEEN THE BMC AT SCAN SITES ON THE RADIUS AND THE THORACIC VERTEBRAE. (n = 18 - 20)

	Thoracic Vertebrae			
	Eighth	Ninth	Tenth	Eleventh
D	.66	.70	.63	.50
DT	.67	.68	.61	.50
M	.67	.69	.60	.42
P	.67	.69	.60	.48

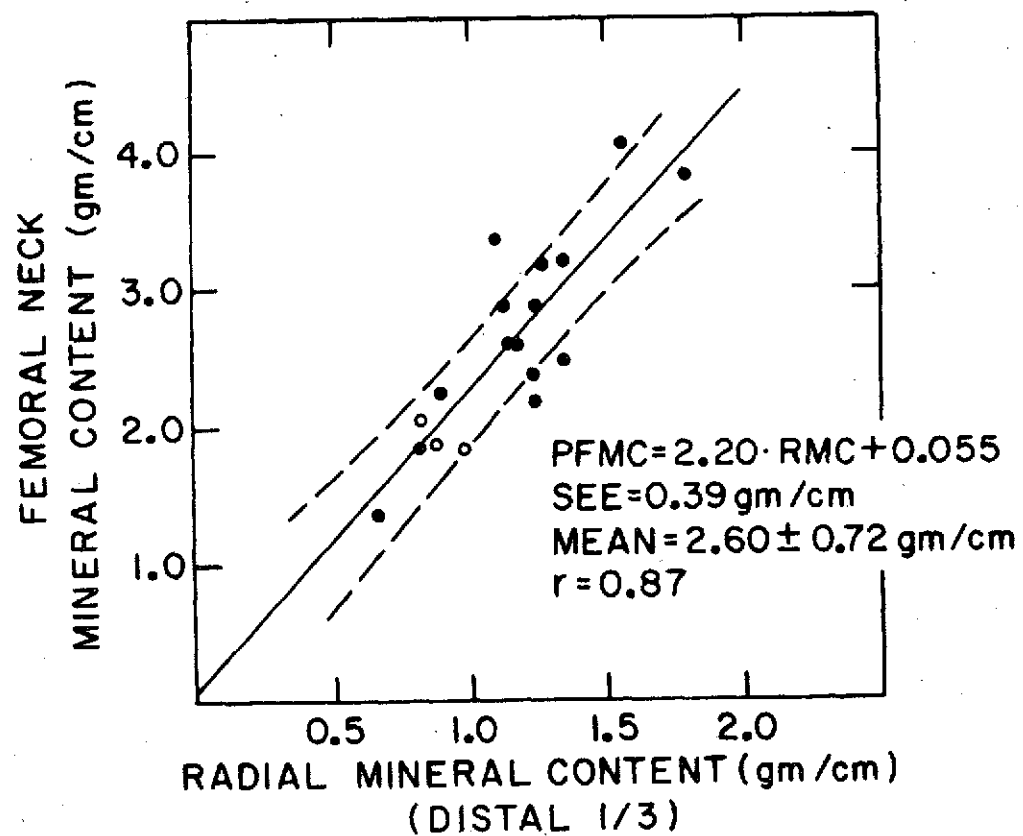


Figure 1 Scattergram between the BMC of the femoral neck and the BMC at the DT scan site on the radius. The regression equation is given; PFMC is the predicted femoral neck mineral content and RMC is the BMC at the DT site on the radius.

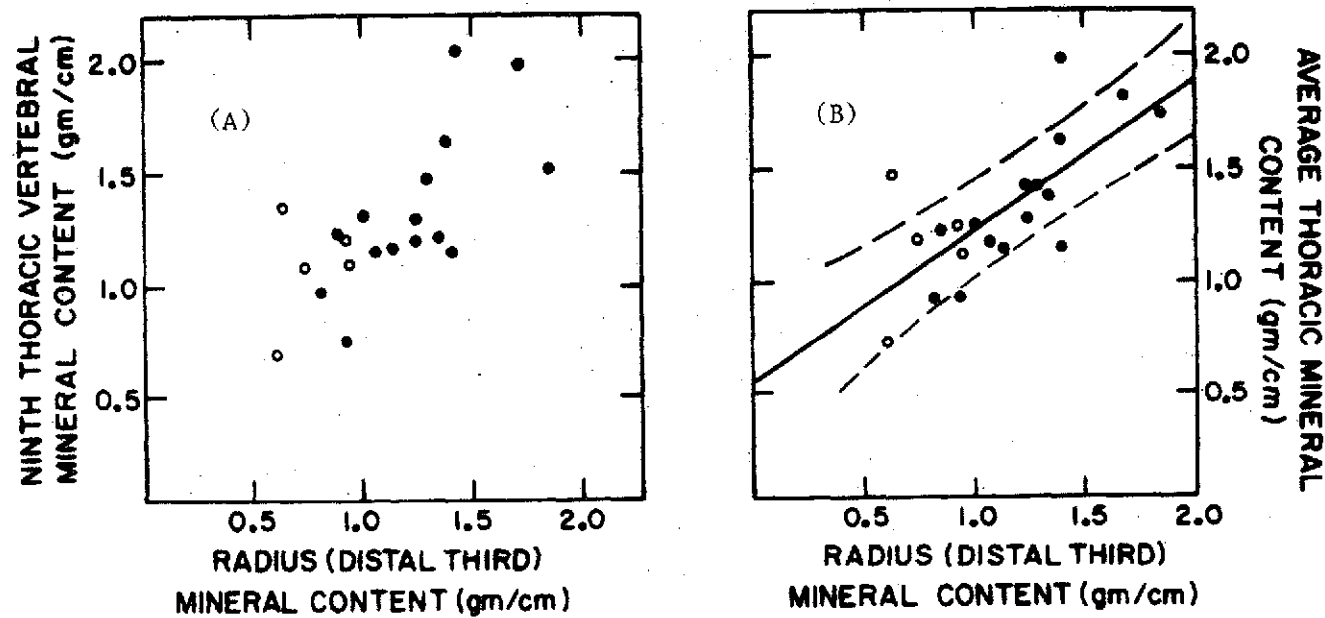


Figure 2 Scattergrams between: (A) Mineral content of the ninth thoracic vertebra and the BMC at the DT scan site on the radius; (B) Average thoracic mineral content of the eighth through eleventh vertebrae and the BMC at the DT site on the radius.

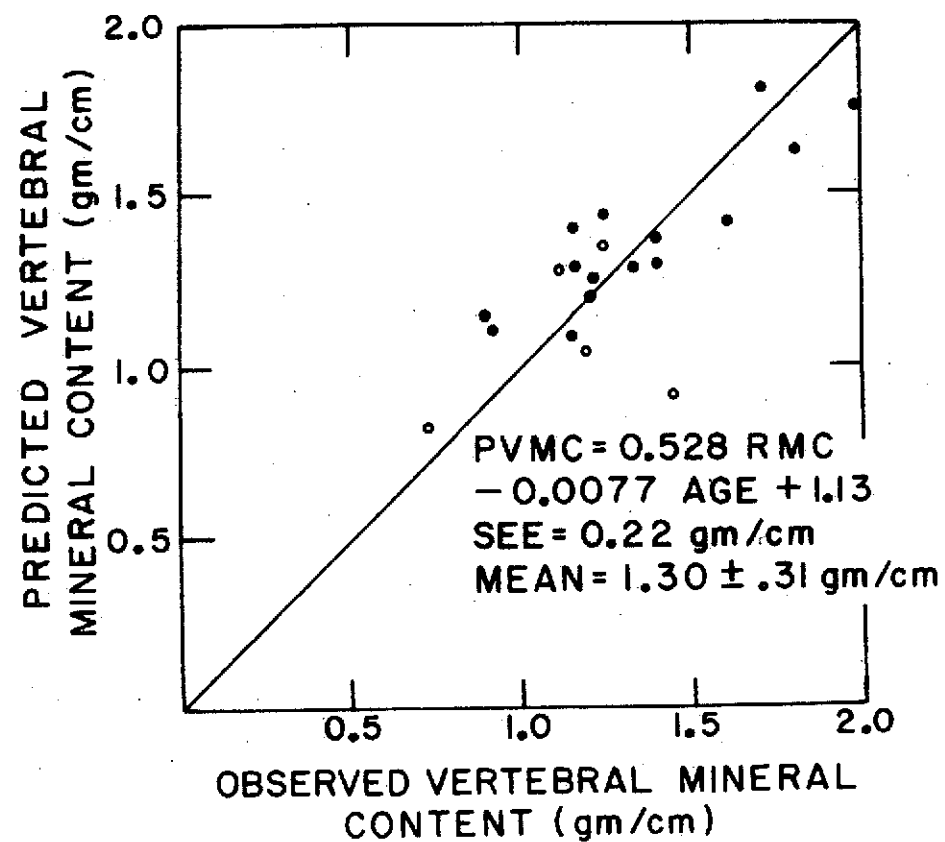


Figure 3 The average vertebral mineral content predicted from the regression equation based on the BMC at the M scan site on the radius and age, plotted versus the observed vertebral mineral content, $r=0.76$. The line of unity slope is drawn.